AD_____

GRANT NUMBER DAMD17-94-J-4401

TITLE: The p53-Deficient Mouse as a Breast Cancer Model

PRINCIPAL INVESTIGATOR: Lawrence A. Donehower, Ph.D.

CONTRACTING ORGANIZATION: Baylor College of Medicine
Houston, Texas 77030

REPORT DATE: October 1997

TYPE OF REPORT: Annual

PREPARED FOR: Commander
U.S. Army Medical Research and Materiel Command
Fort Detrick, Frederick, Maryland 21702-5012

REPORT DOCUMENTATION PAGE

Form Approved
OMB No. 0704-0188

1. AGENCY USE ONLY *(Leave blank)*	2. REPORT DATE	3. REPORT TYPE AND DATES COVERED
	October 1997	Annual (15 Sep 96 - 14 Sep 97)

4. TITLE AND SUBTITLE
The p53-Deficient Mouse as a Breast Cancer Model

5. FUNDING NUMBERS
DAMD17-94-J-4401

6. AUTHOR(S)
Lawrence A. Donehower, Ph.D.

7. PERFORMING ORGANIZATION NAME(S) AND ADDRESS(ES)
Baylor College of Medicine
Houston, Texas 77030

8. PERFORMING ORGANIZATION REPORT NUMBER

9. SPONSORING/MONITORING AGENCY NAME(S) AND ADDRESS(ES)
Commander
U.S. Army Medical Research and Materiel Command
Fort Detrick, Frederick, MD 21702-5012

10. SPONSORING/MONITORING AGENCY REPORT NUMBER

11. SUPPLEMENTARY NOTES

12a. DISTRIBUTION / AVAILABILITY STATEMENT
Approved for public release; distribution unlimited

12b. DISTRIBUTION CODE

13. ABSTRACT *(Maximum 200*

The p53 tumor suppressor gene is mutated in about half of all human cancers and in roughly 30-40% of breast cancers. In order to better understand the role of p53 mutation and loss in breast cancer progression, we have developed a mouse model which is genetically programmed to develop mammary cancer in the presence and absence of p53. By comparison of the mammary tumorigenesis process between the p53 positive and p53 negative animals we hope to obtain further insights into the mechanisms by which loss of p53 accelerates tumor progression. In the first three years of this grant we have shown that in the absence of p53 mammary tumors arise sooner and grow faster than mammary tumors with intact p53. We have also shown that tumors without p53 have higher levels of chromosomal instability and higher rates of cell proliferation than tumors with p53. Rates of apoptosis (programmed cell death) and angiogenesis (tumor vascularization) were not significantly different between p53 positive and negative tumors. We have examined the role of the p53-inducible cyclin-dependent kinase inhibitor p21 in mammary tumor progression and have shown that reduction of p21 accelerates tumor cell proliferation rates. Thus, the model is useful in elucidating the role of p53 loss in tumorigenesis and indicates that p53 has multiple roles in prevention of tumor formation and progression.

14. SUBJECT TERMS	15. NUMBER OF PAGES
p53 Tumor Suppressor Gene, Mammary Tumorigenesis, Genetic Instability, Transgenic Mice, Wnt-1 Oncogene, Preneoplastic Lesions, Breast Cancer	70
	16. PRICE CODE

17. SECURITY CLASSIFICATION OF REPORT	18. SECURITY CLASSIFICATION OF THIS PAGE	19. SECURITY CLASSIFICATION OF ABSTRACT	20. LIMITATION OF ABSTRACT
Unclassified	Unclassified	Unclassified	Unlimited

FOREWORD

Opinions, interpretations, conclusions and recommendations are those of the author and are not necessarily endorsed by the U.S. Army.

____ Where copyrighted material is quoted, permission has been obtained to use such material.

____ Where material from documents designated for limited distribution is quoted, permission has been obtained to use the material.

L.A.D. Citations of commercial organizations and trade names in this report do not constitute an official Department of Army endorsement or approval of the products or services of these organizations.

L.A.D. In conducting research using animals, the investigator(s) adhered to the "Guide for the Care and Use of Laboratory Animals," prepared by the Committee on Care and Use of Laboratory Animals of the Institute of Laboratory Resources, National Research Council (NIH Publication No. 86-23, Revised 1985).

____ For the protection of human subjects, the investigator(s) adhered to policies of applicable Federal Law 45 CFR 46.

L.A.D. In conducting research utilizing recombinant DNA technology, the investigator(s) adhered to current guidelines promulgated by the National Institutes of Health.

L.A.D. In the conduct of research utilizing recombinant DNA, the investigator(s) adhered to the NIH Guidelines for Research Involving Recombinant DNA Molecules.

____ In the conduct of research involving hazardous organisms, the investigator(s) adhered to the CDC-NIH Guide for Biosafety in Microbiological and Biomedical Laboratories.

Lawrence A. Donehower 10/8/97

PI - Signature Date

TABLE OF CONTENTS

Progress Report: The p53-Deficient Mouse as a Breast Cancer Model

Principal Investigator: Lawrence A. Donehower, Ph.D.

Introduction:

The p53 tumor suppressor gene is mutated in roughly half of all human tumors examined to date (1). Approximately 30-40% of human breast cancers have p53 mutations, indicating loss of p53 function is a central event in breast cancer progression (1). Even in those breast cancers where p53 is wild type in structure, it may be abnormally stabilized or localized within the cell, suggesting possible disruption of p53-associated growth control pathways (2). In addition to its loss in spontaneously arising breast cancers, inherited mutations ofthe germ line p53 gene can also occur, giving rise to a familial cancer predisposition called Li-Fraumeni syndrome (3,4). The most frequently observed tumor in affected females of Li-Fraumeni families is breast cancer (5).

The role of p53 in the normal cell appears in large part to be that of a cell cycle checkpoint protein. In response to a variety of DNA damaging agents, p53 levels in the cell increase and mediate one of two cell fates: (i) arrest in G1 of the cell cycle, or (ii) apoptosis (6-8). The decision to undergo arrest versus apoptosis may rely on many factors, including cell type, growth factor levels, and abrogation of function in other growth-related genes, etc. Regardless of which decision is taken, the end result is to prevent the cell from DNA synthesis and division in the presence of damaged DNA templates (9). Thus, the cell is more likely to be spared oncogenic mutations which could lead to cancer. In the absence of p53 (which may occur in preneoplastic cells and does occur in p53-deficient mice), it is hypothesized that cells would be more likely to become tumorigenic through increased mutation rates and genomic instability (9).

The biochemical mechanisms through which p53 mediates its checkpoint functions are likely to be complicated, though clearly transcriptional regulation of key growth related genes is crucial for its G1 arrest function (8,10). Wild type p53 trans-activates the $p21^{WAF1/CIP1}$ gene, which encodes a potent inhibitor of G1 cyclin-dependent kinases (11,12). Transcriptional activation plays a role in p53-mediated apoptosis (13), though which p53 targets are critical for apoptosis are unclear. In other instances, it has been shown that p53 can mediate apoptosis in the absence of transcriptional activation, suggesting multiple mechanisms by which p53 affects cell death (14,15).

There is significant evidence that p53-mediated apoptosis may play an important role in suppression of tumors (16-18). Aberrant expression of certain oncogenes and tumor suppressor genes may induce high levels of p53 (19,20). When cells are induced to proliferate abnormally by these genes, p53 upregulation may induce apoptosis and thus protect the organism from early tumors. This role of p53 tumor suppression through apoptosis has been demonstrated in some mouse tumor models. In situations where Rb function is abrogated in a tissue, G1 arrest capability is

often lost and these abnormally proliferating cells are induced to undergo apoptosis. In the absence of p53, such Rb-deficient tissues may rapidly form aggressive tumors, arguing that attenuated apoptosis due to p53 loss is a rate limiting step in tumor formation (16-18).

Is apoptotic function the primary mechanism by which p53 regulates tumor progression or are there other mechanisms? A number of *in vitro* and *in vivo* studies suggest that loss or mutation of p53 may have additional important biological effects on tumor formation and progression (21). Some of these effects of p53 loss on tumor progression may be: (1) increased rates of cell proliferation independent of apoptotic effects; (2) increased levels of genomic instability in the tumor cells which may lead to further oncogenic lesions; (3) increased rates of angiogenesis, allowing more nutrients to nascent tumor cells; and (4) increased invasiveness and metastases. All of these biological effects are measurable, and an important goal of this proposal is to assess all of these potential tumor progression mechanisms in the context of the *Wnt-1*/p53 tumor model described below.

Initially, to study the role of p53 in tumorigenesis, we developed a p53-deficient mouse by gene targeting methods (22). These mice contained either one (p53+/-) or two (p53-/-) inactivated p53 germ line alleles. In comparison to their normal littermates, the p53-deficient mice showed accelerated tumorigenesis. Half of all p53+/- mice developed tumors by 18 months of age, while 100% of p53-/- mice succumbed to tumors by 10 months of age (23,24). The spectrum of tumors was quite variable, though lymphomas and sarcomas were most frequently observed (23,24).

While the analysis of tumorigenesis in the p53-deficient mice has yielded a number of interesting insights, the study of spontaneous tumor formation in these animals has certain limitations if one wants to examine mechanistic questions in an efficient, well controlled manner. For example, the p53-deficient mice develop a wide array of tumors sometimes with a relatively long latency (particularly the p53+/- mice). Moreover, since p53+/+ mice rarely develop tumors, control tumors which develop in a p53-independent manner are difficult to obtain. To circumvent these disadvantages, investigators have taken two general approaches, either treating the p53-deficient mice with a tissue-specific carcinogen or crossing the p53-deficient mice to a tumor-susceptible transgenic mouse genetically programmed to develop a single tumor type. The resulting models usually develop a single tumor type in a relatively short amount of time and control p53+/+ tumors are available to compare to the p53-deficient tumors.

The model we chose for examination of the role of p53 loss in tumor progression was the *Wnt-1* transgenic/p53-deficient mouse (25). This model was generated by crossing our p53-deficient mice to mammary tumor susceptible *Wnt-1* transgenic mice (26). *Wnt-1* transgenic females, which contain a mouse mammary tumor virus long terminal repeat promoter driving the *Wnt-1* oncogene, specifically develop early mammary gland hyperplasia followed by mammary adenocarcinomas before 12 months of age in a stochastic manner (26). Thus, our prediction was that virtually all of the *Wnt-1* transgenic females would develop mammary adeno-carcinomas either in the presence or absence of wild type p53. Such mice would be

ideal for exploring the biological and genetic effects of p53 presence and absence in mammary tumor formation and progression.

In the third year of our grant, we have supplemented our *Wnt-1* transgenic p53-deficient model with a second model, the *Wnt-1* transgenic p21-deficient mouse. We hypothesized that since the primary effect of the presence of p53 in tumors was to reduce tumor cell proliferation, one possible molecular pathway that p53 reduced proliferation was through induction of $p21^{WAF1/CIP1}$(11,12). We postulated that reduction or elimination of p21 in the *Wnt-1* transgenic mouse might have an effect on tumor progression comparable to that observed in p53-deficient *Wnt-1* transgenic mice.

p21 was first identified in 1993 as a cyclin dependent kinase inhibitor inducible by p53 (11,12,27-29). This protein was found to be associated with inactive cyclin E/CDK2 complexes that normally mediate G1 to S phase transition, indicating that the primary role of p21 is to effect G1 arrest (11,27,29). Overexpression of p21 in proliferating cells does indeed result in G1 arrest (30). Moreover, El Deiry et al. (12) demonstrated that p21 expression is transcriptionally activated by overexpression of p53, providing a potential mechanism through which induced p53 can mediate G1 arrest. Basal p21 expression is independent of p53, but following gamma irradiation increased expression of p21 is partially p53 dependent (31). p21 induction has been observed in cell lines undergoing induction of differentiation or senescence (31,32). p21 also binds PCNA and thus may inhibit DNA replication (33,34).

p21-deficient mice have been generated and p21 nullizygous mice have been shown to be developmentally normal (35,36). p21-deficient mice also do not appear to be tumor prone, indicating that p21, while a cell cycle inhibitor, is not a tumor suppressor in the biological sense. This is corroborated by a failure to find p21 mutations in human tumors. Interestingly, however, embryo fibroblasts from p21 null mice do appear to have enhanced division capabilities and show some defects in G1 arrest following treatment with DNA damaging agents (35,36).

Recent work by LaBaer et al. (37) have revealed that the assembly of G1 cdk/cyclin complexes is actually promoted through binding to p21. Moreover, there appears to be interesting stoichiometric effects based on the level of p21 which binds to the cdk/cyclin complexes. High levels of p21 inhibit the cdk/cyclin complex kinase activity, while absence of p21 results in low kinase activity (probably through failure of cdks and cyclins to form an active complex). However, low to intermediate levels of p21 appear to provide enough activity to promote formation of cdk/cyclin complexes, but not enough to actively inhibit the complex kinase activity. The end result of low to intermediate levels of p21 is enhanced cdk/cyclin activity and enhanced progression of the cell cycle through G1. This model was directly tested in our p21/*Wnt-1* crosses.

Body:

Experimental Methods

Mice

The *Wnt-1* mice used in the crosses described here were the offspring of two *Wnt-1* males from line 303 described previously (Tsukamoto et al., 1988). These mice were of mixed SJL X C57/BL/6 genetic background. The p53-deficient mice were from a pure 129/Sv line of mice containing one or two germ-line *p53* null alleles (38). The two *Wnt-1* males were crossed to heterozygous (*p53*+/-) 129/Sv females to derive F1 mice of four possible genotypes (*p53*+/+; *Wnt-1 p53*+/+; *p53*+/-; *Wnt-1 p53*+/-). F1 *p53*+/- females were crossed to F1 *Wnt-1 p53* +/- males to obtain F2 mice that carried any of the *Wnt-1 p53* genotypes found in the F1 population as well as *Wnt-1 p53*-/- or *p53*-/- . To obtain larger numbers of mice with *p53*-/- genotypes with or without the *Wnt-1* transgene, F2 *p53*-/- females were mated to *Wnt-1 p53* -/- males. All of the mice were monitored visually twice weekly for the appearance of tumors for up to one year. When a tumor of roughly 0.5 centimeters in diameter was detected, the age of the mouse was recorded and used to generate the Kaplan-Meier plots in Fig. 1. After appearance, the growth of the tumor was monitored by measurement in two dimensions of the diameter with a set of calipers. Once a tumor reached 2-2.5 cm in diameter, the tumor-bearing mouse was sacrificed, and tissue sections removed for histopathology. The rest of the tumor was frozen at -70°C for nucleic acid analyses.

The p21-deficient mice used in this study were obtained from Phil Leder and have been described in Deng et al. (35). Female p21-/- mice were crossed to *Wnt-1* transgenic males and F1 mice were intercrossed in a manner similar to that described for the p53-deficient *Wnt-1* transgenic mice described above. Ultimately, when sufficient numbers of p21+/+, p21+/-, and p21-/- *Wnt-1* transgenic females were obtained, these were monitored for mammary tumor formation.

Genotyping of Mice

We determined the *p53* and *Wnt-1* genotypes of the offspring from the crosses using previously described methods (25,26). Briefly, 1 cm of tail was clipped from weanling mice and incubated overnight at 55-60° C in 500 µl of tail lysis buffer (50 mM Tris-HCl pH 7.5, 50 mM EDTA pH 8.0, 100 mM NaCl, 5 mM DTT, 200 µg/ml Proteinase K). Lysates were extracted with phenol chloroform and precipitated in two volumes ethanol. Pellets were resuspended in 100 µl TE (10 mM Tris-HCl, pH 8.0, 1 mM EDTA). Five µl of each tail DNA was cleaved with Bam HI (2-16 hr at 37° C) and subjected to agarose gel electrophoresis on a 0.7% gel. The gel was then blotted to nylon membranes (Bio-Rad Zetaprobe membranes) and hybridized according to the Southern blot hybridization procedures of Reed and Mann (39). *Wnt-1* probes and p53 probes were utilized simultaneously in the hybridization and were labelled with ^{32}P with an oligo labelling kit provided by Boehringer-Mannheim. Filters were rinsed and subjected to autoradiography. The p53 wild type allele (5.0 kb), mutant p53 allele

(6.5 kb), *Wnt-1* transgene (3.0 kb), and endogenous *Wnt-1* gene (2.0 kb) could easily be differentiated by this procedure.

p21 genotypes of p21-deficient *Wnt-1* transgenic mice were determined as described in Deng et al. (35).

p53 Loss of Heterozygosity Assays

These assays were performed by Southern blot hybridization procedures identical to those described above for genotyping except that small pieces of mammary tumor tissue were used instead of tail. Roughly half of the tumors displayed loss of the remaining wild type p53 allele while half retained it by Southern assay (25).

Tumor Transplantation Assays

Either 10^4, 10^5, or 10^6 tumor cells isolated from primary mammary tumors were transplanted into the inguinal mammary fat pads of female SCID hosts 8-16 weeks of age. These tumor cells developed into tumors whose diameter and growth rates were measured by calipers over a period of 6 weeks. The tumor cells were isolated from the tumors by mincing with a sterile razor blade followed by a 3 hour incubation at 37°C in DMEM:F12, collagenase and antibiotics as described by Kittrell et al. (40). The tumor cells were spun down and then rinsed three times with PBS containing 5% ABS to inactivate the Collagenase. The cells were then resuspended in DMEM:F12 and an aliquot was counted on a hemocytometer. Approximately 10 µl containing the appropriate number of cells were then injected into the inguinal fat pad of female SCID hosts.

Mitotic Index Counts

A determination of the number of mitotic figures in each tumor section was performed as follows: Mitotic figures (cells containing obvious condensed chromosomes in various stages of mitosis) were counted in 10 random high power fields at or near the edges of standard hematoxylin and eosin stained tumor cross sections.

BrdU Incorporation

BrdU incorporation was performed using the Cell Proliferation Kit from Amersham (RPN 20). Briefly, 1 ml of BrdU (from kit) per 50 grams body weight of the mouse was injected intraperitoneally. The labeling of cells was allowed to proceed for three hours at which time tumors were harvested and fixed in methacarn fixative solution overnight. Samples were then transferred to acetone for at least three hours and then stored in 95% ethanol until embedding in paraffin. Sections were stained for BrdU incorporation as follows: Samples were deparaffinized by washing twice in xylene, twice in 100% ethanol and once in 70% ethanol. Samples were then

rehydrated in PBS for 20 minutes. Endogenous peroxidase activity was quenched by immersing samples in 3% hydrogen peroxide for five minutes followed by two 10 minute rinses in PBS. The samples were then incubated at 37° C for one hour with nuclease and Anti-BrdU antibody (Kit), followed by a 20 minute wash with PBST and 10 minutes with PBS. This was followed by incubation with the secondary antibody for 30 minutes at 37° C. Samples were then washed for 10 minutes with PBST and twice for 10 minutes with PBS. Substrate was provided in the form of DAB in 1x PBS for 10 minutes. Counterstaining is done with Methyl Green for 5 minutes followed by dipping in butanol, 100% ethanol, and xylene. Samples were then mounted with Permount.

Flow Cytometry

The DNA content of tumor samples was assessed in nuclei isolated from paraffin embedded samples based on a modification of Hedley's method (41). Nuclear suspensions were prepared from five 50 μm sections, a 4 μm section was cut before and after the 50 μm sections to confirm that histologically comparable sections were being used. The samples were deparaffinized using two 50 minute xylene washes at 25° C. The cells were then rehydrated using successive incubations with ethanol, two per dilution, 100%, 95%, 70%, 50% and distilled water. Between each concentration of ethanol there is a 50 minute incubation at 25° C to make a cell suspension. To make this a single cell suspension the cells were treated with a 0.5% pepsin solution at 37° C for 30 minutes. Filtration through a 74 μm mesh (Small Parts Inc., Miami, FL) resulted in a nuclear suspension which was stained using the Vindelov technique (42). For a procedural control fresh chicken erythrocyte nuclei (CEN) (Accurate Chemical & Scientific Co., Westbury, NY) were used. A five microliter solution of a 20,000,000 CEN/ml suspension was added to the sample prior to the DNA staining step.

The sample used for actual DNA flow analysis was acquired of a FACScan flow cytometer using the ModFitLT software with doublet discrimination from Becton Dickinson, San Jose, CA. Twenty thousand events were collected using the gating parameters of FL2-W versus FL2-A. Histograms were generated to determine the percentage of cells in each stage of the cell cycle. The Coefficient of Variation (CV) was determined for the diploid G0/G1 peak for all cases. Only those samples with CV's of less than 8% were used.

DNA Fragmentation Assay

Genomic DNA was isolated from frozen tumor tissue by methods similar to those described for the loss of heterozygosity procedure except that pelleting of the DNA utilized 30 minute centrifugations rather than five minute centrifugations. Twenty micrograms of total DNA from each tumor was then run out on a 1.5% agarose gel. The gel was blotted using standard Southern blot procedures (28) and probed using a total mouse genomic probe cleaved with Hae III and labelled with ^{32}P through the oligo labelling procedure with the High Prime labelling kit (Boehringer-Mannheim). Following autoradiography of the Southern blot, the radioactivity on the filters was imaged and quantitated using a Molecular Dynamics phosphorimager. The amount of

hybridization in the low molecular weight ladder bands (apoptotic fragments) of each lane was divided by the total amount of hybridizing radioactivity (after subtracting background) in that lane to obtain an estimate of the percentage apoptotic DNA.

TUNEL Assay

The TUNEL assay was performed using the TACS™ 2 TdT *In Situ* Apoptosis Detection Kit (Trevigen, Gaithersburg, MD). Briefly, 4 μm sections on slides were deparaffinized by heating at 57° C for 20 minutes followed by placing in xylene for 10 minutes at room temperature. This was followed by another 5 minute xylene wash, a 5 minute 100% ethanol wash, a 5 minute 95% ethanol wash and a 70% ethanol wash for a further 5 minutes. The slides were then rinsed twice in distilled water for 2 minutes each followed by a rehydration in PBS for 10 min. The samples were then digested for 10 minutes at room temperature with Proteinase K (Kit). Endogenous peroxidases were then quenched using 3% hydrogen peroxide for 5 minutes. The fragmented DNA ends present in apoptotic cells were then extended using TdT, Mn^{++}, biotin dNTP's in labeling buffer (Kit). This reaction mix was added to the samples and allowed to incubate at 37° C for 1 hour. The reaction was stopped and rinsed for 2 minutes in PBS. Streptavidin-HRP conjugate was then allowed to bind to the incorporated biotin-dNTPs at room temperature for 15 minutes. Substrate was provided in the form of DAB and the color reaction was allowed to proceed for 5 minutes at room temperature. Counterstaining was performed for 5 minutes with 1.0% methyl green (Kit). Samples were dipped briefly in butanol, 100% ethanol and xylene. Finally, samples were mounted with Permount.

Immunoblot detection of antibodies in mammary tumors

Equivalent amounts of protein from mouse tumors were separated by SDS polyacrylamide gel electrophoresis using 15% resolving gels, transferred to Immobilon P membrane (Millipore), and immunoblotted with either anti-mouse IgG (H+L) antibodies (Pierce), mouse kappa or lambda chain-specific antibodies (Cappell), or tumor bearing serum as previously described (43,44).

Telomerase, telomerase RNA, and telomere assays

The procedures for these assays are described in Broccoli et al. (45).

Angiogenesis assays

Blank slides containing 5 micron sections of tumor tissue were deparafinized by 10 minute and 5 minute incubations in xylene, following by 3 minute sequential incubations in 100% ethanol, 95% ethanol, 70% ethanol, and three incubations in phosphate buffered saline (PBS), one 10 minute incubation in 3% hydrogen peroxide, and two 2 minute washes in PBS. Antigen retrieval was then performed by 15 minute incubation in Proteinase K solution (1 μl enzyme in 50 μl water from the Trevigen

Apoptosis Kit), followed by three washes for 5 minutes in PBS. Blocking was performed by incubation with 10% goat serum in PBS for 30 minutes. Then, the primary Factor VIII antibody (A-0082 from DAKO; 1:200 dilution in 10% goat serum) was incubated on the slide overnight at 4° C in a humidified chamber. The slide was equilibrated to room temperature, and washed three times in PBS (the first wash contained 2% Tween). The secondary biotinylated antibody (DAKO E-0432) was then added (diluted 1:300 in blocking solution) for 45 minutes at room temperature in a humidified chamber. The slide was then washed three times by five minute incubations in PBS (the first wash contained 2% Tween). The slide was then incubated for 30 minutes at room temperature with the ABC reagents (streptavidin peroxidase from Vector Labs), followed by three washes in PBS and incubation in diaminobenzidine (250 µl in 50 ml PBS, 30% H_2O_2 from Trevigen) for 13 minutes. The slide was then washed in PBS for one minute followed by 2 minutes in 1% methyl green and three washes for 30 seconds in butanol, ethanol, and xylene. Finally, the slide was mounted with Permount and visuallized at 200X magnification.

Tumor angiogenesis was quantitated by counting the number of stained capillaries in 10 random high powered fields at 200X magnification along the tumor edge. The mean value of number of microvessels per field was then determined. Ten tumors per p53 genotype group were investigated by this method.

Differential display

Initially, to perform differential display, we isolated mRNAs from 4 *Wnt-1*/p53+/+ tumors, 4 *Wnt-1*/p53+/- LOH tumors, and 4 *Wnt-1*/p53-/- tumors using the Invitrogen mRNA purification kit according to the manufacturer's specifications. cDNAs were then synthesized from these 12 mRNAs using the Clontech Delta RNA Fingerprinting Kit according to the manufacturer's specifications. For each of the 12 cDNAs, one of ninety primer pair combinations provided by the Clontech kit was used to amplify the cDNA through 25 PCR cycles according the Clontech specifications. Each reaction contained alpha ^{33}P-dATP to label the amplified fragments. Each of the 12 amplification reactions were then loaded on a 5% denaturing polyacrylamide gel and electrophoresed. Autoradiography revealed a series of bands for each tumor mRNA which were almost always identical for all twelve tumors. Occasionally, differentially expressed bands were observed for a single tumor. These were usually ignored. However, if differentially expressed bands were observed among three or four tumors of a given given genotype, these bands were isolated from the gel and reamplified with the same primers used initially.

To confirm that the differentially PCR fragments were indeed differentially expressed, candidate reamplified DNAs were labelled with ^{32}P by oligo labelling (Boehringer Mannheim High Prime kit) and hybridized to a Northern blot containing 5 µg of 15 tumor mRNAs, five *from Wnt-1*/p53+/+ tumors, five from *Wnt-1*/p53+/- LOH tumors, and five from *Wnt-1*/p53-/- tumors. Following autoradiography, the comparative expression patterns were observed. In at least one case (out of four candidate fragments examined so far), the initial differential expression pattern was confirmed in the Northern blot analysis.

In Vitro Invasion Assay

Matrigel chambers from Becton-Dickinson were rehydrated with DMEM:F12 medium for two hours. Cell suspensions of 4.4 X 10^5 mammary tumor cells in DMEM:F12 with insulin were prepared. These cell suspensions were placed in the matrigel chamber insert. The insert was then placed ina six well companion plate containing DMEM:F12 with insulin, 2% serum, and EGF. Cell culture inserts were removed after a 24 hour incubation. Cells and matrigel were wiped from the top of the insert using a cotton swab. The bottom of the insert was then stained using a Diff-Quick staining kit from Dade Diagnostics. The insert membraned was removed with a razor blade and placed on a microscope and slide with immersion oil. Cells passing through the membrane were then counted at 200X magnification.

Results

(1) Data from first year of grant

To provide the background for the second and third year's progress, I felt it was necessary to briefly outline the progress in the first year. First, After crossing the p53-deficient mice to the *Wnt-1* transgenic mice, we monitored tumor formation in the various categories of offspring. We will focus on the *Wnt-1* transgenic females in the remainder of this report. Appearance of mammary tumors in the *Wnt-1* transgenic females was greatly accelerated in the absence of p53 (p53-/-) (Figure 1). All of the *Wnt-1* p53-/- females developed mammary adenocarcinomas by 15 weeks of age and very few developed lymphomas or other spontaneous tumors characteristic of the p53-/- mice. *Wnt-1* p53+/+ females showed a delayed mammary tumor incidence with 100% developing adenocarcinomas by 41 weeks of age. Interestingly, *Wnt-1* p53+/- females exhibited the same mammary tumor incidence as *Wnt-1* p53+/+ females, even in those cases where the p53+/- tumor showed loss of the remaining wild type allele.

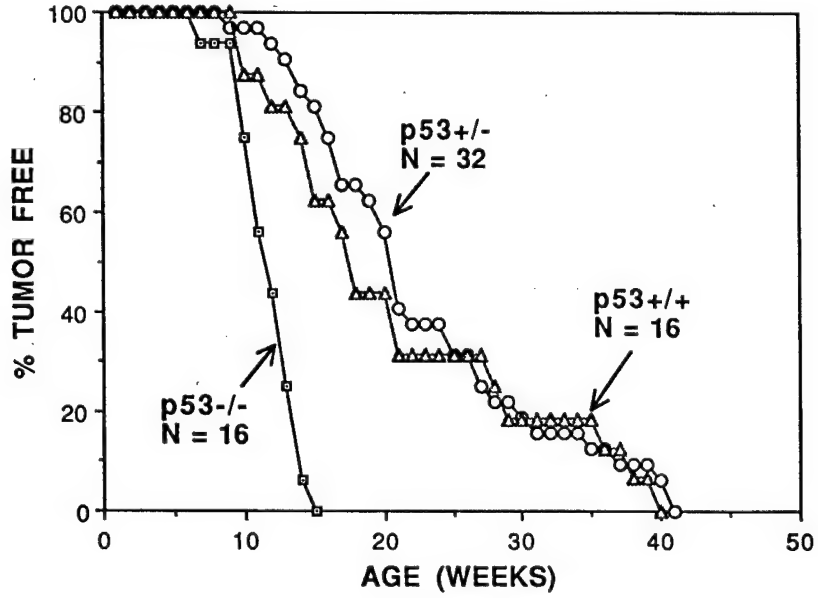

Figure 1.

In order to obtain insights into the mechanisms by which loss of p53 accelerated tumorigenesis, we analyzed the chromosomal complement of the *Wnt-1*-initiated mammary tumors in the presence and absence of p53. Previous *in vitro* studies had shown that the loss of p53 correlated with genomic instability. Using two different methods, classical cytogenetics and comparative genomic hybridization, we showed that loss or absence of p53 correlated quite well with increased genomic instability. A summary of the comparative genomic hybridization (CGH) results is shown on the next page (Table 1). It should be noted here that roughly half of the p53+/- tumors lose their remaining wild type allele (referred to as p53+/- LOH) and roughly half of the tumors appear to retain their wild type allele (referred to as p53+/- no LOH) as assayed by Southern blot hybridizaton. Sequencing of the p53 cDNA in four p53+/- tumors which retained the wild type allele showed no point mutations in the

remaining p53 gene and no downregulation of RNA expression, suggesting that wild type p53 function is retained in this category of p53+/- tumors.

Table 1. Summary of CGH Abnormalities in *Wnt-1* Mammary Adenocarcinomas

p53 Genotype	Tumors with Chromosome Abnormalities	Average Number of Chromosome Abnormalities per Tumor
p53+/+	2/6	0.3
p53+/- (no LOH)	2/4	1.0
p53+/- (LOH)	8/8	4.2
p53-/-	7/7	1.7

Tumors missing p53 (p53+/- LOH and p53-/-) showed significantly higher rates of chromosomal abnormalities, supporting the argument that loss of p53 promotes genomic instability. Surprisingly, Table 1 also shows that p53+/- tumors which lose their remaining wild type p53 allele have even more chromosomal abnormalities than p53-/- tumors. We are unsure why this would be so, but have speculated that p53+/- tumors have to undergo more mutations than p53-/- tumors because of environmental effects (i.e. organisms with no p53 may not be able to express certain extracellular inhibitors of tumor growth). Interestingly, the chromosomal abnormalities observed in the p53-deficient tumors were non-random in nature, suggesting a selection for certain chromosomal lesions which might provide a growth advantage. These results indicate that genomic instability does play a role in the progression of these tumors and that loss or absence of p53 may contribute to tumor progression in part through this mechanism.

(2) Results in second year of grant

In the second year of the grant our primary focus was to determine some of the biological mechanisms by which loss or absence of p53 accelerates mammary tumorigenesis in the *Wnt-1* transgenic p53-deficient model. In the first year we concentrated on the involvement of genomic instability in tumor progression. In the second year we looked at three potential additional mechanisms: (i) cell cycle progression and proliferation; (ii) apoptosis (programmed cell death); and (iii) telomere and telomerase effects. The first two parameters are obviously of critical importance in the growth of the tumor as the tumor growth is a direct function of the rate of cell division minus the rate of cell death. There has been significant evidence from other

tumor models that loss of p53 is accompanied by attenuated apoptosis and that this event might be a rate limiting step in tumor formation (16-18).

(a) mammary tumor growth in the presence and absence of p53

Our first set of studies entailed some followup experiments on the tumor incidence data shown in Figure 1. The data in Figure 1 measures the time to first appearance of a visible tumor. Such curves may reflect early events in tumor formation. However, we wanted to more effectively measure the rates of tumor growth once the tumor is first observed. To do this, we measured the rate of tumor volume growth over time after initial observation. Tumor diameters in two dimensions were measured with calipers at weekly intervals and tumor volumes could then be estimated from these measurements. We found that while the rate of tumor volume growth for each p53 genotype was quite variable, the average growth of tumors missing p53 was faster than those containing p53 (Figure 2).

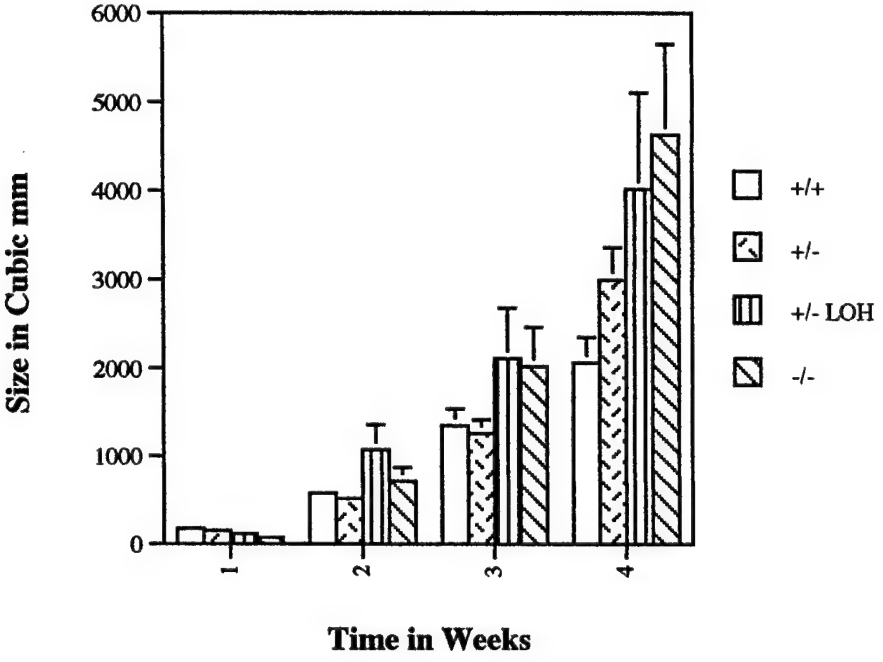

Figure 2.

We also performed tumor transplantation experiments in which we transplanted 10^5 tumor cells from each tumor and injected them into the same inguinal mammary fat pad of genetically indentical recipient SCID mice. Virtually all of the transplantations with 10^5 tumor cells formed tumors which grew gradually enough to easily differentiate between fast growing and slow growing tumors. The transplant experiments also had a number of advantages over the primary tumor measurements. We were starting with the same number of tumor cells (10^5), injected into the same inguinal mammary fat pad, in genetically identical p53+/+ female SCID hosts between 8 and 16 weeks of age. Therefore, tumor growth rates are more likely to be dependent only on the properties of the tumor cells and not those of the host. The results did not show the expected straightforward correlation between growth rate and p53 status. However, the p53+/+ tumors did show the slowest growth rates, and the p53+/- LOH tumors, after a slow start, had the fastest growth rate. Interestingly, the p53-/- tumor cells, which showed the fastest growth rate as primary tumors, showed

slower growth rates than even the p53+/- no LOH tumors. We speculated that such slow rates were attributable to an environmental effect. That is, organisms with intact p53 (such as the p53+/+ SCID hosts in these experiments) may release an inhibitor of tumor growth which p53-/- tumor cells have never been exposed to in the primary tumor. Therefore, it may take more time for the p53-/- tumor cells to evolve the appropriate mutations to overcome this inhibition. However, these experiments partially corroborated the primary tumor data in that the absence or loss of p53 tended to result in an increase in mammary tumor cell growth rates.

(b) tumor cell proliferation and cell cycle progression

Probably the most obvious mechanism by which p53 loss could result in elevated tumor cell growth is through increased rates of cell division. We had shown previously that early passage p53-/- embryo fibroblasts divide more rapidly than their p53+/+ counterparts and have higher percentages of cells in S phase (46). To assess rates of cell division in the mammary tumors in the presence and absence of p53, we employed three different techniques: (i) mitotic index determinations; (ii) BrdU incorporation assays; and (iii) flow cytometry on fixed tumor cells. The mitotic index for each tumor was easily determined by counting the percentage of cells in a tumor in multiple microscopic fields which are clearly in mitosis through the identification of condensed chromatids in the fixed H & E sections. Two individuals performed these counts in a blinded fashion and obtained similar results. These are shown in Table 2 below.

Table 2. Mitotic Index of *Wnt-1* Mammary Adenocarcinomas

p53 Genotype	Mean Mitoses[a]	# Tumors Examined
p53+/+	16.7	9
p53+/- (No LOH)	23.8	6
p53+/- (LOH)	40.0	7
p53-/-	37.0	10

[a]Mean number of mitoses per ten high power fields

The results above clearly indicate that cells which either lack or lose p53 show higher frequencies of mitosis as measured by this assay. To confirm that tumors without p53 also have higher percentages of cells in S phase, we employed a BrdU incorporation assay. BrdU was injected into the tumor bearing animals three hours prior to sacrifice. Tumor cells in S phase during this three hour window were detected

by incubation of the tumor sections with an anti-BrdU antibody. When the results were carefully quantitated, we again found that the p53+/- LOH and p53-/- tumors had higher percentages of cells in S phase than p53+/+ and p53+/- no LOH tumors.

Our final assay for cell proliferation involved flow cytometry on tumor cells from fixed sections of tumors to determine the DNA index and S-phase fraction. 23 *Wnt-1*/p53 tumors were examined by flow cytometry and the results are indicated in Figure 6 of Jones et al. (47; see appended reprint). As expected, tumors losing or missing p53 had higher fractions of cells in S phase. p53+/- LOH showed significantly higher S phase fractions than all other p53 genotypes. This result is consistent with the earlier mitotic index data. Interestingly, flow cytometry indicated that all five p53+/- LOH tumors were aneuploid while none of the other twelve tumors (including p53-/- tumors) appeared to have significant aneuploid fractions. This result was also consistent with the comparative genomic hybridization data presented in Table 1.

(c) apoptosis

The growth rate of a tumor is likely to be influenced by at least two processes, the rate of cell division and the rate of cell death. We have shown strong evidence above that in the *Wnt-1* mammary tumor model the absence of p53 increases cell divison rates over those seen in tumors with intact p53. However, studies on other mouse tumor models have indicated that loss of p53 in a tumor cell may be accompanied by attenuated apoptosis and increased survival (16-18). To determine whether p53 loss was accompanied by decreased apoptosis in our *Wnt-1*/p53 model we analyzed apoptosis by two methods, the TUNEL assay and DNA fragmentation assay. The TUNEL assay specifically labels nuclei with free DNA ends. Such free ends are signature events in apoptotic cells. We employed this assay on both normal and hyperplastic mammary glands and mammary tumors from the *Wnt-1*/p53 mice. Apoptosis levels were very low in both normal and hyperplastic mammary glands in the presence and absence of p53 (47; Figure 3 in Jones et al.) When mammary tumors were examined by TUNEL assay, *Wnt-1* tumors had low levels of apoptosis in both p53 positive and negative tumors and there was not a significant difference among the tumors (47; Figure 2 in Jones et al.)

p53 status plays little or no role in levels of apoptosis in the tumors in this model and this was further confirmed by a DNA fragmentation assay on the tumors. With this assay, there was not a great difference in the intensity of apoptotic DNA (represented by the discrete bands in the low molecular weight region of the gel following quantitation with the Molecular Dynamics Phosphorimager). If anything, we noted that p53-/- tumors had marginally higher percentages of apoptotic DNA compared to p53+/+ tumors (47; Figure 4 of Jones et al.). Thus, our data supports the hypothesis that the increased tumor growth rate observed in the tumors lacking p53 is likely to be a result of increased proliferation rate rather than decreased apoptotic function.

(d) antibody deposition in *Wnt-1* mammary adenocarcinomas

In a collaborative effort with Wafik El-Deiry at the University of Pennsylvania School of Medicine, we investigated $p21^{WAF1/CIP1}$ protein expression in p53-deficient

tumors and *Wnt-1* mammary tumors. Using primarily immunoblot assays, assessment of p21 in the tumors tended to be variable and inconclusive. However, it was quickly noted that tumors from mice which had intact p53 (e.g. *Wnt-1* p53+/+ mice) had high levels of mouse light and heavy chain antibody deposition within the tumor tissue. In contrast, mice without p53 (e.g. *Wnt-1* p53-/- mice) had very low levels of antibody deposition within the tumor. Six of seven *Wnt-1* p53+/+ tumors had high levels of antibodies, while six of seven *Wnt-1* p53-/- tumors had very low levels of antibodies (44; Figure 2C and Table 2 of Shick et al. accompanying progress report). Moreover, sera from tumor-bearing *Wnt-1* p53+/+ mice recognized multiple antigens in extracts from their own tumors. Sera from tumor-bearing *Wnt-1* p53-/- mice had substantially reduced reactivity with tumor antigens in their own tumors.

(e) telomere length, telomerase, and telomerase RNA

In collaboration with Titia de Lange at the Rockefeller, we were fortunate in being able to examine the contribution of telomerase and telomere degradation to tumor initiation and progression in the *Wnt-1* transgenic p53-deficient model (45). Some models of cancer formation implicate activation of telomerase activity as a critical event in tumor formation, since normal human cells in culture show both low telomerase activity and decreasing telomere size with passaging (48). Immortalized human cells and tumor cells often show increased telomere size and high levels of telomerase. It is postulated that early stage tumors may lose telomere function due to progressive shortening (49). This may lead to activation of DNA damage checkpoints, followed by cell cycle arrest and apoptosis. In tumors that have lost the ability to detect uncapped chromosome ends (e.g. p53-deficient cells), telomere malfunction may lead to genomic instability and accelerated tumor progression (49).

To test these possibilities, we compared telomere length, telomerase RNA, and telomerase activities in the normal mammary glands and mammary adenocarcinomas of the *Wnt-1* transgenic p53-deficient mice (45). Interestingly, mouse telomere length did not greatly vary in length between normal and tumor tissue, irrespective of p53 status, suggesting that decreasing telomere length is not an issue in mouse mammary tumorigenesis. Telomerase RNA was increased in amount in the mammary tumors compared to normal mammary glands, but p53 status had no apparent effect on the telomerase RNA levels. The most dramatic result was the high levels of telomerase activity observed in mammary tumors but not in the normal mammary glands or hyperplastic mammary glands (Table 3). There was a slight effect of p53 status on telomerase activity in the mammary tumors. p53-/- mammary tumors had roughly two fold more telomerase activity than p53+/+ tumors. However, it is unclear whether this slight increase in telomerase activity may have a significant effect on tumor initiation and progression in the p53-/- mice. The most likely conclusion is that loss or absence of p53 has little or no effect on telomere status in mouse mammary tumors.

Table 3. Activation of telomerase in *Wnt-1* mammary tumors in mice with different p53 genotypes

Type of sample	Telomerase activity[a]
p53-/- normal mammary gland	
MG 1-/-	9.3
MG 2-/-	4.5
MG 3-/-	18.3
Median	9.3
p53+/+ mammary tumor	
W2	17
W10	11
W30	36
W134	54
W151	24
Median	24
p53-/- mammary tumor	
W98	100
W121	94
W154	56
W177	14
W184	55
Median	54

[a] Telomerase activity is expressed as relative specific activity normalized to a mouse J558 standard. Average percent activity was determined from two to six assays.

(3) Results in third year of grant

(a) angiogenesis assays in *Wnt-1* transgenic, p53-deficient mice

Recent studies have implicated p53 as a potential regulator of angiogenesis. Thrombospondin-1, an inhibitor of angiogenesis, has been shown to be activated by wild type p53 (50). Thus, loss of p53 may positively affect the ability of tumors to undergo neovascularization. To test this possibility, we performed immunostaining on sections taken from the *Wnt-1*/p53 tumors using an anti Factor VIII antibody. Factor VIII staining is frequently used as a marker for capillaries and vasculature. Thus, by

examining the degree of Factor VIII staining in a tumor section, one can get an idea of the degree of vascularization of that tumor. We were successful in obtaining Factor VIII staining in our tumor samples, but when we attempted to quantitate the degree of staining, we were unable to detect significant differences in tumor capillary density by several methods of quantitation (Fig. 3). Thus, in this particular in vivo context, late stage tumors do not show evidence of p53-dependent differences in angiogenesis. However, this does not rule out the possibility that p53 may have an effect during early stages of tumorigenesis.

Figure 3.

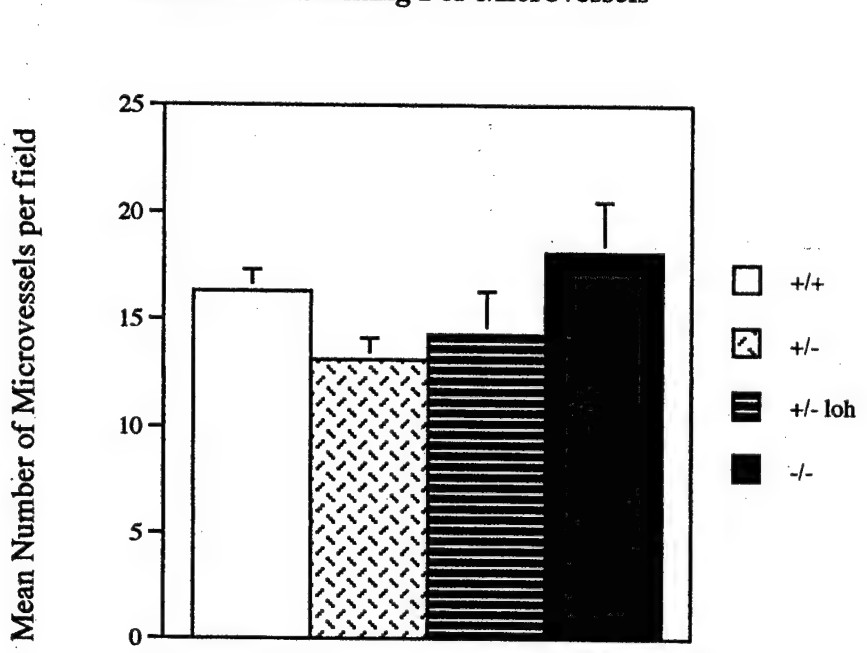

(b) invasiveness and metastasis assays

Evidence from other models suggested that p53 loss could potentially accelerate invasiveness and metastasis. To test this possibility in our Wnt-1/p53 model, we initially tested *Wnt-1*/p53+/+ and *Wnt-1*/p53-/- mammary tumor cells in the Marigel chamber in vitro invasion assay (Becton-Dickinson). Briefly, this assay consists of placing cells on an artificial extracellular matrix overlaying a 8 micron porous membrane. The matrigel matrix serves as a reconstituted basement membrane in vitro. Those cells able to penetrate the matrigel and the porous membrane are considered invasive. Despite many efforts and changing a number of variables with our mammary tumor lines, we were unable to generate any significant numbers of invasive cells regardless of p53 genotype.

To assess metastasis in the *Wnt-1* transgenic model, we have examined the lungs of the tumor bearing mice for metastatic nodules. While metastases are relatively rare in the *Wnt-1* transgenic mouse, when they occur they usually arise in the lungs (H. Varmus, personal communication). So far, in comparing the p53+ and p53- tumors, we have failed to detect any differences in the rate at which the tumor bearing mice display any lung metastases in the presence and absence of p53. Thus, we

have concluded that this model is not a particularly good one for studying the mechanisms of p53 in affecting metastasis.

(c) differential display to identify p53-regulated genes in tumorigenesis

Given the differences in tumor appearance and tumor progression we have observed in our model in the presence and absence of p53, we thought it might be possible to detect p53-dependent differences in gene expression patterns through a differential display approach. Because p53 is a transcriptional regulatory protein which both activates and represses cellular genes, it is possible that at least some genes should show differential expression in the presence and absence of p53. We attempted to identify p53-dependent differences in expression in our p53+ and p53- *Wnt-1* tumors using the differential display approaches originally developed by Liang and Pardee (51,52). Identification of mRNAs expressed only in p53+ tumors or only in p53- tumors could provide insights into the biochemical mechanisms by which p53 loss accelerates tumor growth and progression. In addition, this approach may identify novel p53 target genes. This technique has been well publicized (51,52), so details of the methodology will not be reiterated here.

We have used several variations on this approach in our preliminary experiments, but have recently relied on the Clontech kit (Delta RNA Fingerprinting Kit) which appears to work very well. We have purified mRNA from p53+/+, p53+/- LOH and p53-/- *Wnt-1* mammary tumors (four separate tumors of each genotype) and subjected them to differential display analysis using the 90 different upstream and downstream primer combinations supplied in the kit. We used multiple tumors of each genotype because there is likely to be intertumor variation which is not dependent on p53. Only when we observed consistent differences between p53+ and p53- tumors did we proceed further and isolate the differentially expressed bands. Fragments which showed such p53 specific patterns were isolated from the gel and subjected to a further round of PCR prior to cloning in a vector designed for PCR fragments. We have completed the initial differential display analysis and have isolated 20 fragments which show evidence of consistent differences in the presence and absence of p53. Corroboration of the differential expression patterns has been initiated by Northern blot analysis of the mRNAs from the p53+ and p53- tumors. An example of one probe which has displayed p53-specific genotype differences is shown below in Fig. 4.

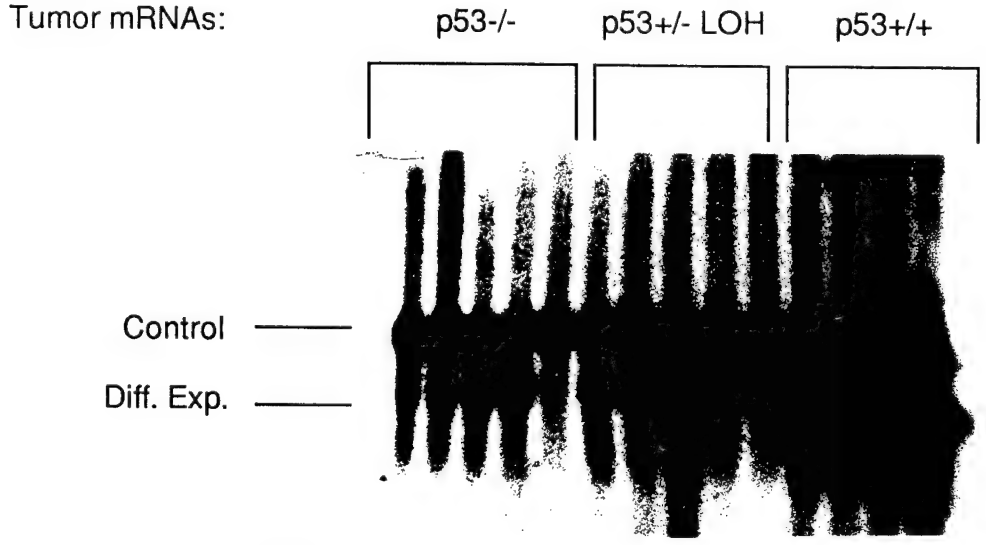

Figure 4.

Note that while all of the p53+/+ tumors demonstrate high levels of expression of this message, only 2 of 5 p53-/- tumors express this message, and at considerably lower levels than p53+/+ tumors. Moreover, the p53+/- LOH tumors also display decreased levels of this message, suggesting that this message is expressed in a partially p53-dependent manner. The upper band represents a control probe for loading which is expressed equally in all genotypes. Once we have identified all of the differentially expressed fragments by Northern blot analysis, the inserts will then be sequenced at the local sequencing core to determine their identity.

(d) tumor incidence and growth in *Wnt-1* transgenic p21-deficient mice

Recently, we have crossed the *Wnt-1* mice to p21 knockout mice obtained from Phil Leder. The *Wnt-1* transgenic female offspring of all three p21 genotypes have been examined for mammary tumor incidence and tumor growth rates. We found that while p21 status (p21+/+, p21+/-, or p21-/-) had little discernable effect on when the *Wnt-1* initiated mammary tumors arose, the growth rates of the tumors did show p21-dependent differences. p21+/+ tumors showed the similar slow growth observed in p53+/+ *Wnt-1* transgenic mice. However, the *Wnt-1*/p21+/- tumors showed dramatically higher growth rates than p21+/+ tumors, similar to the growth rates previously observed for *Wnt-1*/p53-/- tumors (Fig. 5).

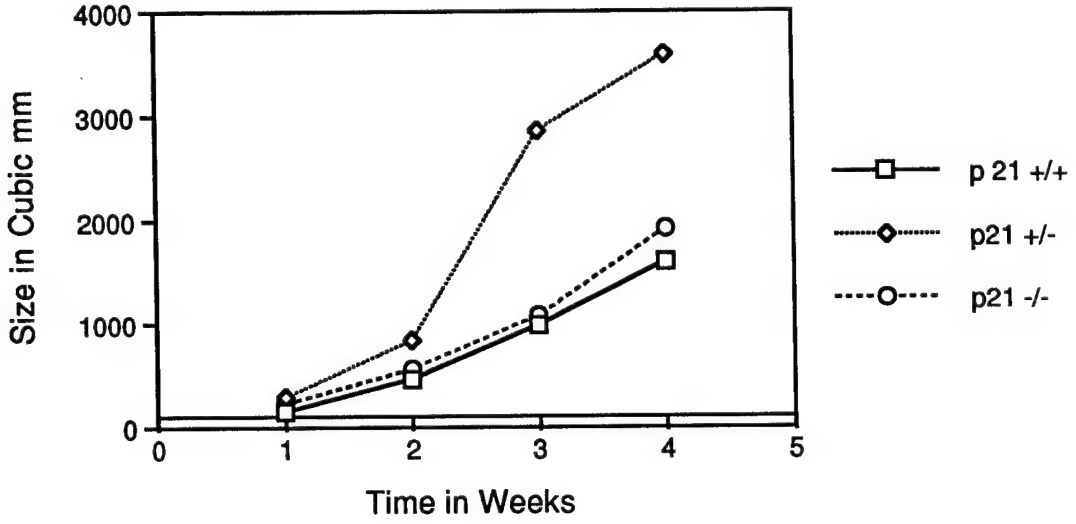

Figure 5.

Interestingly, the *Wnt-1*/p21-/- tumors showed growth rates equivalent to the *Wnt-1*/p21+/+ tumors. These growth rate differences were confirmed by mitotic index assays and BrdU incorporation assays which demonstrated significantly higher fractions of p21+/- tumor cells in mitosis and S phase compared to p21+/+ and p21-/- tumor cells. Figure 6 on the next page shows the relative mitotic index for the *Wnt-1* transgenic tumors of all three p21 genotypes. While the differences in mitotic index are not as dramatic as in the tumor growth curves, they are significant by t-test.

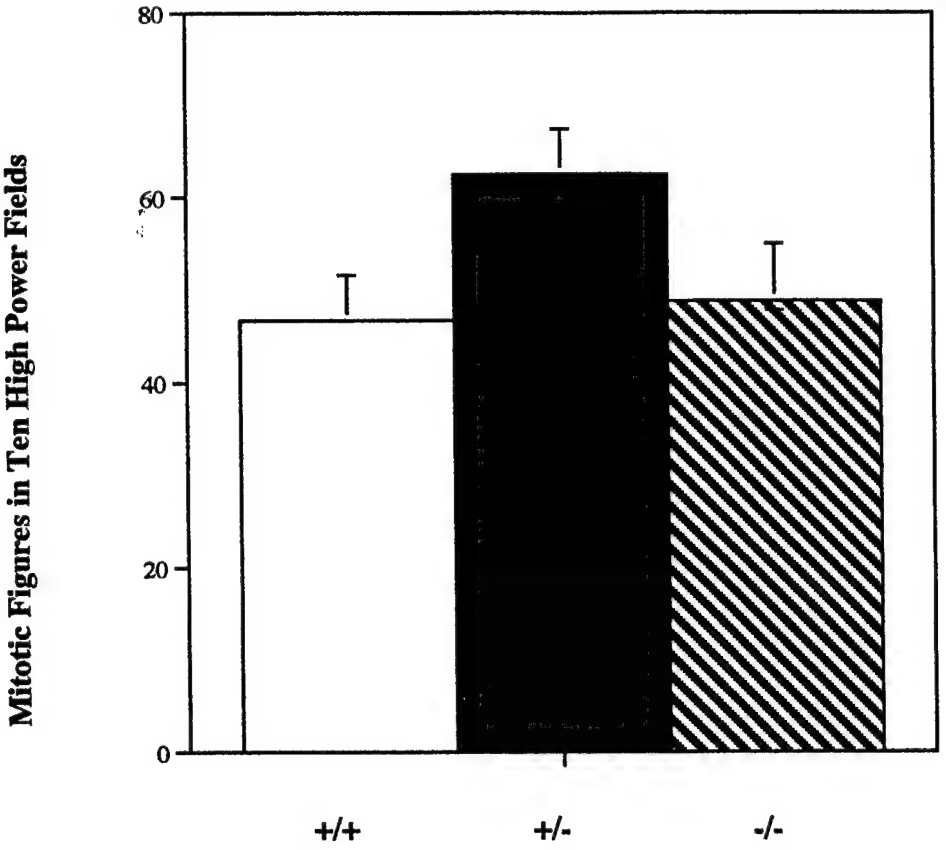

Figure 6.

Note again that the p21+/- tumors appear to have the highest mitotic rates. No differences in apoptosis rates were observed among the tumor types, indicating that the growth rate differences were driven by proliferation rather than cell death. These results were a bit surprising since it was expected that absence of p21 altogether might have an accelerated effect on tumor growth as well. However, the recent paper by LaBaer et al. (37) provides a potential explanation. High levels of p21 inhibit the kinase activity of cyclin/cdk complexes, while the absence of p21 is important in assembly of the cyclin/cdk complexes. However, low to intermediate levels of p21 appear to be sufficient to allow assembly of the cyclin/cdk complexes without being inhibitory to kinase activity of the complex. The apparent result is enhanced cell cycle progression in the presence of reduced p21 (as is observed for the p21+/- tumors).

(e) p21 protein assays

To further understand the mechanisms by which a reduced level of p21 accelerates tumor growth rates while absence of p21 has little or no effect on tumor growth, we have initiated assays to directly examine p21 protein levels in the p21/Wnt-1 tumors. Initially, we have performed western blots on tumor lysates from p21+/+, p21+/-, and p21-/- Wnt-1 transgenic tumors. However, with a series of commercially available antibodies to p21, we have failed to consistently detect p21 in our lysates (including positive controls). Recently, we have obtained a polyclonal antibody to mouse p21 from Wafik El-Deiry and preliminary indications are that this antibody works quite well. We will continue to use this in Westerns to determine whether reduction in p21 protein is associated with increased tumor growth rates and then we will attempt to determine the association of p21 with the cyclin/cdk complexes and the kinase activity of these complexes.

CONCLUSIONS

The data presented in this report argue that p53 loss or absence may contribute to tumorigenesis by a variety of different mechanisms. Tumors without p53 appear to grow and progress faster than tumors which contain p53. Surprisingly, while other mouse tumor models have demonstrated that loss of p53 is accompanied by attenuated apoptosis (16-18), we have shown in our model that apoptosis is likely to have little or no role in tumor progression. The reasons for the apoptotic independence in our model are unclear but it may have to do with the growth factor environment of the nascent tumor cells. *In vitro* assays often show that apoptosis can only be induced in the absence of certain growth factors. The nascent *Wnt-1*-initiated tumor cell may be bathed in Wnt-1 growth factor and this may prevent any apoptotic pathways from being activated. However, this apoptotic independence makes our model particularly useful in teasing out other p53-dependent mechanisms which may influence tumor progression.

In the first two years of this grant we have attempted to identify some of these alternative mechanisms. Among these are increased genomic instability in the absence of p53 and increased proliferative capacity. Interestingly, while the tumors with the most genomic instability, the p53+/- (LOH) tumors, have the highest proliferative rates, they do not arise any sooner than p53+/+ tumors. This suggests that genomic instability plays a role in tumor progression but not tumor initiation. In addition, tumor cells missing or losing p53 appear to have a higher percentage of cells in S phase, suggesting that p53 may play a direct role in decreasing tumor growth rate through its growth arrest function (through checkpoint inhibition of progression through G1 and G2 or through direct inhibition of DNA replication).

We also examined the effects of p53 loss on telomere function in the presence and absence of p53 in our mammary tumor model. Telomeres themselves appear to maintain their structure during tumor progression, though telomerase activity is greatly increased. However, this telomerase increase appears to be mostly p53-independent, arguing against a role for p53 in this particular aspect of the tumorigenesis process.

Through serendipity, we discovered that *Wnt-1* mice lacking p53 have greatly reduced amounts of heavy and light chain antibodies deposited in their tumors than *Wnt-1* mice with intact p53. The *Wnt-1* p53-/- mice also seem to be less able to mount an immune response to tumor antigens that *Wnt-1* p53+/+ mice are quite capable of recognizing. Such results argue that immune surveillance of nascent tumors in mice lacking p53 may be deficient and this may be part of the reason for the accelerated tumor incidence in *Wnt-1* p53-/- mice (see Figure 1).

In the third year of the grant we have extended our work on the *Wnt-1*/p53 model and have attempted to detect a p53-dependent effect on angiogenesis in the mammary tumors. However, we have failed to detect significant differences in the degree of vascularization of p53+ and p53- tumors, suggesting either that p53 does not affect angiogenesis in this model or that it does have a rate limiting effect, but only

in the early stages of tumor initiation and formation. If so, then it would be difficult for us to discern this early effect by looking at end stage tumors.

Since the p53-dependent effects on tumor progression in our model are primarily related to cell proliferation, we decided to explore this mechanistically by investigating the role of p21 in this process. Since p21 is induced by p53 and retards cell cycle progression through binding cyclin/cdk complexes, it is a natural candidate for investigation of p53 dependent mechanisms of tumor cell proliferation. When we crossed the p21 knockout mice to the *Wnt-1* transgenic mice, we found that the *Wnt-1* transgenic females developed tumors at about the same incidence regardless of p21 status. However, only the p21+/- *Wnt-1* females exhibited fast growing tumors. This dosage effect of reduced p21 is consistent with the stoichiometric model proposed by Harlow and colleagues (37) in which high levels of p21 (e.g. in p21+/+ tumors) inhibit the kinase activity of the cyclin/cdk complex, but that low levels (e.g. in p21+/- tumors) can stimulate the complex activity. Moreover, since p21 appears actually to be an important assembly factor for some cyclin/cdk complexes, its complete absence (e.g. in p21-/- tumors) may actually be inhibitory for cell cycle progression. We hope to investigate this model further in the final year of the grant by examining p21 protein and its effects on the cyclin/cdk complexes in the tumor cells.

In summary, in the first three years of this grant, we have attempted to more fully answer mechanistic questions about the role of p53 loss in mammary tumor progression in our *Wnt-1* p53 model. We have shown that increased genomic instability and increased cell proliferation rates (independent of apoptosis) accompany loss of p53. Through collaborative efforts we have also examined telomere status and immune function in our model. The roles of angiogenesis and p21 in the tumorigenesis process have also been explored in the last year. In the next year, we hope to identify other mechanisms, further understand the role of p21 in the tumor progression process, and identify particular genes (through differential display) which may mediate these important mechanisms. We do believe that the results achieved so far validate the *Wnt-1* transgenic p53-deficient mouse as a highly useful model for these types of studies.

Efforts to Fulfill the Statement of Work:

AIM 1: FURTHER CHARACTERIZATION OF TUMORIGENESIS IN THE p53/*Wnt-1* MICE

MONTHS 25-36:
COMPLETION OF TUMOR BIOLOGY STUDIES OF p53/Wnt-1 MICE
1. TUMOR GROWTH RATES - Completed
2. TUMOR CELL APOPTOTIC RATES - Completed
3. IN VIVO TUMOR CELL PROLIFERATION RATES - Completed
4. IN VITRO TUMOR CELL PROLIFERATION RATES - Completed

MONTHS 25-48:
COMPLETION OF TUMOR BIOLOGY STUDIES OF p53/Wnt-1 MICE
1. INVASIVENESS AND METASTASIS ASSAYS -Completed
2. TUMOR ANGIOGENESIS ASSAYS - Completed

Aim 1 Comments:

This specific aim has been completed and the results have been published in the Cell Growth & Differentiation paper (see appendix). The invasiveness/metastasis assays and angiogenesis assays have been largely negative in showing any difference between p53+ and p53- tumors and thus these approaches have not been pursued further.

AIM 2: FURTHER BIOLOGICAL STUDIES OF CO-FACTORS WHICH INFLUENCE TUMORIGENESIS IN p53/Wnt-1 MICE

MONTHS 25-48:
CHARACTERIZATION OF RNA EXPRESSION PATTERNS OF KNOWN GENES WHICH MAY INFLUENCE TUMORIGENESIS IN THE PRESENCE AND ABSENCE OF p53
1. p21 - In progress
2. Bax - Not yet performed
3. Bcl-2 - Not yet performed
4. Histone H4 - In progress
5. Cyclin D1 - Not yet performed
6. bFGF - Not yet performed
7. VEGF - In progress
8. Thrombospondin-1 - In progress

Aim 2 comments:

So far, we have placed most of our efforts in studying the role of p21 in affecting tumor progression through the p21-*Wnt-1* crosses and western blot assays. We have initiated RNAse protection assays for VEGF and thrombospondin-1 mRNA expression, but the technical aspects of RNAse protection are still being worked out. Since apoptosis has not really been affected by the presence or absence of p53 in this model, we have placed less priority in studying Bax and Bcl-2.

AIM 3: IDENTIFICATION OF OTHER ONCOGENE AND TUMOR SUPPRESSOR GENE LOCI ASSOCIATED WITH MAMMARY TUMORIGENESIS

MONTHS 25-48:
DIFFERENTIAL DISPLAY TO IDENTIFY NOVEL GENES DIFFERENTIALLY EXPRESSED IN THE PRESENCE AND ABSENCE OF p53
In Progress

MONTHS 37-48:
ISOLATION AND CHARACTERIZATION OF DIFFERENTIALLY EXPRESSED GENES
In Progress

Aim 3 Comments:

We have made good progress on this specific aim, having screened 90 primer pairs in the differential display procedures and identifying 20 differentially expressed candidate fragments. Initial screening of several candidate fragments by Northern blot analysis has revealed at least one bona fide differentially expressed gene (see Fig. 4).

References

1. Greenblatt MS, Bennett W, Hollstein M, Harris CC (1994) Mutations in the p53 tumor suppressor gene: clues to cancer etiology and molecular pathogenesis. Cancer Research 54:4855-4878

2. Moll U, Giou G, Levine A (1992) Two distinct mechanisms alter p53 in breast cancer: Mutation and nuclear exclusion. Proc Natl Acad Sci USA 89:7262-7266

3. Malkin D, Li FP, Strong LC, Fraumeni JF, Nelson CE, Kim DH, Kassell J, Gryka MA, Bischoff FZ, Tainsky MA, Friend SH (1990) Germ line p53 mutations in a familial syndrome of breast cancer, sarcomas, and other neoplasms. Science 250:1233-1238

4. Srivastava S, Zou Z, Pirollo K, Blattner W, Chang EH (1990) Germ-line transmission of a mutated p53 gene in a cancer-prone family with Li-Fraumeni syndrome. Nature 348:747-749

5. Malkin D (1994) Germline p53 mutations and heritable cancer. Annu. Rev. Genet. 28:443-465

6. Kastan MB, Canman CE, Leonard CJ (1995) p53, cell cycle control and apoptosis. Cancer and Metastasis Rev 14:3-15

7. Bates S, Vousden KH (1996) p53 in signaling checkpoint arrest or apoptosis. Curr Opin Genet & Develop 6:12-19

8. Ko LJ, Prives C (1996) p53: puzzle and paradigm. Genes & Develop 10:1054-1072

9. Lane DP (1992) p53, guardian of the genome. Nature 358:15-16

10. Gottlieb TM, Oren M (1996) p53 in growth control and neoplasia. BBA Rev Cancer 1287:77-102

11. Harper JW, Elledge SJ, Keyomarsi K *et al* (1995) Inhibition of cyclin-dependent kinases by p21CIP1/WAF1 Molecular Biology of the Cell 6 387-400

12. El-Deiry WS, Tokino T, Velculescu VE *et al* (1993) WAF1, a potential mediator of p53 tumor suppression. Cell 76 817-825

13. Sabbatini P, Lin J, Levine AJ, White E (1995) Essential role for p53-mediated transcription in E1A-induced apoptosis. Genes & Develop 9:2184-2192

14. Caelles C, Helmberg A, Karin M (1994) p53-dependent apoptosis in the absence of transcriptional activation of p53-target genes. Nature 370:220-223

15. Haupt Y, Rowan S, Shaulian E, Vousden KH, Oren M (1995) Induction of apoptosis in HeLa cells by trans-activation deficient p53. Genes & Development 9:2170-2183

16. Pan HC, Griep AE (1994) Altered cell cycle regulation in the lens of HPV-16 E6 or E7 transgenic mice - implications for tumor suppressor gene function in development Genes & Dev 8:1285-1299

17. Howes KA, Ransom N, Papermaster DS, Lasudry JGH, Albert, DM, Windle JJ (1994) Apoptosis or retinoblastoma - alternative fates of photoreceptors expressing the HPV-16 E7 gene in the presence or absence of p53 Genes & Dev 8:1300-1310

18. Symonds H, Krail L, Remington L, Saenz-Robles M, Lowe S, Jacks T, Van Dyke T (1994) p53-dependent apoptosis suppresses tumor growth and progression in vivo. Cell 78:703-711

19. Hermeking H and Eick D (1994) Mediation of c-myc-induced apoptosis by p53. Science 265:2091-2093

20. Lowe SW, Jacks T, Housman DE, Ruley HE (1994) Abrogation of oncogene-associated apoptosis allows transformation of p53-deficient cells. Proc Natl Acad Sci USA 91:2026-2030

21. Donehower LA (1996) Effects of p53 mutation on tumor progression: recent insights from mouse tumor models. BBA Rev Cancer 1242:171-176

22. Donehower LA, Harvey M, Slagle BL, McArthur MJ, Montgomery, CA Jr, Butel JS, Bradley A (1992) Mice deficient for p53 are developmentally normal but susceptible to spontaneous tumours. Nature 356:215-221

23. Harvey M, McArthur MJ, Montgomery CA, Butel JS, Bradley A, Donehower LA (1993) Spontaneous and carcinogen-induced tumorigenesis in p53-deficient mice. Nature Genet 5:225-229

24. Donehower LA, Harvey M, Vogel H, McArthur MJ, Montgomery CA Jr, Park SH, Thompson T, Ford RJ and Bradley A (1995) Effects of genetic background on tumorigenesis in p53-deficient mice. Mol Carcinog 14:16-22

25. Donehower LA, Godley LA, Aldaz CM, Pyle R, Shi Y-P, Pinkel D, Gray J, Bradley A, Medina D, Varmus HE (1995) Deficiency of p53 accelerates mammary tumorigenesis in *Wnt-1* transgenic mice and promotes chromosomal instability. Genes & Dev 9:882-895.

26. Tsukamoto AS, Grosschedl R, Guman RC, Parslow T, Varmus HE (1988) Expression of the *int-1* gene in transgenic mice is associated with mammary gland hyperplasia and adenocarcinomas in male and female mice. Cell 55:619-625.

27. Gu Y, Turck CW, Morgan DO. (1993) Inhibition of CDK2 activity in vivo by an associated 20K regulatory subunit. Nature 366:707-710.

28. Noda A, Ning Y, Venable SF, Pereira-Smith OM, Smith JR. (1994). Cloning of senescent cell-derived inhibitors of DNA synthesis using an expression screen. Exp. Cell Res. 211:90-98.

29. Xiong Y, Hannon GJ, Zhang H, Casso D, Kobayashi R, Beach, D. (1993). p21 is a universal inhibitor of cyclin kinases. Nature 366:701-704.

30. Harper JW, Elledge SJ, Keyomarsi K, Dynlacht B, Tsai L-H, Zhang P, Dobrowolski S, Bai C, Connell-Crowley L, Swindell E, Fox MP, Wei N. (1995). Inhibition of cyclin-dependent kinases by p21. Mol. Biol. Cell 6:387-400.

31. Macleod KF, Sherry N, Hannon G, Beach D, Tokino T, Kinzler K, Vogelstein B, Jacks T. (1995). p53-dependent and independent expression of p21 during cell growth, differentiation, and DNA damage. Genes & Dev. 9:935-944.

32. Parker SB, Eichele G, Zhang P, Rawls A, Sands AT, Bradley A, Olson EN, Harper JW, Elledge SJ. (1995). p53-independent expression of p21Cip1 in muscle and other terminally differentiating cells. Science 267:1024-1027.

33. Flores-Rozas H, Kelman Z, Dean FB, Pan Z, Harper JW, Elledge SJ, O'Donnell M, Hurwitz J (1994). Cdk-interacting protein-1 (Cip1, WAF1) directly binds with proliferating cell nuclear antigen and inhibits DNA replication catalyzed by the DNA polymerase holoenzyme. Proc. Natl. Acad. Sci USA 91:8655-8659.

34. Waga S, Hannon GJ, Beach D, Stillman B (1994). The p21 inhibitor of cyclin-dependent kinases controls DNA replication by interacting with PCNA. Nature 369:574-578.

35. Deng C, Zhang P, Harper JW, Elledge SJ, Leder P. (1995). Mice lacking $p21^{CIP1/WAF1}$ undergo normal development, but are defective in G1 checkpoint control. Cell 82:675-684.

36. Brugarolas J, Chandrasekaran C, Gordon JI, Beach D, Jacks T, Hannon, G.J. (1995). Radiation-induced cell cycle arrest compromised by p21 deficiency. Nature 377:552-556.

37. LaBaer J, Garrett MD, Stevenson LF, Slingerland JM, Sandhu C, Chou HS, Fattaey A, Harlow E. (1997). Genes & Dev. 11:847-862.

38. Harvey M, McArthur MJ, Montgomery CA, Bradley A, Donehower LA (1993) Genetic background alters the spectrum of tumors that develop in p53-deficient mice. FASEB J 7:938-943

39. Reed KC, Mann DA (1985) Rapid transfer of DNA from agarose gels to nylon membranes. Nucleic Acids Res 13:7207-7221

40. Kittrell FS, Oborn CJ, Medina D (1992) Development of mammary preneoplasias *in vivo* from mouse mammary epithelial cell lines *in vitro* . Cancer Res 52:1924-1932

41. Hedley DW, Friedlander ML, Taylor IW, Rugg CA, Musgrove EA (1993) Method of analysis of cellular DNA content of paraffin-embedded pathological material using flow cytometry. J Histochem Cytochem 21:1333-1335.

42. Vindelov LL, Christensen IJ, Nissen NI (1993) A detergent-trypsin method for the preparation of nuclei for flow cytometric DNA analysis. Cytometry 3:323-327

43. El-Deiry WS, Harper JW, O'Connor PM, Velculescu VE, Canman CE, Jackman J, Pietenpol JA, Burrell M, Hill DE, Wang Y, Wiman KG, Mercer WE, Kastan MB, Kohn KW, Elledge SJ, Kinzler KW, Vogelstein B (1994) WAF1/CIP1 is induced in p53-mediated arrest and apoptosis. Cancer Res 54:1169-1174

44. Shick L, Carman JH, Choi JK, Somasundarum K, Burrell M, Hill DE, Zeng Y-X, Wang Y, Wiman KG, Salhany K, Kadesch TR, Monroe JG, Donehower LA, and El-Deiry WS (1997). Decreased immunoglobulin deposition in tumors and increased immature B cells in p53-null mice. Cell Growth & Different. 8, 121-131

45. Broccoli D, Godley LA, Donehower LA, Varmus HE, de Lange T (1996) Telomerase activation in mouse mammary tumors: lack of detectable telomere shortening and evidence for regulation of telomerase RNA with cell proliferation. Mol Cell Biol 16:3765-3772

46. Harvey M, Sands AT, Weiss RS, Hegi M, Wiseman RW, Panayotis P, Biovanella BC, Tainsky MA, Bradley A, Donehower LA (1993) In vitro growth characteristics of embryo fibroblasts isolated from p53-deficient mice. Oncogene 8:2457-2467

47. Jones JM, Attardi L, Godley LA, Laucirica R, Medina D, Jacks T, Varmus HE, Donehower LA (1997) Absence of p53 in a mouse mammary tumor model promotes tumor cell proliferation without affecting apoptosis. Cell Growth & Different. 8:829-838

48. de Lange T (1995) Telomere dynamics and genome instability in human cancer In Blackburn EH and Greider CW (eds). *Telomeres*, pp. 265-293, Cold Spring Harbor Laboratory Press, Cold Spring Harbor, New York

49. Harley CB, Kim NW, Prowse KR *et al* (1994) Telomerase, cell immortality, and cancer *Cold Spring Harbor Symposia on Quantitative Biology* **59** 307-315

50. Dameron KM, Volpert OV, Tainsky MA, Bouck N. (1994) Control of angiogenesis in fibroblasts by p53 regulation of thrombospondin-1. Science 265, 1582-1584.

Appendix:

Two reprints published in the last year which describe some of the work outlined above are appended here:

Jones JM, Attardi L, Godley LA, Laucirica R, Medina D, Jacks T, Varmus HE, Donehower LA (1997) Absence of p53 in a mouse mammary tumor model promotes tumor cell proliferation without affecting apoptosis. Cell Growth & Different. 8:829-838

Shick L, Carman JH, Choi JK, Somasundarum K, Burrell M, Hill DE, Zeng Y-X, Wang Y, Wiman KG, Salhany K, Kadesch TR, Monroe JG, Donehower LA, and El-Deiry WS (1997). Decreased immunoglobulin deposition in tumors and increased immature B cells in p53-null mice. Cell Growth & Different. 8, 121-131.

In addition to the above two reprints, I have included our original *Genes & Development* paper which describes the *Wnt-1*/p53 model in more detail and provides the foundation for the subsequent work reported here:

Donehower LA, Godley LA, Aldaz CM, Pyle R, Shi Y-P, Pinkel D, Gray J, Bradley A, Medina D, Varmus HE (1995) Deficiency of p53 accelerates mammary tumorigenesis in *Wnt-1* transgenic mice and promotes chromosomal instability. Genes & Dev 9:882-895.

Absence of p53 in a Mouse Mammary Tumor Model Promotes Tumor Cell Proliferation without Affecting Apoptosis[1]

Jeffrey M. Jones, Laura Attardi, Lucy A. Godley, Rodolfo Laucirica, Daniel Medina, Tyler Jacks, Harold E. Varmus, and Lawrence A. Donehower[2]

Program in Cell and Molecular Biology [J. M. J.], Division of Molecular Virology [J. M. J., L. A. D.], Department of Pathology and The Methodist Hospital [R. L.], Department of Cell Biology [D. M.], Baylor College of Medicine, Houston, Texas 77030; Center for Cancer Research, Massachusetts Institute for Technology and Howard Hughes Medical Institute, Cambridge, Massachusetts 02139 [L. A., T. J.]; and National Cancer Institute, NIH, Bethesda, Maryland 20892 [L. A. G., H. E. V.]

Abstract

Loss or mutation of p53 may have multiple biological and genetic effects that result in accelerated tumor progression. Loss of p53 in some tumors has been correlated with a marked decrease in tumor cell apoptosis. p53 loss may also accelerate tumor growth through an increase in cell proliferation rates. To examine the effects of p53 loss on tumor progression in a controlled experimental context, we previously crossed p53-deficient mice to mammary tumor-susceptible *Wnt-1* transgenic (*TG*) mice. The resulting female *Wnt-1 TG* offspring of this cross all developed mammary tumors, regardless of p53 status (p53+/+, p53+/−, or p53−/−). However, female p53−/− *Wnt-1 TG* mice developed tumors much sooner than their p53+/+ counterparts. In this report, we demonstrate that the average growth rates of tumors missing (p53−/−) or losing p53 (p53+/− with loss of heterozygosity) are accelerated compared to tumors with both wild-type *p53* alleles (p53+/+). This accelerated growth rate appears to be due primarily to increases in rates of tumor cell proliferation. Tumor cell apoptotic levels were modest and were not measurably different in the presence or absence of wild-type p53. These results differ substantially from other mouse tumor models in which p53 loss was closely correlated with accelerated growth rates through attenuated apoptosis. Thus, the mechanisms by which p53 loss influences tumor progression may differ, depending on the tissue type and/or the oncogenic pathways involved.

Received 4/30/97; revised 5/30/97; accepted 5/30/97.
The costs of publication of this article were defrayed in part by the payment of page charges. This article must therefore be hereby marked *advertisement* in accordance with 18 U.S.C. Section 1734 solely to indicate this fact.
[1] This work was funded by grants from the United States Army Breast Cancer Program and National Cancer Institute (to L. A. D.).
[2] To whom requests for reprints should be addressed, at Division of Molecular Virology, Baylor College of Medicine, One Baylor Plaza, Houston, TX 77030. E-mail: larryd@bcm.tmc.edu.

Introduction

The importance of *p53* as a tumor suppressor gene is indicated by its being lost or mutated in almost one-half of all human cancers (1). Human breast cancers have been found to have mutated *p53* alleles in 28% of all cases (2). With respect to the role of p53 dysfunction in breast tumors, this number may be an underestimate, because it does not include tumors found to contain p53 protein rendered nonfunctional through cytoplasmic sequestration (3, 4) or by binding to the overexpressed oncogenic protein Mdm2 (5–7).

p53 is a cell cycle checkpoint protein that regulates progression through G_1 (8, 9) and G_2-M (10–12) phases of the cell cycle. p53 levels are greatly increased in cells following treatment by a variety of DNA-damaging agents, particularly those that introduce DNA strand breaks (8, 9, 13). Up-regulated p53 can induce either cell cycle arrest in late G_1 (8, 9, 13, 14) or apoptosis (15–17). The decision to enter apoptosis rather than arrest in G_1 may be influenced by a number of endogenous and exogenous factors including cell type (18), p53 levels (19), and environmental growth factor concentrations (14, 20). Wild-type p53 is a potent inducer of apoptosis in tumor cells following treatment with ionizing radiation or anticancer agents (21). Moreover, wild-type p53 may inhibit tumor growth and progression by inducing apoptosis when cells are rapidly dividing following altered expression of an oncogene or tumor suppressor gene (22–25).

Multiple groups have shown in mouse tumor models that loss of wild-type p53 converts a tissue or slow-growing tumor with high levels of apoptotic cells to a rapidly growing tumor with minimal numbers of cells undergoing apoptosis (26–28). For example, Symonds *et al.* (26) have demonstrated that transgenic mice that express high levels of a truncated large T antigen (which inactivates Rb protein but not p53) in the choroid plexus develop slowly growing choroid plexus tumors with high levels of apoptosis. When these mice are crossed to p53-deficient mice, the progeny with the T antigen transgene, but missing p53 (p53−/−), develop rapidly growing choroid plexus tumors with a low apoptotic index. This indicates that p53-induced apoptosis may be the primary mechanism governing the slow growth rate of these tumors.

Loss or mutation of p53 in human tumors has been correlated with increased aggressiveness and poor prognosis (2, 29, 30). Although this increased aggressiveness may be due in part to attenuated apoptosis, loss of p53 may affect tumor progression by additional mechanisms. One possible effect of p53 loss is an increase in genomic instability. Cell culture studies have documented that loss of p53 is closely associated with chromosomal instability (31–34). If loss of p53 in a tumor cell confers genomic instability, then the rate of appearance of further oncogenic lesions is likely to be increased. Some of these oncogenic lesions could result in a

significant growth advantage and accelerate tumor progression. There appears to be a high degree of correlation between p53 mutation and increased chromosomal instability in a variety of human tumor types (35–38).

Another result of p53 loss in a tumor might be an increase in the rate of cell proliferation due to a higher percentage of tumor cells entering and progressing through the cell cycle. Wild-type p53 is known to activate expression of the $p21^{WAF1/CIP1}$ cyclin-dependent kinase inhibitor (39), a protein important in mediating G_1 arrest (40). Loss of p53 may prevent activation of p21 and other cell cycle inhibitors and allow a higher fraction of cells to traverse G_1 and enter S phase. In support of this, we have shown that early passage mouse fibroblasts from p53−/− embryos proliferate more rapidly and have a higher percentage of cells in S phase and mitosis than p53+/+ fibroblasts cultured under identical conditions (34). Human tumors with overexpressed mutant p53 also tend to express markers that suggest a higher rate of proliferation than tumors with intact p53 (41–44).

To examine the effects of p53 presence or absence on tumor progression in a controlled experimental breast cancer model, we have used the offspring of mammary tumor-susceptible *Wnt-1 TG*[3] mice crossed to p53-deficient mice. The *Wnt-1 TG* mice contain multiple copies of the *Wnt-1* oncogene expressed ectopically at high levels in the mammary gland (45). The p53-deficient mice, generated by gene targeting in embryonic stem cells, contain one (p53+/−) or two (p53−/−) disrupted germ-line *p53* alleles and are susceptible to a wide array of tumor types (46). By crossing the p53-deficient mice to the *Wnt-1 TG* mice, we were able to obtain a tumor model with distinct advantages: (*a*) *Wnt-1 TG* females all develop the same type of mammary tumor (type B adenocarcinoma), regardless of p53 status (p53+/+, p53+/−, or p53−/−); (*b*) the mice all develop tumors within a relatively short amount of time (2–9 months after birth); (*c*) mammary tumorigenesis can be monitored both in the presence and absence of p53 (the p53+/+ *Wnt-1 TG* females serve as controls to monitor p53-independent mechanisms of tumorigenesis); and (*d*) the mammary tumors are s.c. and therefore, can be detected early and measured easily for rates of growth (47).

In an earlier study of *Wnt-1 TG* p53-deficient mice (47), we showed that in the absence of p53, *Wnt-1* females all developed mammary tumors by 15 weeks of age, whereas p53+/+ and p53+/− *Wnt-1* females had longer survival rates and did not all develop tumors until 42 weeks of age. We also found that mammary tumors from p53−/− mice and from p53+/− mice that lost their remaining wild-type allele (LOH) had significantly higher rates of chromosomal instability than p53+/+ tumors. In the earlier study, we focused on tumor initiation (*i.e.,* when the tumors first appeared). In this study, we have attempted to address the issue of tumor growth after initial formation. Does the presence or absence of p53 influence tumor growth rates, and if so, what are the biological mechanisms for the differential growth? Here, we provide evidence that the loss of p53 does accelerate tumor growth rates during mammary tumorigenesis. However, the increased growth rate appears to be due largely to increased cell proliferation rather than to reduced rates of tumor cell apoptosis. This result contrasts with some of the other mouse tumor models (26–28) and indicates that p53 loss may promote tumor progression by multiple biological mechanisms.

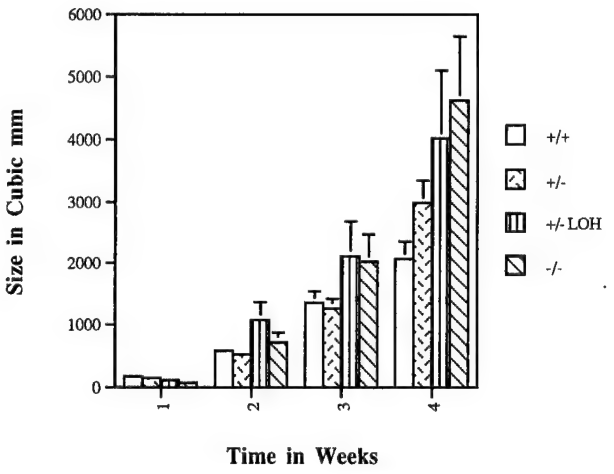

Fig. 1. Growth rates of mammary tumors arising in *Wnt-1 TG* p53-deficient female mice. Tumor size was measured once per week, and the tumor volume was determined as described by Miller *et al.* (48). Time zero is the first date at which the tumor was observed and measured. Four p53 genotypes are represented: p53+/+, $n = 17$; p53+/−, $n = 13$; p53+/− LOH, $n = 10$; p53−/−, $n = 10$. *Bars,* SE for each genotype.

Results

Loss of p53 Promotes Accelerated Mammary Tumor Growth Rates. To directly assess tumor growth rate, we monitored *Wnt-1 TG* females of all three p53 genotypes for the appearance of mammary tumors by palpation and visual examination. When a small tumor was noted, its diameter was measured in two dimensions with calipers and then measured weekly for another 3 weeks. Tumor volumes were then calculated from these measurements as has been described by Miller *et al.* (48). The tumor-bearing animals were then sacrificed, and part of the tumor was analyzed for histopathology. High molecular weight DNA was prepared from p53+/− tumors, and the status of the remaining wild-type *p53* allele was assessed by Southern blot hybridization as described previously (46). Roughly one-half of the *Wnt-1TG* p53+/− tumors delete the remaining wild-type *p53* allele, and the rest retain it. We have shown previously that in those tumors that retain the wild-type allele, the *p53* gene remains wild type in sequence (47). A compilation of the tumor growth data for each of the p53 genotypes is shown in Fig. 1. Note that after 4 weeks of growth, the p53−/− tumors displayed significantly higher tumor volumes than p53+/+ tumors ($P = 0.04$ as measured by t test). p53+/− tumors with LOH also had significantly higher tumor volumes at 4 weeks than p53+/+ tumors ($P = 0.02$). p53+/− tumors

[3] The abbreviations used are: TG, transgenic; LOH, loss of heterozygosity; TUNEL, terminal deoxynucleotidyl transferase-mediated nick end labeling; MMTV, mouse mammary tumor virus.

without LOH showed on average marginally increased growth rate compared to p53+/+ tumors, but this difference was not significant by *t* test.

Apoptosis Levels Are Low and Independent of p53 Status. The measurements of the mammary tumors revealed that the loss or absence of p53 significantly enhanced tumor growth rates. One potential mechanism for this enhanced tumor growth could be a result of a reduction in apoptotic cell fraction as seen in other mouse tumor models missing p53 (26, 27). A net growth advantage would result if fewer tumor cells die in the p53-deficient tumors compared to the tumors with wild-type p53. To address this possibility, we examined formalin-fixed mammary tumor sections by the TUNEL apoptosis assay. Fig. 2, *A* and *B*, shows examples of this staining in a p53+/+ tumor (Fig. 2*A*) and a p53−/− tumor (Fig. 2*B*). The results of the TUNEL assays are represented by the graph in Fig. 2*C*. There does not appear to be any correlation between the p53 status of a tumor and the degree of apoptosis observed. Apoptotic cells appeared to be randomly distributed throughout the tumor sections.

We also performed the TUNEL assay on hyperplastic mammary gland tissue from the p53−/−, p53+/−, and p53+/+ *Wnt-1* females. Normal mammary glands were not available, because the *Wnt-1* transgene induces a very early hyperplasia throughout each of the mammary glands (45). It is possible that in hyperplastic tissue, wild-type p53 might delay tumor formation through increased apoptosis of abnormally proliferating mammary gland cells. This could explain the delay in onset of mammary tumors in p53+/+ and p53+/− *Wnt-1* mice compared to p53−/− *Wnt-1* mice. However, results of the TUNEL assays revealed that apoptosis in *Wnt-1 TG* female mammary glands was very low (on average, below 0.5% of total cells) and not appreciably different among p53−/−, p53+/−, and p53+/+ hyperplastic tissues (Fig. 3). These results suggest that differences in apoptotic rates in the presence and absence of p53 are not a major factor either in the initiation or progression of the mammary tumors.

To confirm the results of the TUNEL assay, we also examined the total tumor DNA for apoptotic DNA fractions using a DNA laddering assay. DNA from cells undergoing apoptosis forms a ladder of bands that are rough multiples of 170 bp (49). Using this assay, we were again able to show that the apoptotic DNA fraction in *Wnt-1* mammary tumors of all three *p53* genotypes was relatively low and did not differ appreciably according to p53 status (Fig. 4). The apoptotic DNA fraction ranged from 2–7%, as calculated following Southern blot hybridization (see "Materials and Methods"). Transfer of high molecular weight DNA to the blots was inefficient in comparison to low molecular weight apoptotic DNA; thus, calculations of apoptotic fractions are likely to be overestimates. The critical point is that there were no significant differences in the apoptotic DNA fractions between p53+/+ and p53−/− tumors (as measured by *t* test).

The Absence of p53 Promotes Cell Proliferation. If apoptosis is not playing a major role in the increased growth rates of the p53-deficient *Wnt-1 TG* tumors, the obvious alternative is that tumor cells are dividing more rapidly in the absence of p53. To test this possibility, we first examined the number of mitotic cells in the mammary tumors as a simple marker for the relative number of cells undergoing division. This was performed by counting mitotic figures in H&E-stained tumor cross-sections. The total number of mitotic figures was determined in 10 high power microscopic fields (×400) for each tumor. The fields were randomly selected near the edge of the expanding tumor because this area usually has the highest growth rates. The total number of mitotic figures per 10 fields was also converted to percentages of mitotic figures per total number of cells in the 10 fields to control for any possible size differences between tumor cells of different p53 genotypes. However, with both measurements, the relative mitotic index was significantly higher in the p53−/− and p53+/− LOH tumors than in the p53+/+ tumors as measured by *t* test ($P = 0.001$ and 0.006, respectively; Fig. 5). The p53+/− tumor cells had on average higher mitotic indexes than p53+/+ tumor cells, although the difference here was not statistically significant.

The second assay used to assess cell proliferation in the tumor samples was flow cytometric analysis for DNA content. This assay provides an approximation of the percentage of the tumor cells in each phase of the cell cycle. This assay was performed on tumor cell nuclei obtained by cutting 50-μm sections from paraffin-embedded samples as described previously by Demirel *et al.* (50). Three representative flow cytometry profiles for the tumors are shown in Fig. 6, *A–C*. Note the higher percentages of cells in S phase and G_2-M phase in the p53−/− sample when compared to the p53+/+ tumor cells. Note also that the p53+/− LOH tumor has substantial aneuploidy among its tumor cell population. This aneuploid profile was consistently observed for all five p53+/− LOH tumors examined. Only one of seven p53−/− tumors exhibited an aneuploid profile (data not shown). This result was consistent with chromosomal instability studies performed on this tumor model previously (47). The results for all four p53 genotypes are compiled in Fig. 6*D*. Note that the p53+/− LOH tumors have on average the highest levels of cells in S phase. Although this estimate for the p53+/− LOH S phase fraction may be slightly distorted due to aneuploidy (Fig. 6*C*), we have attempted to be conservative in the interpretations of the profiles. p53+/− LOH tumor cells showed significantly higher numbers of cells in S phase on average (17.3%) than did p53+/+ cells (6.9%) by *t* test ($P = 0.001$). The p53−/− tumor cells also exhibited significantly higher fractions of S-phase cells (11.7%) than p53+/+ tumor cells ($P = 0.03$ by *t* test). The flow cytometry results show that absence or loss of p53 results in a higher percentage of tumor cells proceeding through S phase and G_2-M.

Discussion

In an earlier study using the *Wnt-1 TG* p53-deficient model, we showed that the absence of p53 accelerates tumorigenesis (47). One-half of p53−/− *Wnt-1 TG* females developed mammary tumors by 11.5 weeks of age, whereas one-half of p53+/+ and p53+/− *Wnt-1* females developed mammary tumors by 23 weeks of age (47). In this study, we show that not only does the absence of p53 promote early tumor formation, but once formed, tumors lacking p53 grow significantly faster on average than tumors in their p53+/+ coun-

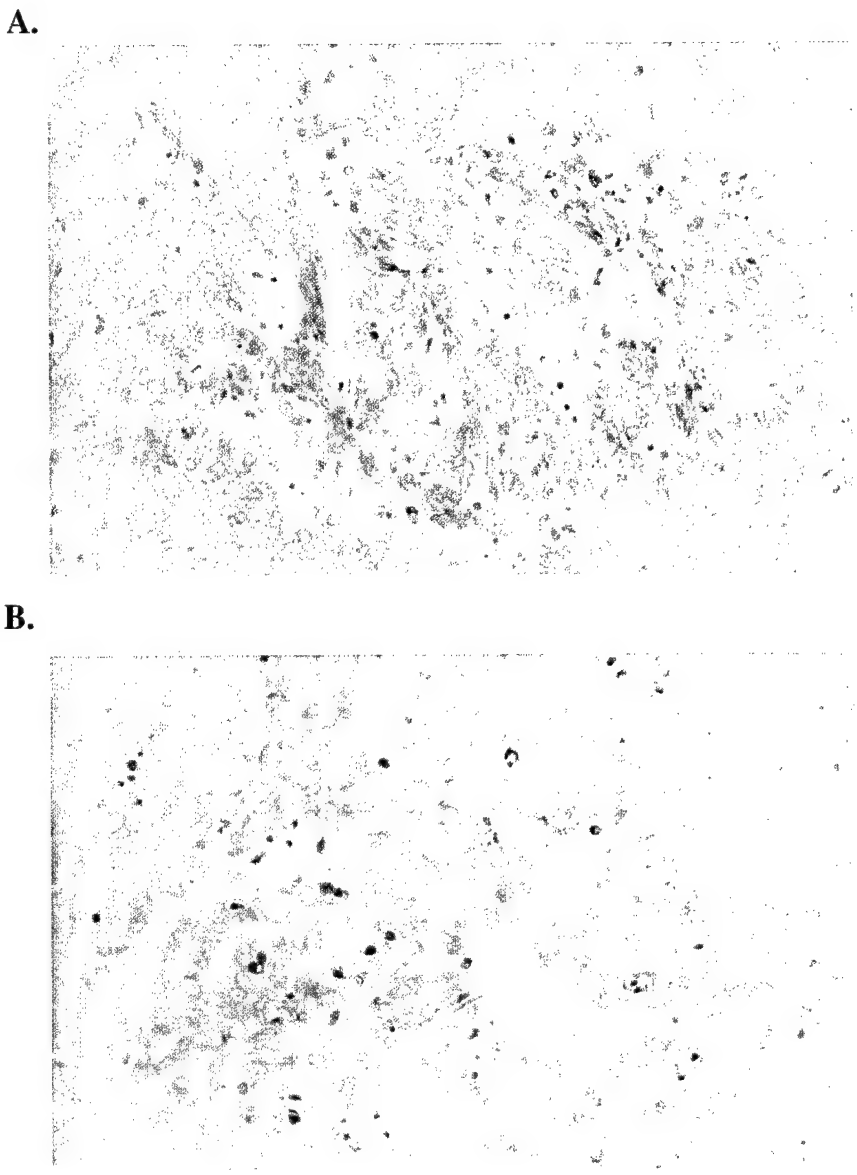

Fig. 2. TUNEL assay on mammary tumors in the presence and absence of p53. The two pictures are examples of the TUNEL assay performed on mammary tumor samples. *A*, p53+/+ tumor at ×400 with brown-stained apoptotic cells. *B*, p53−/− tumor at ×400 with brown-stained apoptotic cells. *C*, estimates of average levels of apoptosis in mammary tumors in the presence and absence of p53, showing the results of the TUNEL assay when performed on individual mammary tumors. Each *column* represents a separate tumor. The approximate level of apoptosis across each tumor is indicated by the number of pluses. +, very few apoptotic cells per high power field (0–1); ++, 2–10 apoptotic cells in a field; +++, 10–20 apoptotic cells in each field. *Columns* showing intermediate values between + and ++ indicate tumors displaying an overall level of TUNEL staining corresponding to + tumors but exhibiting occasional patches with higher levels of staining.

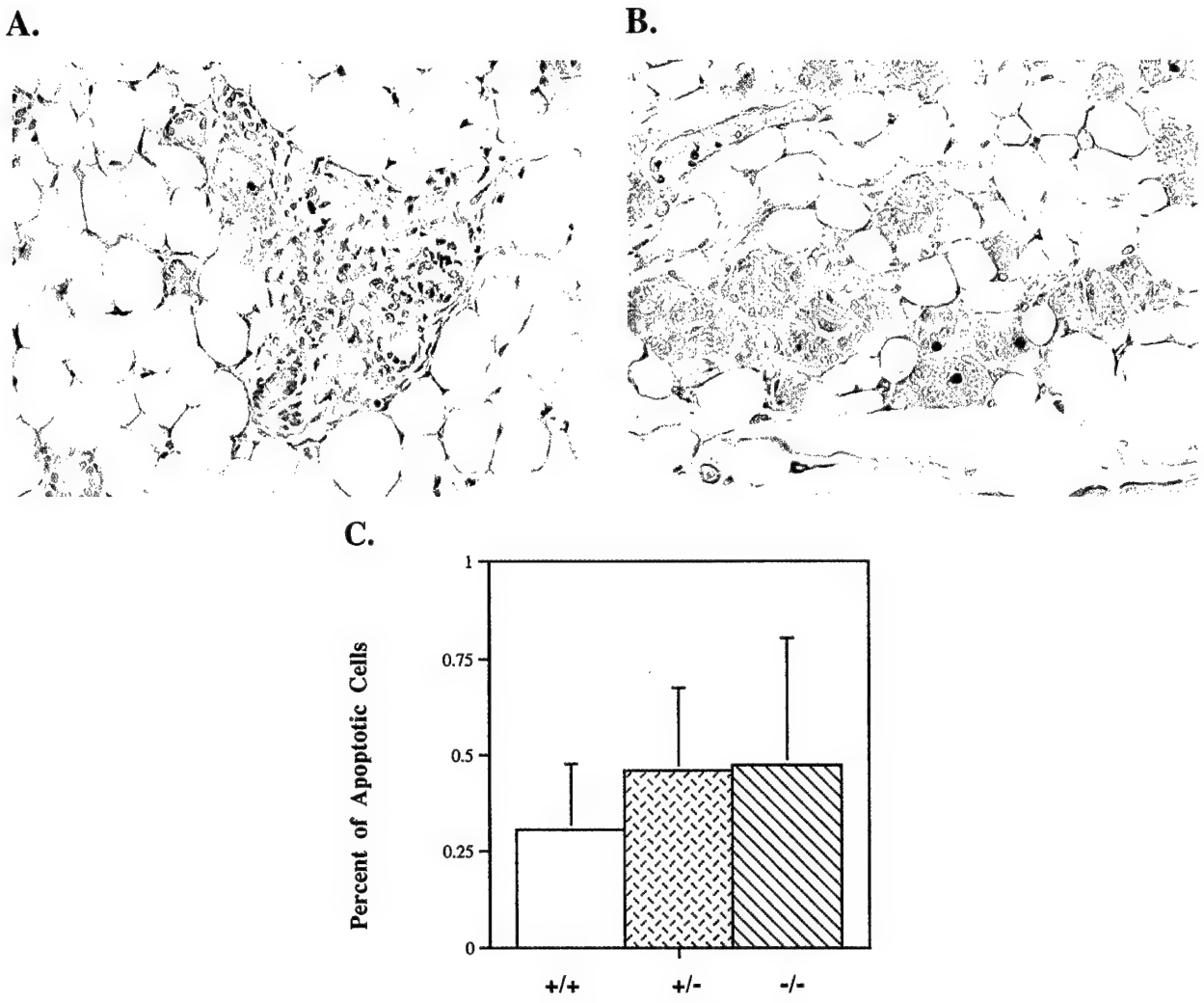

Fig. 3. Apoptosis in *Wnt-1* hyperplastic mammary glands in the presence and absence of p53 as measured by the TUNEL assay. *A,* hyperplastic mammary gland at ×400 from a *Wnt-1 TG* p53+/+ female. Apoptotic cells are stained *dark brown* by the TUNEL assay. *B,* hyperplastic mammary gland at ×400 from a *Wnt-1 TG* p53−/− female. Apoptotic cells are stained *dark brown*. *C,* TUNEL staining for apoptosis in hyperplastic mammary glands of *Wnt-1 TG* females. The data are expressed as the average percentage of epithelial cells undergoing apoptosis (for over 1000 cells counted per slide). For p53+/+ hyperplastic mammary glands, $n = 8$; p53+/−, $n = 10$; p53−/−, $n = 4$. *Bars,* SE.

terparts. The tumor growth assays indicated a higher rate of growth in tumor cells missing p53 (p53−/−) or having lost p53 (p53+/− LOH) compared to tumor cells with a full complement of p53 (p53+/+).

The maintenance of normal tissue homeostasis is dependent on balancing the rate of cell division and the rate of cell death. An increase in cell proliferation rates or a decrease in cell death rates can upset the balance that maintains the normal cellular integrity of the tissue, and the end result can be a tumor. Loss of normal p53 function could play a role in affecting tissue homeostasis either by increasing the fraction of cells progressing through the cell cycle or by reducing the levels of cellular apoptosis. Previous animal model studies have examined the mechanisms by which absence of p53 may confer a growth advantage during tumor progression (26–28). In general, these studies have supported the concept that p53 loss accelerates tumor growth primarily through loss of normal apoptotic function. The data presented here indicate that in the *Wnt-1*/p53 model, the absence of p53 has little or no effect on apoptosis (though subtle differences in apoptosis not detectable by our assays cannot be ruled out). However, the loss or absence of p53 does result in tumor cells with significantly higher rates of proliferation. Whether this increased proliferation is a direct effect of p53 loss or an indirect effect due to such factors as genomic instability remains unclear. In a recent study by Hundley *et al.* (51), the offspring of MMTV-c-*ras* mice mated to p53-deficient mice also demonstrated increased tumor cell proliferation in the absence of p53. Moreover, the p53-deficient c-*ras* tumors did not show the p53-dependent differences in apoptotic cell levels described in other models (26–28). These results, together with the observation of increased genomic instability in the p53-deficient tumors, closely paralleled our own results and suggest that p53 loss

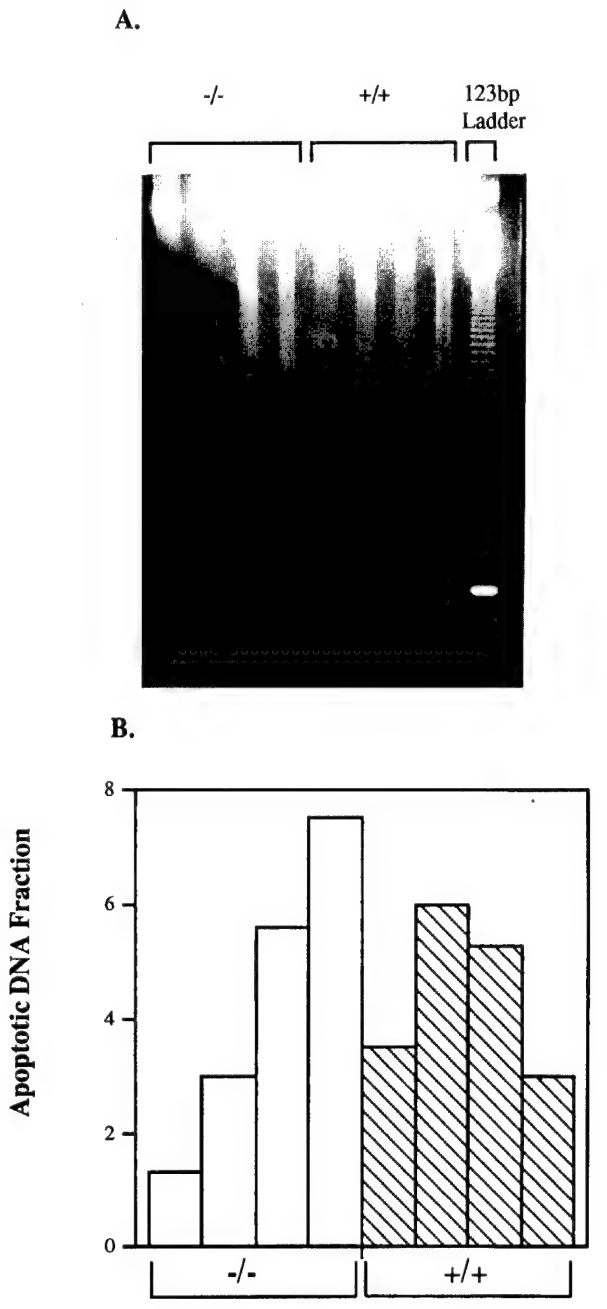

Fig. 4. Apoptotic DNA laddering assays for *Wnt-1 TG* p53+/+ and *Wnt-1 TG* p53−/− tumors. *A,* agarose gel electrophoresis of total genomic p53+/+ and p53−/− tumor DNA from *Wnt-1 TG* females. An ethidium bromide-stained 1.2% agarose gel shows the apoptotic DNA ladders characteristic of cells undergoing apoptosis. A 123-bp ladder is on the *right* to provide a size marker. *B,* quantitation of the apoptotic DNA fraction in each *Wnt-1 TG* tumor in the presence and absence of p53. The gel shown in Fig. 4*A* was blotted to nylon and hybridized to a total mouse genomic DNA probe. Hybridization of the probe to the low molecular weight and high molecular weight DNA fractions of the gel was quantitated by a Molecular Dynamics PhosphorImager. This analysis was performed on three additional samples of each genotype, and the results fell within the same range for both p53+/+ and p53−/− genotypes. Each *column* represents the percentage of total DNA in the apoptotic fraction of an individual mammary tumor.

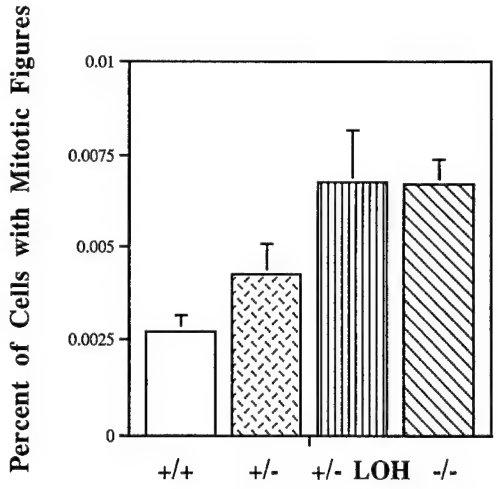

Fig. 5. Mitotic figures in *Wnt-1 TG* tumors in the presence and absence of p53. The percentage of mammary tumor cells with visible mitotic figures was determined by counting at least 10 randomly selected fields near the outer edge of the tumor section (over 5000 cells/sample were counted). For p53+/+ tumors, $n = 8$; p53+/−, $n = 6$; p53+/− LOH, $n = 7$; p53−/−, $n = 10$. *Bars,* SE.

may affect tumor progression by different mechanisms, depending on the type of model.

Why does p53 loss in the *Wnt-1*/p53 model affect tumor progression by different mechanisms than in the previously characterized Rb/p53-based models? The differences between the two models may provide some clues. One difference could be in the tissue type. Previous models developed tumors in the retinal tissue (27, 28) or the choroid plexus of the brain (26). Loss of p53 in mammary epithelial tissue in our model may have profoundly different effects on tumor progression. As described above, crossing of p53-deficient mice to mammary tumor-susceptible MMTV-c-*ras* transgenic mice resulted in tumors in which absence of p53 correlated well with higher tumor cell proliferation without effects on apoptosis levels (51). It has been demonstrated that mammary gland apoptosis during involution proceeds independently of the p53 status of the animal (52). Thus, mammary tissue may be relatively insensitive to p53-dependent apoptosis.

An alternative explanation for the absence of an apoptotic effect is that the oncogenic pathways used in the Rb/p53 and *Wnt-1*/p53 models to generate tumors are different. Loss of function of the tumor suppressor Rb could have different effects on p53 activities than overexpression of the *Wnt-1* oncogene product. Moreover, because Wnt-1 acts as a transforming growth factor in mammary tissue (53, 54), it may also be acting as a survival factor, preventing apoptosis. *In vitro* studies have demonstrated that the addition of cytokines or growth factors to p53-containing cells can inhibit p53-induced apoptosis (15, 20). Thus, some oncogenic pathways may be relatively insensitive to p53-mediated apoptosis, and tumors arising through such pathways may be less likely to incur loss of p53 during tumor progression. Perhaps a single dominant mutation in another oncogene could provide the same growth advantage that mutation of

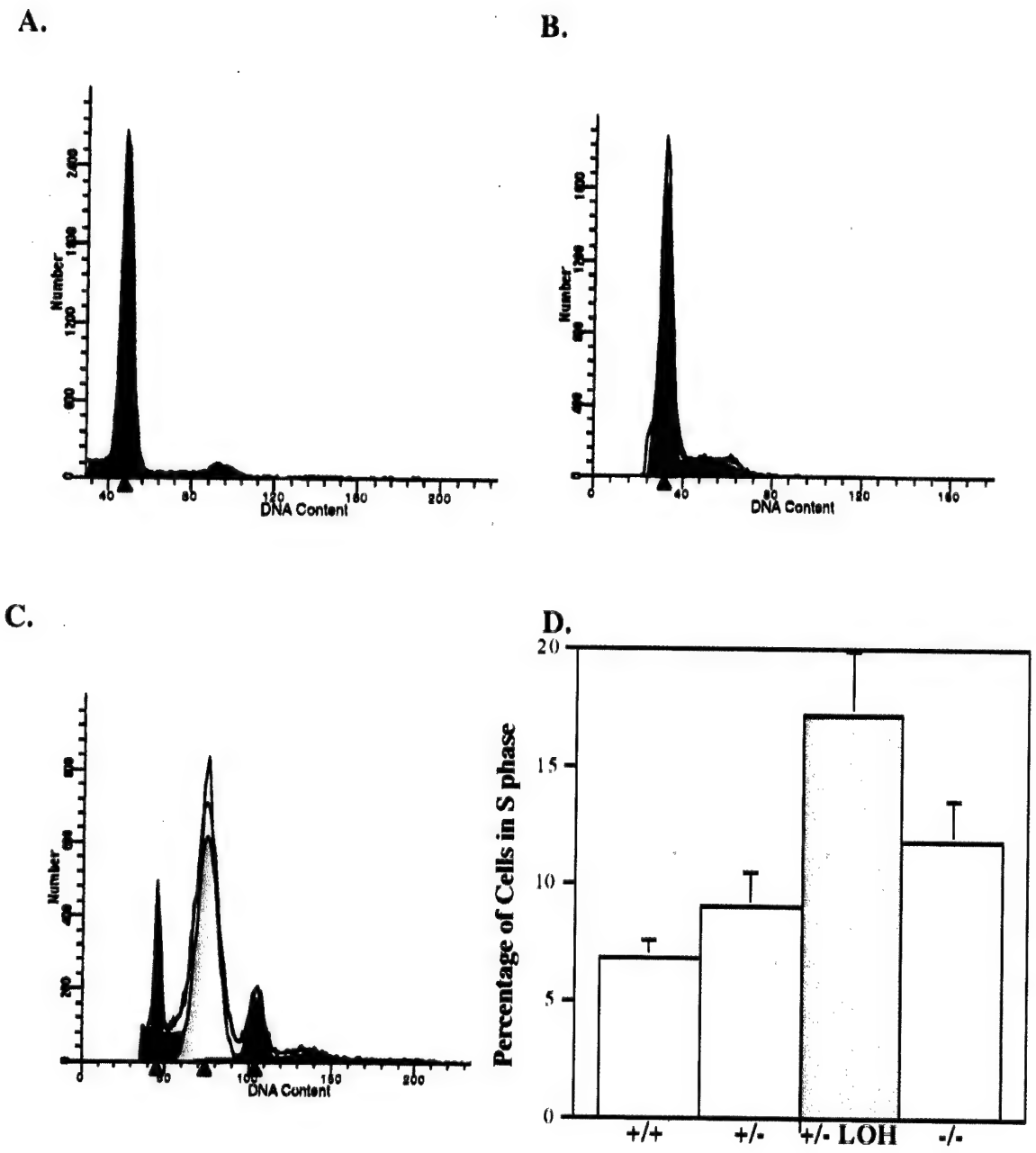

Fig. 6. Flow cytometry for DNA content in *Wnt-1*/p53 mammary tumors. *A,* representative flow cytometry profile of *Wnt-1 TG* p53+/+ tumor. This tumor has an estimated diploid S-phase fraction of 7.8%. Colors under each peak are for clarification purposes only. *Red,* diploid peak; *yellow,* aneuploid peak. *B,* representative flow cytometry profile of a *Wnt-1 TG* p53−/− tumor. This tumor has an estimated diploid S-phase population of 20%. *C,* representative flow cytometry profile of *Wnt-1 TG* p53+/− LOH tumor. This tumor exhibits two aneuploid stemlines with DNA indices of 1.7 and 2.3 (second and third peaks to the *right* of the diploid G_0-G_1). This high degree of aneuploidy was observed in all tumors that are p53+/− LOH. *D,* average percentage of mammary tumor cells in S phase for each *Wnt-1* p53 genotype. For p53+/+ tumors, $n = 7$; p53+/−, $n = 4$; p53+/− LOH, $n = 5$; p53−/−, $n = 7$. *Bars,* SE.

both *p53* alleles provides. This may explain why p53 mutations have yet to be found in p53+/+ *Wnt-1* tumors (47).[4]

In summary, we have demonstrated that in addition to its previously characterized ability to accelerate tumor growth through loss of apoptotic function, p53 loss can also increase cell proliferation levels. In this system, and in the MMTV-c-*ras* model recently described by Hundley *et al.* (51), enhanced proliferation levels appear to be more significant than decreased apoptosis in the acceleration of mammary tumor progression and growth rates. However, both apoptosis and proliferation may be affected by p53 loss in other models or in human tumors. There may also be other biological effects of p53 deficiency on tumor progression, some

[4] V. Pecenka and H. E. Varmus, unpublished data.

of which have been suggested by experiments in mouse models and in cell culture systems. These include increased levels of angiogenesis (55, 56) and an increased likelihood of metastasis (57). Further studies are needed to clarify some of these issues.

Materials and Methods

Histological Sample Preparation. Tumors were surgically removed, and cross-sections were cut with a sterile razor blade. These samples were then fixed overnight in 10% neutral buffered formalin and embedded in paraffin using standard methods. Samples were cut with a microtome at a size of 4 μm. Samples were fixed on slides and left unstained for TUNEL analysis or stained with H&E under standard conditions.

DNA Laddering Assay. Genomic DNA was isolated from frozen tumor tissues using standard phenol/chloroform extraction. Following ethanol precipitation of the total DNA, it was centrifuged at 12,000 $\times$ *g* at 4°C for 30 min. Following resuspension in TE [10 mM Tris-HCl (pH 8.0), 1 mM EDTA], 10 μg of total DNA from each tumor were then subjected to electrophoresis on a 1.2% agarose gel. DNA was visualized under UV illumination after ethidium bromide staining, and the gel was blotted using standard Southern blot procedures (60) and probed with a ^{32}P-labeled total mouse genomic probe. To determine the approximate apoptotic fraction of DNA, the hybridization signal (quantified by Molecular Dynamics PhosphorImager analysis) in the low molecular weight portion of the gel (<2000 bp) was divided by the signal intensity of the entire lane. This resulted in the approximate percentage of apoptotic DNA present in an individual tumor.

Detection of Apoptotic Cells in Tumors and Hyperplastic Mammary Gland Sections. Mammary gland and tumor sections were prepared as described above. Cells undergoing apoptosis were detected using the TACS 2 TdT *In Situ* Apoptosis detection kit (Trevigen, Gaithersburg, MD). Samples were deparaffinized and treated with proteinase K (2 μg/ml) for 15 min. Endogenous peroxidase was quenched by immersing samples for 5 min in 2% H_2O_2. Samples were then incubated with terminal deoxynucleotidyltransferase and biotinylated nucleotides for 1 h at 37 °C. Cells that had incorporated the biotinylated nucleotide were detected by incubation with streptavidin-horseradish peroxidase followed by 3,3'-diaminobenzidine for 10 min. Samples were then counterstained with 1% methyl green for 5 min. Finally, samples were washed with butanol, ethanol, and xylene and then mounted with Permount.

Mitotic Indexes. A determination of the number of mitotic figures in tumor samples was performed by counting the number of visible mitotic figures within cells in 10 random high power fields (×400). These fields were all within three high power fields of the edge of standard H&E-stained tumor cross-sections. The total number of mitotic figures was determined for all 10 high power fields as well as the percentage of tumor cells in the field with visible mitotic figures. The mitotic counts were performed blind with respect to p53 genotype.

Flow Cytometric Analysis of DNA Content of Tumor Cells. The DNA content of tumor samples was assessed in nuclei isolated from paraffin-embedded samples based on a modification of Hedley's method (41, 58). Nuclear suspensions were prepared from five 50-μm sections; a 4-μm section was cut before and after the 50-μm sections to confirm that histologically comparable sections were being used. The samples are deparaffinized using two 50-min xylene washes at 25 °C. The cells are then rehydrated using successive incubations with ethanol, two per dilution, 100, 95, 70, and 50% and distilled water. Between each concentration of ethanol there was a 50-min incubation at 25 °C to make a cell suspension. To make a single cell suspension, the cells were treated with a 0.5% pepsin solution for 37 °C for 30 min (Sigma Chemical Co., St. Louis, MO). Filtration through a 74-μm-pore mesh (Small Parts, Inc., Miami, FL.) resulted in a nuclear suspension, which was stained using the Vindelov technique (59). For a procedural control, fresh chicken erythrocyte nuclei (Accurate Chemical & Scientific Co., Westbury, NY) were used. A five-μl solution of a 20,000,000 chicken erythrocyte nuclei/ml suspension was added to the sample prior to the DNA staining step. The sample used for DNA flow analysis was acquired on a FACScan flow cytometer with doublet discrimination (Becton Dickinson, San Jose, CA). Twenty thousand events were collected using the gating parameters of FL2-W *versus* FL2-A. Histograms were generated to determine the percentage of cells in each stage of the cell cycle. Cell cycle analysis was performed using the ModFitLT software (Topsham, ME).

Acknowledgments

We thank Wendy Hively and Francis Kittrell for technical assistance.

References

1. Hollstein, M., Rice, K., Greenblatt, M. S., Soussi, T., Fuchs, R., Sorlie, T., Hovig, E., Smith-Sorensen, B., Montesano, R., and Harris, C. C. Database of *p53* gene somatic mutations in human tumors and cell lines. Nucleic Acids Res., *22:* 3551–3554, 1994.

2. Greenblatt, M. S., Bennett, W. P., and Harris, C. C. Mutations in the *p53* tumor suppressor gene: clues to cancer etiology and molecular pathogenesis. Cancer Res., *54:* 4855–4878, 1994.

3. Moll, U. M., Riou, G., and Levine, A. J. Two distinct mechanisms alter p53 in breast cancer: mutation and nuclear exclusion. Proc. Natl. Acad. Sci. USA, *89:* 7262–7266, 1992.

4. Moll, U. M., Ostermeyer, A. G., Haladay, R., Winkfield, B., Frazier, M., and Zambetti, G. Cytoplasmic sequestration of wild-type p53 protein impairs the G1 checkpoint after DNA damage. Mol. Cell. Biol., *16:* 1126–1130, 1996.

5. Momand, J., Zambetti, G. P., Olson, D. C., George, D., and Levine, A. J. The *mdm-2* oncogene product forms a complex with the p53 protein and inhibits p53-mediated transactivation. Cell, *69:* 1237–1245, 1992.

6. Oliner, J. D., Kinzler, K. W., Meltzer, P. S., George, D. L., and Vogelstein, B. Amplification of a gene encoding a p53-associated protein in human sarcomas. Nature (Lond.), *358:* 80–83, 1992.

7. McCann, A. H., Kirley, A. Carney, D. N., Corbally, N., Magee, H. M., Keating G., and Dervan, P. Amplification of the *MDM2* gene in human breast cancer and its association with MDM2 and p53 protein status. Br. J. Cancer, *71:* 981–985, 1995.

8. Kuerbitz, S. J., Plunkett, B. S., Walsh, W. V., and Kastan, M. B. Wildtype p53 is a cell cycle checkpoint determinant following irradiation. Proc. Natl. Acad. Sci. USA, *89:* 7491–7495, 1992.

9. Kastan, M. B., Zhan, Q., El-Deiry, W. S., Carrier, F., Jacks, T., Walsh, W. V., Plunkett, B. S., Vogelstein, B., and Fornace, A. J., Jr. A mammalian cell cycle checkpoint pathway utilizing p53 and GADD45 is defective in ataxia-telangiectasia. Cell, *71:* 587–597, 1992.

10. Stewart, N., Hicks, G. G., Paraskevas, F., and Mowat, M. Evidence for a second cell cycle block at G_2-M by p53. Oncogene, *10:* 109–115, 1995.

11. Agarwal, M. L., Agarwal, A., Taylor, W. R., and Stark, G. R. p53 controls both the G_2-M and the G1 cell cycle checkpoints and mediates reversible growth arrest in human fibroblasts. Proc. Natl. Acad. Sci. USA, *92:* 8493–8497, 1995.

12. Cross, S. M., Sanchez, C. A., Morgan, C. A., Schimke, M. K., Ramel, S., Idzerda, R. L., Raskind, W. H., and Reid, B. J. A p53-dependent mouse spindle checkpoint. Science (Washington DC), *267:* 1353–1356, 1995.

13. Lu, X., and Lane, D. P. Differential induction of transcriptionally active p53 following UV or ionizing radiation: defects in chromosome instability syndromes? Cell, *75:* 765–778, 1993.

14. Di Leonardo, A., Linke, S. P., Clarkin, K., and Wahl, G. M. DNA damage triggers a prolonged p53-dependent G1 arrest and long-term induction of Cip1 in normal human fibroblasts. Genes Dev., *8:* 2540–2551, 1994.

15. Yonish-Rouach, E., Pesnitzky, D., Lotem, J., Sachs, L., Kimchi, A., and Oren, M. Wild type p53 induces apoptosis of myeloid leukaemic cells that is inhibited by interleukin-6. Nature (Lond.), *352:* 345–347, 1991.

16. Lowe, S. W., Schmitt, E. M., Smith, S. W., Osborne, B. A., and Jacks, T. p53 is required for radiation-induced apoptosis in mouse thymocytes. Nature (Lond.), *362:* 847–849, 1993.

17. Clarke, A. R., Purdie, C. A., Harrison, D. J., Morris, R. G., Bird, C. C., Hooper, M. L., and Wyllie, A. H. Thymocyte apoptosis induced by p53-dependent and independent pathways. Nature (Lond.), *362:* 849–852, 1993.

18. Midgley, C. A., Owens, B., Briscoe, C. V., Thomas, D. B., Lane, D. P., and Hall, P. A. Coupling between gamma irradiation, p53 induction and the apoptotic response depends upon cell type *in vivo*. J. Cell Sci., *108:* 1843–1848, 1995.

19. Chen, X., Ko, L. J., Jayaraman, L., and Prives, C. p53 levels, functional domains, and DNA damage determine the extent of the apoptotic response of tumor cells. Genes & Dev., *10:* 2438–2451, 1996.

20. Canman, C. E., Gilmer, T. M., Coutts, S. B., and Kastan, M. B. Growth factor modulation of p53-mediated growth arrest *versus* apoptosis. Genes Dev., *9:* 600–611, 1995.

21. Lowe, S. W., Ruley, H. E., Jacks, T., and Housman, D. E. p53-dependent apoptosis modulates the cytotoxicity of anticancer agents. Cell, *74:* 957–967, 1993.

22. Hermeking, H., and Eick, D. Mediation of c-myc-induced apoptosis by p53. Science (Washington DC), *265:* 2091–2093, 1996.

23. Wagner, A. J., Kokontis, J. M., and Hay, N. Myc-mediated apoptosis requires wild-type p53 in a manner independent of cell cycle arrest and the ability of p53 to induce $p21^{waf1/cip1}$. Genes Dev., *8:* 2817–2830, 1994.

24. Lowe, S. W., Jacks, T., Housman, D. E., and Ruley, H. E. Abrogation of oncogene-associated apoptosis allows transformation of p53-deficient cells. Proc. Natl. Acad. Sci. USA, *91:* 2026–2030, 1994.

25. Morgenbesser, S. D., Williams, B. O., Jacks, T., and DePinho, R. A. p53-dependent apoptosis produced by Rb-deficiency in the developing mouse lens. Nature (Lond.), *371:* 72–74, 1994.

26. Symonds, H., Krall, L., Remington, L., Saenz-Robles, M., Lowe, S., Jacks, T., and Van Dyke, T. p53-dependent apoptosis suppresses tumor growth and progression *in vivo*. Cell, *78:* 703–711, 1994.

27. Howes, K. A., Ransom, N., Papermaster, D. S., Lasudry, J. G. H., Albert, D. M., and Windle, J. J. Apoptosis or retinoblastoma: alternative fates of photoreceptors expressing the HPV-16 *E7* gene in the presence or absence of p53. Genes Dev., *8:* 1300–1310, 1994.

28. Pan, H., and Griep, A. E. Temporally distinct patterns of p53-dependent and p53-independent apoptosis during mouse lens development. Genes Dev., *9:* 2157–2169, 1995.

29. Kern, S. E., Fearon, E. R., Tersmette, K. W., Enterline, J. P., Leppert M., Nakamura, Y., White, R., Vogelstein, B., and Hamilton, S. R. Clinical and pathological associations with allelic loss in colorectal carcinoma. J. Am. Med. Assoc., *261:* 3099–3103, 1989.

30. Harris, C. C., and Hollstein, M. Clinical implications of the *p53* tumor-suppressor gene. N. Engl. J. Med., *329:* 1318–1327, 1993.

31. Bischoff, F. Z., Yim, S. O., Pathak, S., Grant, G., Siciliano, M. J., Giovanella, B. C., Strong, L. C., and Tainsky, M. A. Spontaneous abnormalities in normal fibroblasts from patients with Li-Fraumeni cancer syndrome: aneuploidy and immortalization. Cancer Res., *50:* 7979–7984, 1990.

32. Livingstone, L. R., White, A., Sprouse, J., Livanos, E., Jacks, T., and Tlsty, T. D. Altered cell cycle arrest and gene amplification potential accompany loss of wild type p53. Cell, *70:* 605–620, 1992.

33. Yin, Y., Tainsky, M. A., Bischoff, F. Z., Strong, L. C., and Wahl, G. M. Wild type p53 restores cell cycle control and inhibits gene amplification in cells with mutant p53 alleles. Cell, *70:* 937–948, 1992.

34. Harvey, M., Sands, A. T., Weiss, R. S., Hegi, M. E., Wiseman, R. W., Pantazis, P., Giovanella, B. C., Tainsky, M. A., Bradley, A., and Donehower, L. A. *In vitro* growth characteristics of embryo fibroblasts isolated from p53-deficient mice. Oncogene, *8:* 2457–2467, 1993.

35. Galipeau, P. C., Cowan, D. S., Sanchez, C. A., Barrett, M. T., Emond, M. J., Levine, D. S., Rabinovitch, P. S., and Reid, B. J. 17p (p53) allelic losses, 4N (G2/tetraploid) populations, and progression to aneuploidy in Barrett's esophagus. Proc. Natl. Acad. Sci. USA, *93:* 7081–7084, 1996.

36. Soder, A. I., Hopman, A. H. N., Ramaekers, F. C. S., Conradt, C., and Bosch, F. X. Distinct nonrandom patterns of chromosomal aberrations in the progression of squamous cell carcinomas of the head and neck. Cancer Res., *55:* 5030–5037, 1995.

37. Kihana, T., Tsuda, H., Teshima, S., Okada, S., Matsuura, S., and Hirohashi, S. High incidence of *p53* gene mutation in human ovarian cancer and its association with nuclear accumulation of p53 protein and tumor DNA aneuploidy. Jpn. J. Cancer Res., *83:* 978–984, 1992.

38. Eyfjord, J. E., Thorlacius, S., Steinarsdottir, M., Valgardsdottir, R., Ogmundsdottir, H. M., and Anamthawat-Jonsson, K. *p53* abnormalities and genomic instability in primary human breast carcinomas. Cancer Res., *55:* 646–651, 1995.

39. El-Deiry, W. S., Tokino, T., Velculescu, V. E., Levy, D. B., Parsons, R., Trent, J. M., Lin, D., Mercer, W. E., Kinzler, K. W., and Vogelstein, B. *WAF1,* a potential mediator of p53 tumor suppression. Cell, *75:* 817–825, 1993.

40. Harper, J. W., Adami, G. R., Wei, N., Keyomarsi, K., and Elledge, S. J. The p21 cdk-interacting protein Cip1 is a potent inhibitor of G1 cyclin-dependent kinases. Cell, *75:* 805–816, 1993.

41. Papadopoulos, I., Rudolph, P., Wirth, B., and Weichert-Jacobsen, K. p53 expression, proliferation marker Ki-S5, DNA content and serum PSA: possible biopotential markers. Urology, *48:* 261–268, 1996.

42. Nawa, G., Ueda, T., Mori, S., Yoshikawa, H., Fukuda, H., Ishiguro, S., Funai, H., and Uchida, A. Prognostic significance of Ki67 (MIB1) proliferation index and p53 over-expression in chondrosarcomas. Int. J. Cancer, *69:* 86–91, 1996.

43. Gelsleichter, L., Gown, A. M., Zarbo, R. J., Wang, E., and Coltrera, M. D. p53 and mdm-2 expression in malignant melanoma: an immunocytochemical study of expression of p53, mdm-2, and markers of cell proliferation in primary *versus* metastatic tumors. Mod. Pathol., *8:* 530–535, 1995.

44. Sirvent, J. J., Salvado, M. T., Santafe, M., Martinez, S., Brunet, J., Alvaro, T., and Palacios, J. p53 in breast cancer. Its relation to histological grade, lymph-node status, hormone receptors, cell-proliferation fraction (ki-67) and c-erbB-2. Immunohistochemical study of 153 cases. Histol. Histopathol., *10:* 531–539, 1995.

45. Tsukamoto, A. S., Grosschedl, R., Guzman, R. C., Parslow, T., and Varmus, H. E. Expression of the *int-1* gene in transgenic mice is associated with mammary gland hyperplasia and adenocarcinomas in male and female mice. Cell, *55:* 619–625, 1988.

46. Donehower, L. A., Harvey, M., Slagle, B. L., McArthur, M. J., Montgomery, C. A., Jr., Butel, J. S., and Bradley, A. Mice deficient for p53 are developmentally normal but susceptible to spontaneous tumors. Nature (Lond.), *356:* 215–221, 1992.

47. Donehower, L. A., Godley, L. A., Aldaz, C. M., Pyle, R., Shi, Y-P., Pinkel, D., Gray, J., Bradley, A., Medina, D., and Varmus, H. E. Deficiency of *p53* accelerates mammary tumorigenesis in *Wnt-1* transgenic mice and promotes chromosomal instability. Genes Dev., *9:* 882–895, 1995.

48. Miller, B. E., Miller, F. R., Wiburn, D., and Heppner, G. H. Dominance of a tumor subpopulation in mixed heterogeneous mouse mammary tumors. Cancer Res., *48:* 5747–5753, 1988.

49. Kerr, J. F. R., and Harmon, B. V. Definition and incidence of apoptosis: an historical perspective. *In:* L. D. Tomei and F. O. Cope (eds.), The Molecular Basis of Cell Death, pp. 5–29. Cold Spring Harbor, NY: Cold Spring Harbor Laboratory, 1991.

50. Demirel, D., Laucirica R., Fishman, A., Owens, R. G., Grey, M. M., Kaplan, A. L., and Ramzy, I. Ovarian tumors of low malignant potential. Correlation of DNA index and S-phase fraction with histopathologic grade and clinical outcome. Cancer (Phila.), *77:* 1494–1500, 1996.

51. Hundley, J. E., Koester, S. K., Troyer, D. A., Hilsenbeck, S. G., Subler, M. A., and Windle, J. J. Increased tumor proliferation and genomic instability without decreased apoptosis in MMTV-ras mice deficient in p53. Mol. Cell. Biol., *17:* 723–731, 1997.

52. Li, M., Hu, J., Heermeier, K., Hennighausen, L., Furth, P. A. Apoptosis and remodeling of mammary gland tissue during involution proceeds through p53-independent pathways. Cell Growth & Differ., *7:* 13–20, 1996.

53. Jue, S. F., Bradley, R. S., Rudnicki, J. A., Varmus, H. E., and Brown, A. M. C. The mouse *Wnt-1* gene can act via a paracrine mechanism in transformation of mammary epithelial cells. Mol. Cell. Biol., *12:* 321–328, 1992.

54. Bradley, R. S., and Brown, A. M. C. A soluble form of *Wnt-1* protein with mitogenic activity on mammary epithelial cells. Mol. Cell. Biol., *15:* 4616–4622, 1995.

55. Dameron, K. M., Volpert, O. V., Tainsky, M. A., and Bouck, N. Control of angiogenesis in fibroblasts by p53 regulation of thrombospondin-1. Science (Washington DC), *265:* 1582–1584, 1994.

56. Van Meir, E. G., Polverini, P., Chazin, V. R., Su Huang, H. J., de Tribolet, N., and Cavenee, W. K. Release of an inhibitor of angiogenesis upon induction of wild type p53 expression in glioblastoma cells. Nat. Genet., *8:* 171–176, 1994.

57. Thompson, T. C., Park, S. H., Timme, T. L., Ren, C., Eastham, J. A., Donehower, L. A., Bradley, A., Kadmon, D., and Yang, G. Loss of p53 function leads to metastasis in *ras* + *myc*-initiated mouse prostate cancer. Oncogene, *10:* 869–879, 1995.

58. Hedley, D. W., Friedlander, M. L., Taylor, I. W., Rugg, C. A., and Musgrove, E. A. Method of analysis of cellular DNA content of paraffin-embedded pathological material using flow cytometry. J. Histochem. Cytochem., *21:* 1333–1335, 1983.

59. Vindelov, L. L., Christensen, I. J., and Nissen, N. I. A detergent-trypsin method for the preparation of nuclei for flow cytometric DNA analysis. Cytometry, *3:* 323–327, 1993.

Decreased Immunoglobulin Deposition in Tumors and Increased Immature B Cells in p53-null Mice[1]

Lawton Shick, Julie H. Carman, John K. Choi, Kumaravel Somasundaram, Marilee Burrell, David E. Hill, Yi-Xin Zeng, Yisong Wang, Klas G. Wiman, Kevin Salhany, Thomas R. Kadesch, John G. Monroe, Lawrence A. Donehower, and Wafik S. El-Deiry[2]

Laboratory of Molecular Oncology and Cell Cycle Regulation [L. S., K. S., Y-X. Z., W. S. E-D.], and Departments of Medicine [L. S., K. So., Y-X. Z., W. S. E-D.], Immunology [J. H. C., J. G. M.], Genetics [T. R. K., W. S. E-D.], and Pathology-Laboratory Medicine [J. K. C., K. Sa.]; Howard Hughes Medical Institute, University of Pennsylvania School of Medicine, Philadelphia, Pennsylvania 19104 [J. K. C., K. So., Y-X. Z., T. R. K., W. S. E-D.]; Oncogene Science, Inc. [M. B.], Oncogene Research Products [D.E.H.], Calbiochem, Cambridge, Massachusetts 02142; Department of Tumor Biology, Karolinska Institutet, Stockholm, Sweden [Y. W., K. G. W.]; and Division of Molecular Virology, Baylor College of Medicine, Houston, Texas 77030 [L. A. D.]

Abstract

Recent studies have hinted that there may be a relationship between p53 and the immune response. In preliminary experiments, we found significantly decreased levels of immunoglobulin deposition in 13 of 16 p53-null tumors compared with 2 of 17 tumors derived from $p53^{+/-}$ mice. We further explored the effect of p53 on B-cell development and function. p53-null mice contained more splenic white pulp and more immature B cells in the bone marrow compared with $p53^{+/-}$ mice. p53-null B cells were hyperresponsive to proliferative challenge but were not more resistant to signal-induced apoptosis. Several p53 DNA-binding sites were localized to the regulatory regions of immunoglobulin heavy and light chain genes, including the KII site, which serves as an enhancer for rearrangement of the mouse κ chain J cluster genes. Levels of p53 protein and the κ chain sterile transcript increased after exposure of pre-B cells to the DNA damaging agents etoposide and Adriamycin. Our observations suggest that p53 may be involved in B-cell maturation and may relay certain stress signals to affect B-cell function.

Received 7/15/96; revised 11/19/96; accepted 12/13/96.
The costs of publication of this article were defrayed in part by the payment of page charges. This article must therefore be hereby marked *advertisement* in accordance with 18 U.S.C. Section 1734 solely to indicate this fact.
[1] This work was supported in part by NIH Training Grant DK-07066 (to L. S.). W. S. E-D. is an Assistant Investigator of the Howard Hughes Medical Institute.
[2] To whom requests for reprints should be addressed, at Laboratory of Molecular Oncology and Cell Cycle Regulation, Howard Hughes Medical Institute, University of Pennsylvania School of Medicine, 415 Curie Boulevard, CRB 437, Philadelphia, PA 19104. Phone: (215) 898-9015; Fax: (215) 573-9139.

Introduction

The p53 tumor suppressor protein is a transcription factor that regulates growth arrest and apoptosis pathways in mammalian cells (reviewed in Ref. 1). *p53* target genes include cell cycle regulators ($p21^{WAF1/CIP1}$, MDM2, and GADD45), apoptosis inducers (bax and FAS/Apo1), and secreted proteins (Thrombospondin 1, GD-AiF, and IGF-BP3). Recent studies have suggested a possible relationship between p53 and the immune response. p53 induction was correlated with differentiation and κ light chain gene expression in γ-irradiated pre-B cells (2). In addition, it has been possible to partially rescue VDJ[3] recombination and T-cell development in SCID mice that are $p53^{+/-}$ but not $p53^{-}$ (3).

While investigating p21 expression as a marker of p53 status, we found evidence for decreased immunoglobulin deposition in tumors derived from $p53^{-}$ *versus* $p53^{+/-}$ mice. To further explore the relationship between p53 and this immunoglobulin deposition, we investigated B-cell maturation and responsiveness in p53-null and $p53^{+/-}$ mice. We also searched for evidence for direct p53 regulation of VDJ rearrangement. We found that p53-null mice contain increased splenic white pulp, increased numbers of immature B cells in their bone marrow, and B cells that are hyperresponsive to proliferative challenge. We identified several p53 DNA-binding sites in the regulatory regions of immunoglobulin heavy and light chain genes, including the KII site recently shown to be important for rearrangement of κ light chain genes (4) and the DQ52 region important for heavy chain gene rearrangement (5). p53 bound to these putative sites, and we detected induction of sterile (germ line) transcription at the κ chain and *Jμ* loci after p53 induction. Our observations raise the possibility that p53 may be involved in B-cell maturation, a role that has implications with respect to normal and antitumor immune function, as well as the high prevalence of lymphoid malignancies in p53 knockout mice. p53 binding to immunoglobulin regulatory sites suggests the possibility that p53 may serve as a relay of certain stress signals to affect B-cell function.

Results

Analysis of Tumors from $p53^{+/-}$ and $p53^{-/-}$ Mice. Our initial studies used tumors derived from $p53^{+/-}$ and $p53^{-/-}$ mice to examine p21 expression in tumors as a marker of p53 status. We raised antibodies that specifically and sensitively recognized mouse p21 (Fig. 1). Three anti-mouse p21 mAbs (Fig. 1*A–C*) and a rabbit polyclonal antibody (Fig. 1*D*)

[3] The abbreviations used are: VDJ, Variable Diversity Joining segments of immunoglobulin gene family; sIgM, surface Immunoglobulin class M; LPS, lipopolysaccharide; GST, glutathione *S*-transferase; EMSA, electrophoretic mobility shift assay; FACS, fluorescence-activated cell sorting; RT, reverse transcription.

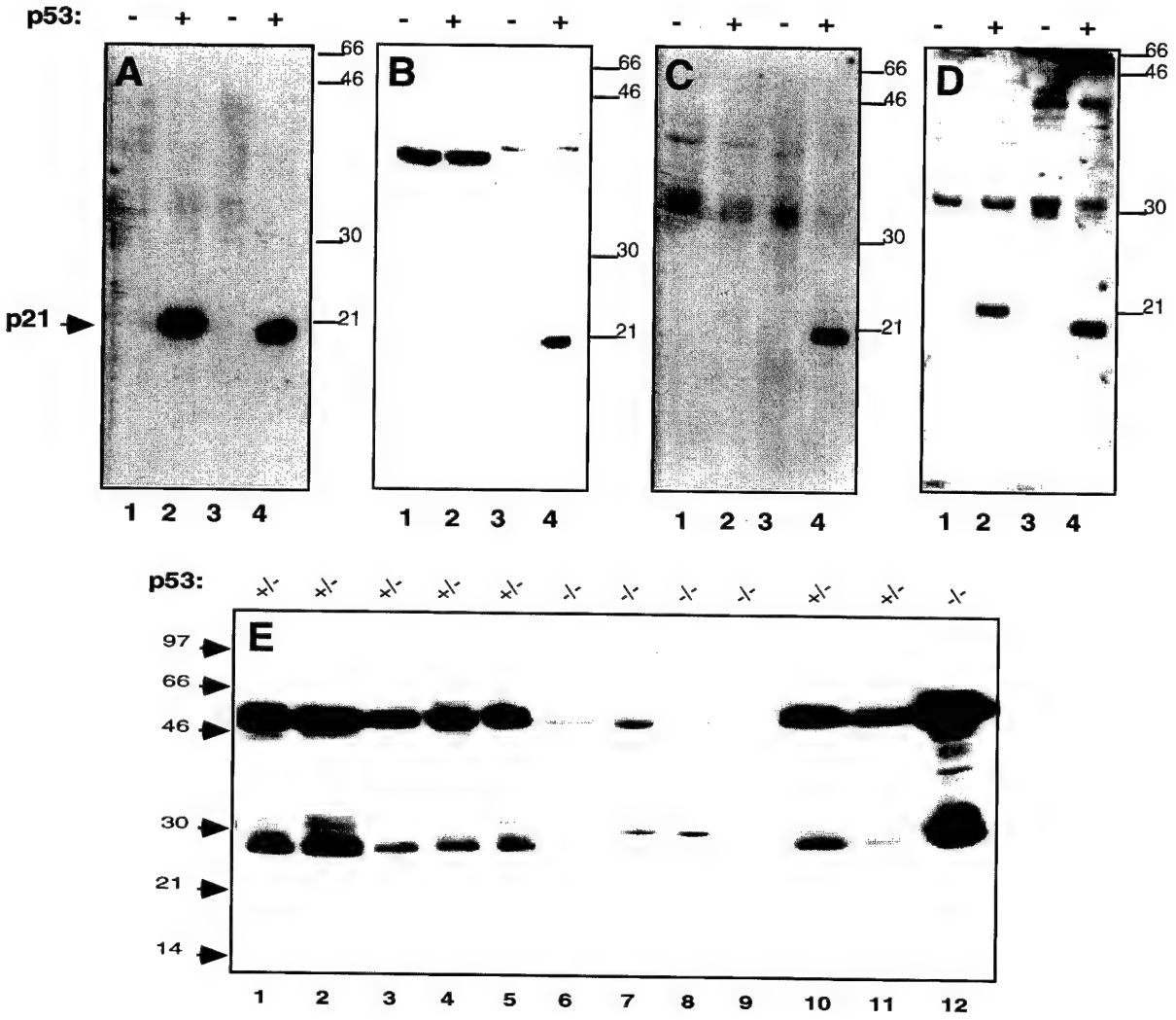

Fig. 1. *A–D*, reactivity of anti-mouse $p21^{WAF1/CIP1}$ antibodies. Western blot analysis of lysates derived from human GM cells incubated in the absence (*Lane 1*) or presence (*Lane 2*) of dexamethasone, or lysates derived from mouse M3 cells incubated at 37°C (*Lane 3*) or 32°C (*Lane 4*) were immunoblotted with either anti-mouse p21 mAb 22A (*A*), anti-mouse p21 mAb 75A (*B*), anti-mouse p21 mAb 65A (*C*), or anti-mouse p21 polyclonal sera OS100 (*D*). +, presence of wild-type p53 protein. Protein molecular weight size markers are indicated to the *right* of each panel (in thousands). The predicted mobility of p21 is indicated by an *arrow* to the *left* of *A*. *E*, analysis of tumors from $p53^{+/-}$ and $p53^{-/-}$ mice using an anti-mouse $p21^{WAF1/CIP1}$ mAb. Western blot analysis of a subset of the tumors shown in Table 1 was performed using anti-mouse $p21^{WAF1/CIP1}$ mAb 75A as described in "Materials and Methods." The p53 genotype of the mice from which the tumors were derived is indicated above each lane. +/−, one wild-type *p53* allele and one null allele; −/−, two null *p53* alleles. Protein molecular weight size markers (in thousands) are indicated by *arrows* to the *left* of the figure. The identity of each tumor shown in this figure can be found in Table 1 (*Lane 1*, tumor 967; *Lane 2*, tumor 1337; *Lane 3*, tumor 1005; *Lane 4*, tumor 1087; *Lane 5*, tumor 1239; *Lane 6*, tumor 1280; *Lane 7*, tumor 1367; *Lane 8*, tumor 1687; *Lane 9*, tumor 1706; *Lane 10*, tumor 1334; *Lane 11*, tumor 1640; and *Lane 12*, tumor 1683).

recognized a M_r 20,000 band by Western blot analysis of M3 murine lymphoma cells (6) at 32°C (Fig. 1*A–D*, *Lane 4*), but not at 37°C (*Lane 3*). The M3 lymphoma cells express a temperature-sensitive *p53* gene (6) that adopts a transcriptionally active "wild-type" conformation at 32°C, but is functionally mutant at 37°C. One of the monoclonal antibodies (22A; Fig. 1*A*) and the polyclonal antibody (OS100; Fig. 1*D*) also showed reactivity against human p21 protein (*Lane 2*) in GM cells treated with dexamethasone to induce p53, but not in untreated GM cells (*Lane 1*). Cross-reacting protein bands were detected but were least prominent when mAb 75A (Fig. 1*A*) was used for immunoblotting (compare with Fig.1*B–D*). These four antibodies also immunoprecipitated p21 and associated cyclin-dependent kinase 2 protein from M3 cells at 32°C, but not at 37°C (data not shown).

In a blinded fashion, we used the anti-mouse p21 antibodies to immunoblot 19 tumors derived from $p53^{+/-}$ (n = 10) and $p53^{-/-}$ (n = 9) mice. The 19 tumors (see Table 1) included a representative sampling of neoplasms, which spontaneously arise in p53-deficient mice (7). The monoclonal antibodies recognized a slower migrating band (M_r ~25,000) in several tumors (Fig. 1*E*), but no band at M_r 21,000, leading us to suspect a posttranslationally modified p21 *in vivo*. The M_r 25,000 band was not recognized by anti-p27 antibodies (data not shown). We found no evidence for interaction between the M_r 25,000 band and either cyclin-

Table 1 Predicted p53 status of tumors derived from $p53^{+/-}$ and $p53^{-/-}$ mice

Tumor	Tumor type	Predicted p53 status[a]	Host's p53 genotype
967	Lymphoma	wt	+/−
971	Lymphoma	-	+/−
1005	Undifferentiated sarcoma	wt	+/−
1064	Osteosarcoma	wt	+/−
1087	Hemangiosarcoma	wt	+/−
1239	Lung adenocarcinoma	wt	+/−
1280	Lymphoma	-	−/−
1327	Lymphoma	-	−/−
1334	Undifferentiated sarcoma	wt	+/−
1337	Leiomyosarcoma	wt	+/−
1339	Rhabdomyosarcoma	-	−/−
1367	Lymphoma	-	−/−
1434	Osteosarcoma	wt	+/−
1640	Osteosarcoma	-	+/−
1680	Hemangiosarcoma	wt	−/−
1683	Hemangiosarcoma	wt	−/−
1687	Lymphoma	-	−/−
1706	Lymphoma	-	−/−
1713	Lymphoma	-	−/−

[a] wt, wild-type; −, non-wild-type.

dependent kinase 2 or proliferating cell nuclear antigen (data not shown). We also found no evidence that the M_r 25,000 band was a hyperphosphorylated form of p21 (data not shown). Thus, it would appear that the M_r 25,000 protein is neither structurally nor functionally related to p21. However, based on the expression level of the M_r 25,000 protein, we correctly predicted the p53 genotype of 15 of 19 mice (Table 1). Since the M_r 25,000 band intensity appeared helpful in predicting p53 genotype, we further attempted to identify it.

Decreased Immunoglobulin Deposition in p53-null Tumors. Analysis of several tumors with high levels of the M_r 25,000 band and several tumors with little or no detectable M_r 25,000 protein revealed that the M_r 25,000 protein was immunoglobulin light chain (Fig. 2*A*, *Lanes 1-3 versus Lanes 4-6*). In tumors in which the M_r 25,000 protein was easily detected, a M_r 50,000 band was also easily detected (Figs. 2*A, Lanes 1-3*, and 1*E*), likely corresponding to immunoglobulin heavy chain. Five tumors derived from $p53^{+/-}$ mice contained higher levels of both immunoglobulin κ and λ chains compared with five tumors derived from $p53^{-/-}$ mice (Fig. 2*B*, compare *Lanes 1-5* with *Lanes 6-10*). Thus, both κ and λ chains appear to be deposited at decreased levels in p53-null tumors. We checked whether tissue origin of the tumor could account for the difference in immunoglobulin deposition. We found examples of lymphomas that overexpressed immunoglobulin when obtained from a $p53^{+/-}$ mouse, whereas other lymphomas had relatively low levels of immunoglobulin if they arose in $p53^{-/-}$ mice (Table 1).

We reproduced the difference in immunoglobulin deposition between wild-type p53-expressing tumors and p53-null tumors by examining breast cancers obtained from *wnt1* mice crossed with either $p53^{+/+}$ or $p53^{-/-}$ mice (8). Fig. 2*C* shows that immunoglobulin light chain deposition was observed in 6 of 7 tumors derived from $p53^{+/+}$/*Wnt1* mice, but not 6 of 7 breast tumors derived from $p53^{-/-}$/*Wnt1* mice (Table 2).

The anti-mouse p21 OS100 polyclonal antibody, when used at a titer of 1:1000, detected a doublet at M_r 21,000-22,000 in most of the original tumors derived from $p53^{+/-}$ and $p53^{-/-}$ mice (Fig. 3). We found a poor correlation between p21 expression and p53 genotype; *i.e.,* one of two tumors that highly expressed p21 (Fig. 3, *Lanes 2* and *9*) was $p53^{-/-}$, and in the tumors that expressed p21 at lower levels (*e.g.,* Fig. 3, *Lanes 1, 3-7,* and *10-12*), there was no apparent difference between the level of p21 expression in tumors derived from $p53^{+/-}$ and $p53^{+/-}$ mice. Therefore, at least for the case of tumors derived from $p53^{+/-}$ and $p53^{-/-}$ mice, p21 expression levels did not correlate with p53 status.

Reactivity of Mouse Sera against Tumor Antigens. Immunohistochemical staining of two immunoglobulin-positive and two immunoglobulin-negative tumors (Fig. 4*A*) revealed that some immunoglobulin was extracellular, possibly associated with cellular fragments, some was associated with tumor cells, and some with rare small round cells. The precise origin of the tumor-associated immunoglobulin or the target of this immunoglobulin deposition was not clear.

We found no differences in the levels of serum immunoglobulin between $p53^{+/+}$, $p53^{+/-}$, and $p53^{-/-}$ mice (data not shown). We investigated the reactivity of sera derived from wild-type p53-containing *versus* $p53^{-/-}$ tumor-bearing mice against tumor antigens. Fig. 4*B, a–c*, shows results of immunoblotting a tumor derived from a $p53^{-/-}$ mouse and two tumors derived from $p53^{+/-}$ mice with sera derived from each of the same three tumor-bearing mice. One of the sera (Fig. 4*Bc*) from the tumor-bearing mouse whose tumor specimen is shown in *Lane 2* strongly recognized novel antigens (M_r ~35,000 and ~75,000-80,000 proteins) in the same tumor, but not in the tumor derived from a $p53^{-/-}$ mouse (*Lane 1*) or another $p53^{+/-}$ mouse (*Lane 3*). These antigens were not recognized by sera from another $p53^{+/-}$ tumor-bearing mouse, whose tumor is shown in *Lane 3* (Fig. 4*Bb*), and at least the M_r ~35,000 band was not recognized in *Lane 2* when probed by sera from a $p53^{-/-}$ mouse whose tumor is shown in *Lane 1* (Fig. 4*Ba*).

Fig. 4*B, d* and *e*, shows that pooled sera from $p53^{+/+}$/*Wnt1* tumor-bearing mice recognized several protein bands (range, M_r ~70,000-150,000) in tumors derived from either wild-type p53-expressing or p53-null mice (Fig. 4*Be*; *arrows*), whereas pooled sera from $p53^{-/-}$/*Wnt1* tumor-bearing mice had substantially reduced reactivity (Fig. 4*Bd*).

Increased Immature B Cells in p53-null Bone Marrow. Lymphoid tissues (spleen, mesenteric lymph nodes, and bone marrow) were harvested from four $p53^{-/-}$, two $p53^{+/-}$, and four $p53^{+/+}$ 6-week-old mice. No significant differences were noted in the gross appearance or weight of the organs. Histological examination revealed an architectural difference with increased white pulp and relatively decreased red pulp in p53-null splenic tissue (Fig. 5*A, a–d*). We found no differences in the numbers of B and T lymphocytes in the spleen and lymph nodes in these groups of mice (data not shown). Although similar numbers of cells were recovered from the bone marrow of $p53^{-/-}$, $p53^{-/+}$, and $p53^{+/+}$ mice, the bone marrow of $p53^{-/-}$ mice contained a higher percentage of pre-B cells ($B220^+$ $sIgM^-$) compared with $p53^{+/+}$ mice (Fig. 5*B, a* and *b*). The percentages of B cells ($B220^+$ $sIgM^+$) were

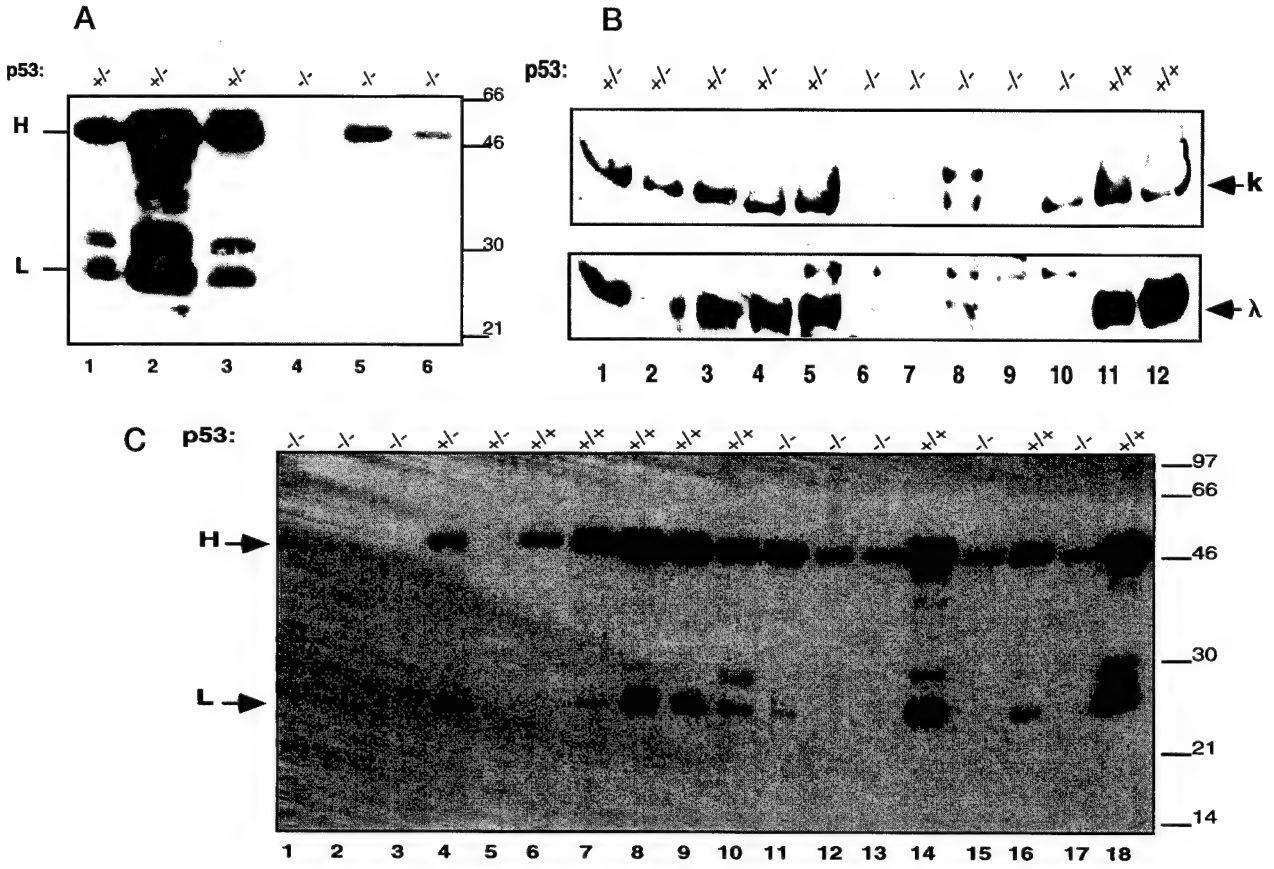

Fig. 2. *A*, analysis of tumors from $p53^{+/-}$ and $p53^{-/-}$ mice using anti-mouse immunoglobulin antibodies. Western blot analysis of a subset of tumors shown in Table 1 was performed using anti-mouse immunoglobulin (heavy and light) antibody as described in "Materials and Methods." The p53 genotype of the mice from which the tumors were derived is indicated *above* each lane. Protein molecular weight size markers (in thousands) are indicated by *arrows* to the *right*. The identity of each tumor shown can be found in Table 1 (*Lane 1*, tumor 1239; *Lane 2*, tumor 1337; *Lane 3*, tumor 1434; *Lane 4*, tumor 1280; *Lane 5*, tumor 1339; and *Lane 6*, tumor 1706). *B*, Western blot analysis of a subset of tumors shown in Table 1 was performed using either anti-mouse κ (*top*) or λ (*bottom*) antibody as described in "Materials and Methods." The p53 genotype of the mice from which the tumors were derived is indicated *above* each lane. The identity of each tumor shown can be found in Table 1 (*Lane 1*, tumor 967; *Lane 2*, tumor 1064; *Lane 3*, tumor 1334; *Lane 4*, tumor 1337; *Lane 5*, tumor 1434; *Lane 6*, tumor 1280; *Lane 7*, tumor 1339; *Lane 8*, tumor 1367; *Lane 9*, tumor 1706; *Lane 10*, tumor 1713; *Lane 11*, 1 μg of mouse immunoglobulin; and *Lane 12*: 2 μg of mouse immunoglobulin). *C*, analysis of tumors derived from $p53^{+/+}$/*Wnt1* and $p53^{-/-}$/*Wnt1* mice using anti-mouse immunoglobulin antibodies. Western blot analysis of tumors shown in Table 2 was performed using anti-mouse immunoglobulin (heavy and light) antibody as described in "Materials and Methods." The p53 genotype of the mice from which the tumors were derived is indicated *above* each lane. Protein molecular weight size markers (in thousands) are indicated by *arrows* to the *right*. The identity of each tumor shown can be found in Table 2 (*Lane 1*, tumor 460; *Lane 2*, tumor 477B; *Lane 3*, tumor Null-9; *Lane 4*, tumor Het-65B; *Lane 5*, tumor Het-73; *Lane 6*, tumor 2; *Lane 7*, tumor 10; *Lane 8*, tumor 30; *Lane 9*, tumor 70; *Lane 10*, tumor 75; *Lane 11*, tumor 98; *Lane 12*, tumor 154; *Lane 13*, tumor 162; *Lane 14*, tumor 372; *Lane 15*, tumor 388B; *Lane 16*, tumor 430; *Lane 17*, tumor 455; and *Lane 18*, 1 μg of mouse immunoglobulin). *Lanes 3, 4,* and *5* represent tumors derived from a $p53^{-/-}$ mouse and two $p53^{\pm}$ mice, respectively.

comparable between the two groups of mice. Consistent with the increased percentage of pre-B cells, bone marrow from $p53^{-/-}$ mice contained an increased percentage of cells expressing high levels of the heat-stable antigen, a protein expressed at high levels on pre-B and immature B cells (Ref. 9; data not shown). Frequencies of S7+ cells were not changed in the $p53^{-/-}$ bone marrow.

Mitogenic Responses of $p53^{-/-}$ *versus* $p53^{+/+}$ B Cells. To examine a potential relationship between p53 status and the ability of B lymphocytes to enter the cell cycle, we cultured the lymphocytes with different mitogens and measured S-phase entry by uptake of [^{3}H]thymidine into newly synthesized DNA (Fig. 5*C*). Ligation of sIgM using $F(ab')_2$ fragments of polyclonal anti-IgM antibody induces mature B cells to reenter the cell cycle (10). When cultured with increasing concentrations of $F(ab')_2$ fragments of anti-IgM antibody, splenic B cells from $p53^{-/-}$ synthesized significantly more DNA compared with splenic B cells from either $p53^{+/+}$ or $p53^{-/+}$ mice (Fig. 5*Ca*). This increased proliferative response could not be attributed to increased expression of sIgM by $p53^{-/-}$ B cells. Splenic B cells from all three groups of mice expressed comparable levels of sIgM, sIgD, heat-stable antigen, and the B cell-specific form of CD45 (B220) as determined by flow cytometry (data not shown).

The increased proliferative response of $p53^{-/-}$ B cells was not specific for sIgM ligation. When cultured with the polyclonal mitogen LPS, $p53^{-/-}$ splenic B cells synthesized significantly more DNA compared with splenic B cells derived from either $p53^{-/+}$ or $p53^{+/+}$ mice (Fig. 5*Cb*).

Table 2 Predicted p53 status of tumors derived from $p53^{+/+}$/*wnt1* and $p53^{-/-}$/*wnt1* mice

wnt1 tumor	Predicted p53 status[a]	Host's p53 genotype
2	-	+/+
10	wt	+/+
30	wt	+/+
70	wt	+/+
75	wt	+/+
98	wt	−/−
154	-	−/−
162	-	−/−
372	wt	+/+
388B	-	−/−
430	wt	+/+
455	-	−/−
460	-	−/−
477B	-	−/−

[a] wt, wild-type; −, non-wild-type.

The increased proliferative responses of B lymphocytes from the lymph nodes of $p53^{-/-}$ mice could not be attributed to increased numbers of B cells in $p53^{-/-}$ lymph nodes, because the percentages of lymph node B lymphocytes were comparable between all groups of mice (data not shown). In addition, we found no evidence that the increased proliferative responses of $p53^{-/-}$ B cells could be explained by a decreased apoptotic fraction when compared with $p53^{+/+}$ cells (data not shown). The results from Fig. 5*C* suggest that B lymphocytes derived from $p53^{-/-}$ mice are significantly more responsive to mitogenic stimulation, synthesizing more RNA (data not shown) and DNA in response to B-cell polyclonal stimuli.

p53 DNA-binding Sites in the Regulatory Regions of Immunoglobulin Genes. To further explore a potential relationship between p53 and regulation of immunoglobulin gene expression or immune function, we searched for p53 DNA binding sites in the regulatory regions of immunoglobulin genes. GenBank searches identified two potential p53 DNA consensus sites in both the human DQ52 region important for heavy chain rearrangement (4) and the human *VH6* gene promoter region important for regulation of immunoglobulin chain transcription (11). Analysis of the corresponding DQ52 region in the mouse revealed the presence of at least two potential p53 sites, suggesting that regulation by p53 may be conserved. In addition, we noticed a remarkable similarity of the KII site (4) to the p53 recognition element.

We tested the candidate sites for their ability to bind to p53 protein *in vitro* (Fig. 6*A*). Fig. 6*A* demonstrates a mobility shift of a p53 binding site from p21 (*Lanes 2*), as well as mobility shifts of homologous consensus p53 binding sites from the immunoglobulin gene regulatory regions KII (*Lane 6*), DQ52 (*Lanes 8* and *10*), and VH6 (*Lane 12*). No mobility shifts were evident in the absence of baculovirus p53 protein (Fig. 6*A*, *Lanes 1, 3, 5, 7, 9,* and *11*). Competition experiments showed that a high-affinity p53 binding site derived from the *p21* gene could compete with p53 binding to the KII site (Fig. 6*B*, *Lanes 3* and *4*), whereas a non-p53 binding site was a much weaker competitor (Fig. 6*B*, *Lanes 5* and *6*).

Correlation of p53 Induction with Sterile Transcription. Before the rearrangement of immunoglobulin genes, noncoding transcripts initiating upstream and extending beyond potential rearrangement sites are produced, spliced, and polyadenylated. The expression of the sterile transcripts $I\mu$ and μ^o, derived from the heavy chain locus and the light chain locus, respectively, may be a necessary prerequisite for immunoglobulin gene rearrangement (12-15). To determine whether p53 binding might regulate the expression of sterile transcripts and thus B-cell development, Ba/F3 (early B-cell progenitor cell line), HAC6 (pro-B-cell line), and μ (pre-B-cell line) were treated with the DNA damaging agent Adriamycin to induce p53. Adriamycin treatment of all three cell lines induced p53 protein (Fig. 7). In Adriamycin-treated Ba/F3 cells, the level of $I\mu$ transcripts increased 2- to 3-fold (Fig. 7). κ light chain sterile transcripts were not expected and were not detected in Ba/F3 cells due to their early stage of B-cell development. Adriamycin treatment of both HAC6 and μ cells resulted in the induction of the κ germ line sterile transcripts, but not $I\mu$ transcripts, which were already present at elevated levels.

Discussion

Our experiments provide a novel link between p53 and the immune response, and suggest the following model. Conserved p53 DNA binding sites located in the regulatory regions of immunoglobulin heavy and light chain genes may enhance sterile transcription and immunoglobulin gene rearrangement, which could facilitate B-cell maturation. Previous studies have implicated a role for p53 in B-cell maturation (2, 16-18). Host deficiency in p53 may lead to less efficient immunoglobulin gene rearrangement, abnormal B-cell maturation, and decreased tumor-specific immunoglobulin. Abnormal B-cell maturation in the context of complete p53 deficiency may predispose the host to lymphoid malignancy and infection. A significant number of $p53^{-/-}$ mice die due to infectious abscesses, in the absence of evident tumor (19).

It has been shown previously that exposure of pre-B cells to ionizing radiation induced differentiation and κ chain gene expression (2). We would propose that binding of p53 to the KII site upstream of the mouse κ chain J cluster genes may facilitate the differentiation of B cells and the production of κ chain after DNA damage. The results showing induction of germ line κ chain expression after p53 induction (Fig. 7*B*) are consistent with this hypothesis. Future experiments will determine whether p53 is required for the DNA damage-induced sterile transcription.

It is not clear that the decreased immunoglobulin deposition in p53-null mice is due to a loss of an antitumor response, and the precise origin of the immunoglobulin within the tumors of $p53^{+/-}$ mice is unknown. We speculate that plasma cells whose normal maturation was stimulated by the tumors may secrete immunoglobulin, which is then deposited within the tumors. The immunoglobulin deposition may recruit other effectors with the capacity to eliminate tumor cells. We suspect that some of the immunoglobulin we found

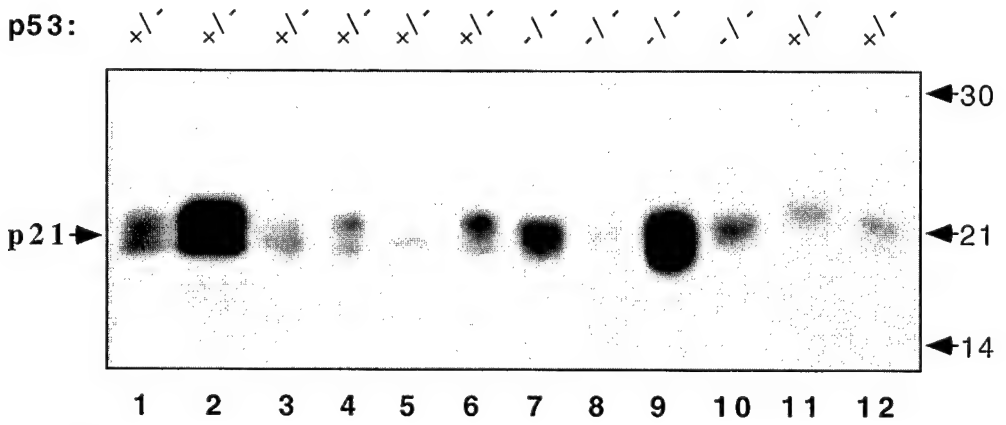

Fig. 3. Analysis of $p21^{WAF1/CIP1}$ expression in tumors derived from $p53^{+/-}$ and $p53^{-/-}$ mice. Western blot analysis of a subset of the tumors shown in Table 1 was performed using anti-mouse $p21^{WAF1/CIP1}$ polyclonal antibody OS100 as described in "Materials and Methods." The p53 genotype of the mice from which the tumors were derived is indicated *above* each lane. Protein molecular weight size markers (in thousands) are indicated by *arrows* to the *right*. The identity of each tumor shown in this figure can be found in Table 1 (*Lane 1*, tumor 967; *Lane 2*, tumor 1434; *Lane 3*, tumor 971; *Lane 4*, tumor 1005; *Lane 5*, tumor 1087; *Lane 6*, tumor 1239; *Lane 7*, tumor 1327; *Lane 8*, tumor 1367; *Lane 9*, tumor 1687; *Lane 10*, tumor 1713; *Lane 11*, tumor 1334; *Lane 12*, tumor 1640).

associated with cellular fragments may represent residue of dying cells. However, the deposited immunoglobulin did not appear to be specific for such fragments because some was associated with tumor cells and some with rare small round cells.

It is also not clear if less efficient immunoglobulin gene rearrangement in the host is the underlying mechanism of decreased immunoglobulin deposition in p53-deficient tumors. Because our initial studies involved the p53 status of the host mice, we favor a host factor to explain the differences in immunoglobulin deposition. It is interesting that one of the mouse tumors (1337) from a $p53^{+/-}$ mouse acquired a second hit in the *p53* gene with a resultant $p53^{-/-}$ tumor genotype.[4] The relatively high levels of immunoglobulin in this tumor are consistent with the hypothesis that a host factor may be responsible for the difference in immunoglobulin deposition between tumors from $p53^{+/-}$ and $p53^{-/-}$ mice. Our observation that sera derived from wild-type p53-containing tumor-bearing mice cross-reacted with antigens from tumors derived from both $p53^{+/+}$ and $p53^{-/-}$ mice also correlates the p53 status of the host to the presumptive immune response.

It is well known that in ataxia telangiectasia there is defective VDJ recombination, immune deficiency, and an increased incidence of lymphoid malignancy (20). It has been shown that p53 induction after exposure of AT cells to DNA damaging agents is abnormally delayed (21). Therefore, it is conceivable that the defect in VDJ recombination may be due to abnormal p53 function in AT cells, *i.e.*, a downstream effect of abnormal ATM signaling (22). The ability of p53 to bind to regulatory regions of immunoglobulin genes, which are critical for VDJ recombination, coupled with the increased numbers of immature B cells in $p53^{-/-}$ mice, is consistent with the possibilities that p53 may regulate VDJ recombination and that defects in such regulation may underlie certain defects in ataxia telangiectasia. Future studies will examine the effects of replacement of p53 on VDJ recombination and maturation of B cells derived from AT patients.

Because $p53^{-/-}$ mice appear to be predisposed to infectious disease (19), it is unlikely that the p53 status of the host is only important after tumors have developed. In addition, the high prevalence of lymphoid malignancy in $p53^{-/-}$ mice has not been adequately explained. We would propose that the absence of p53 contributes to a B-cell maturation defect that may then predispose p53-null mice to developing lymphomas.

[4] L. A. Donehower, unpublished observations.

Materials and Methods

Cell Lines and Culture Conditions. The human glioblastoma cell line GM was a gift from W. Edward Mercer (Thomas Jefferson University). GM cells were maintained in culture as described previously (23). Induction of the exogenous mouse mammary tumor virus promoter-driven wild-type *p53* gene in GM cells was accomplished by incubating them in the presence of 1 μM dexamethasone for 20 h as described previously (24). M3 murine lymphoma cells were maintained in culture as described previously (6). Temperature shift to 32°C, to induce the wild-type conformation of the exogenous p53 temperature-sensitive mutant, was carried out for 24 h before harvesting the cells as described previously (25). The murine cell lines μ (26), HAC6 (27), and Ba/F3 (Ref. 28; a gift from Richard J. Jones, Johns Hopkins University, Baltimore, MD) were cultured as described previously and treated with 0.2 μg/ml Adriamycin for 20 h before harvesting.

Anti-Mouse $p21^{WAF1/CIP1}$ Antibodies. GST-muWAF1/CIP1 fusion protein, containing amino acids 1-164 of $p21^{WAF1/CIP1}$, was expressed in *Escherichia coli* after induction with isopropyl-1-thio-β-D-galactopyranoside for 2 h at 37°C. Cells were lysed by passage through a French Pressure Cell (SLM Instruments), and the insoluble GST-muWAF1/CIP1 was recovered by centrifugation. Approximately 10 mg of insoluble GST-muWAF1/CIP1 protein was resuspended in 2.5 ml of SDS-PAGE sample buffer and applied to a Bio-Rad PrepCell for purification. Eluted fractions from the PrepCell containing GST-muWAF1/CIP1 protein were pooled and dialyzed against 1× PBS overnight at 4°C. At this point, the protein remained soluble and was further concentrated using an Amicon Stir Cell.

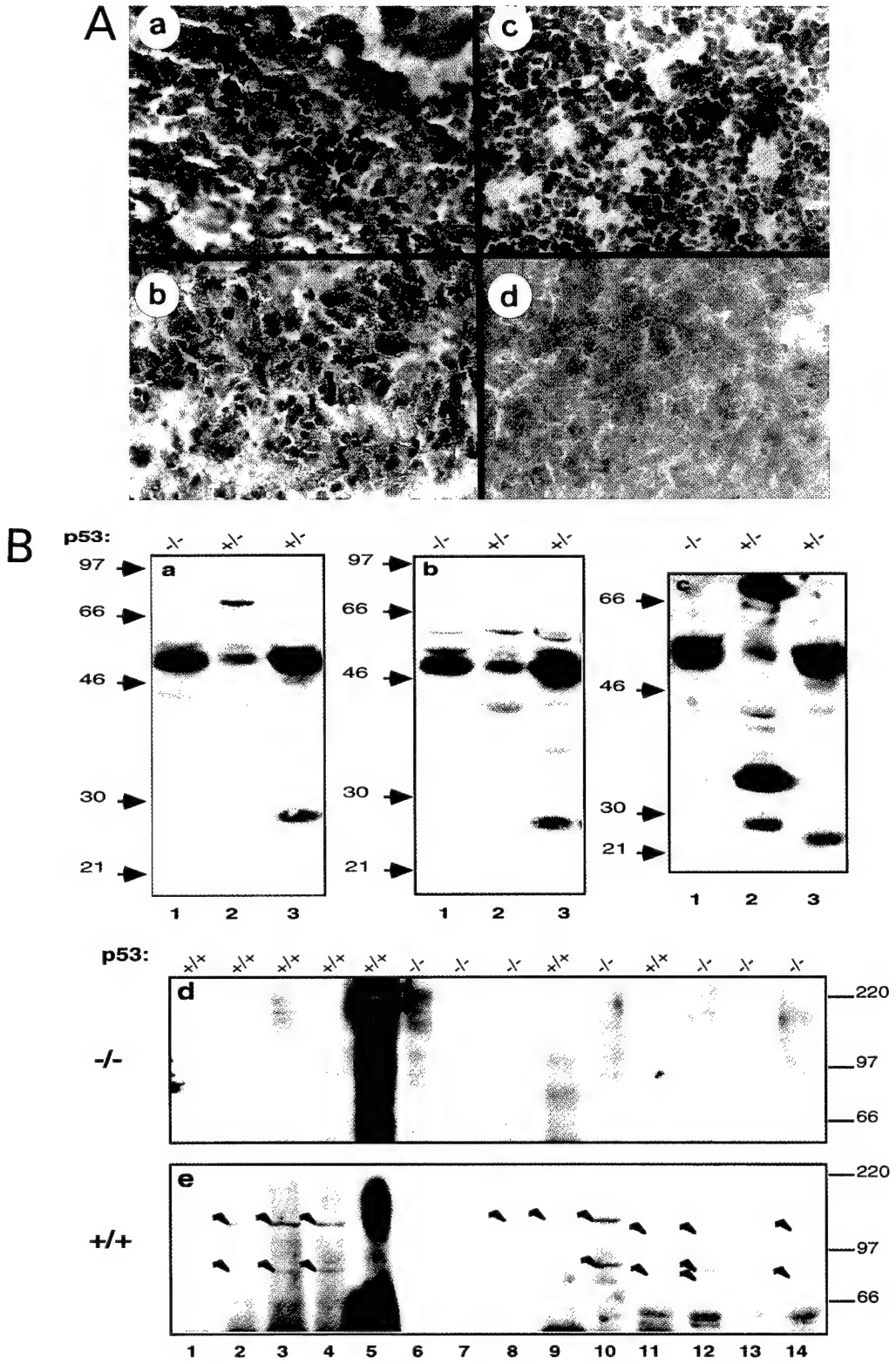

Fig. 4. *A*, immunohistochemical staining of tumors derived from $p53^{+/-}$ and $p53^{-/-}$ mice. *a–d*, antibodies directed against murine IgG were used to stain tumors derived from $p53^{+/-}$ (*a* and *b*) and $p53^{-/-}$ (*c* and *d*) mice. The identity of each tumor shown can be found in Table 1 (*a*, tumor 1239; *b*, tumor 1337; *c*, tumor 1280; *d*, tumor 1706). *B*, reactivity of wild-type p53 or $p53^{-/-}$ host sera against tumor antigens. *a–c*, tumor lysates were prepared from spontaneously arising tumors in a $p53^{-/-}$ mouse (*Lane 1*), or two different $p53^{+/-}$ mice (*Lanes 2* and *3*) and immunoblotted using sera derived from the same mice (sera in *A*: tumor in *Lane 1*; sera in *B*: tumor in *Lane 3*; sera in *C*: tumor in *Lane 2*) as described in "Materials and Methods." The p53 genotype of the mice from which the tumors were derived is indicated *above* each lane. Protein molecular weight size markers (in thousands) are indicated by *arrows* to the *left* of each panel. *d* and *e*, Western analysis of $p53^{+/+}$/*Wnt1* and $p53^{-/-}$/*Wnt1* tumors using pooled sera derived from either $p53^{-/-}$/*Wnt1* (*D*) or $p53^{+/+}$/*Wnt1* (*E*) tumor-bearing mice. The identity of each tumor shown can be found in Table 2 (*Lane 1*, tumor 2; *Lane 2*, tumor 10; *Lane 3*, tumor 30; *Lane 4*, tumor 70; *Lane 5*, tumor 75; *Lane 6*, tumor 98; *Lane 7*, tumor 154; *Lane 8*, tumor 162; *Lane 9*, tumor 372; *Lane 10*, tumor 388B; *Lane 11*, tumor 430; *Lane 12*, tumor 455; *Lane 13*, tumor 460; *Lane 14*, tumor 477).

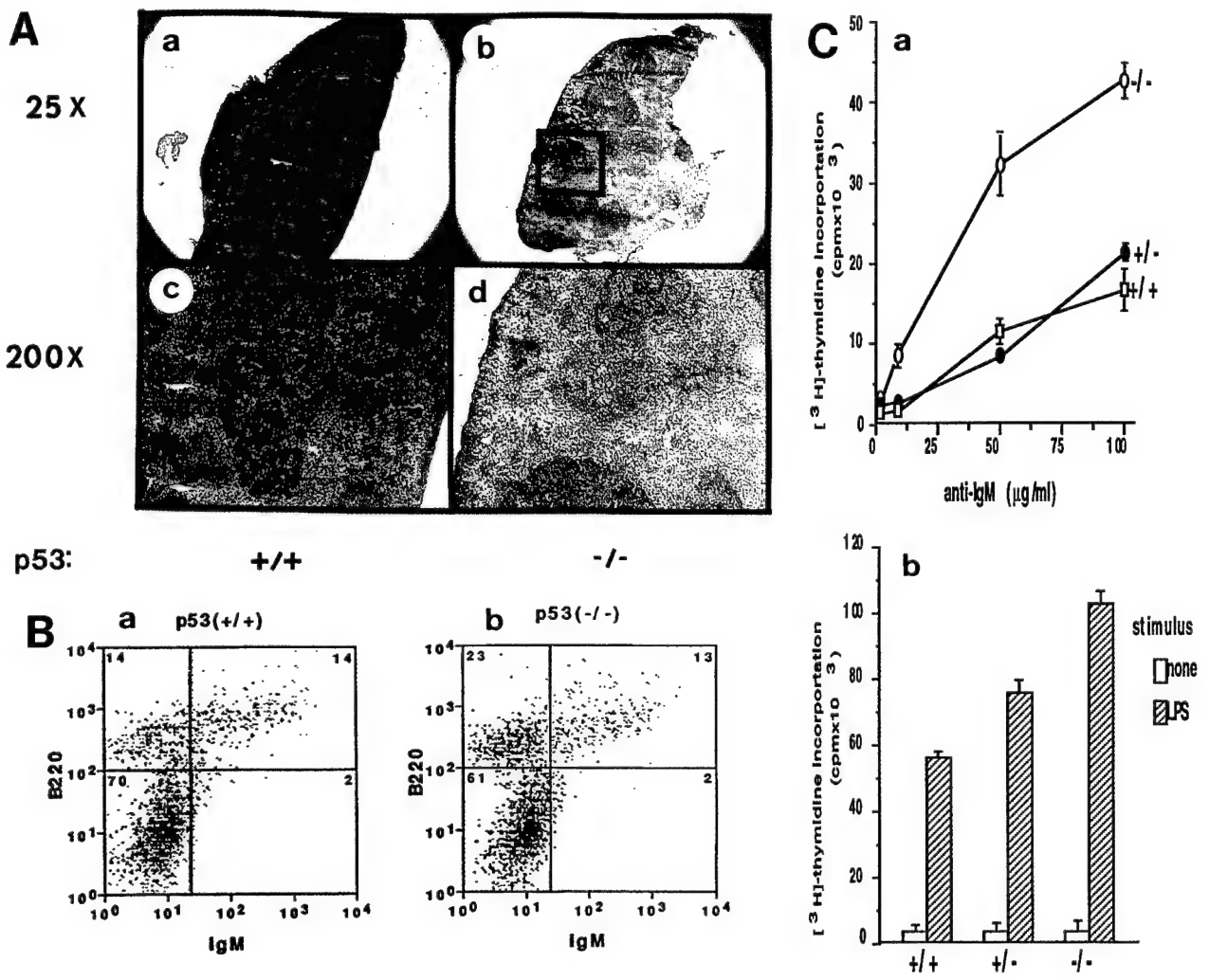

Fig. 5. *A, a–d*, increased white pulp in spleens derived from $p53^{+/+}$ and $p53^{-/-}$ mice. Spleens from a $p53^{+/+}$ (*left*) or a $p53^{-/-}$ mouse (*right*) were cryosectioned and stained with H&E. Photomicrographs are shown at 25× (*top*) or 200× (*bottom*). Bottom photomicrographs represent a magnification of the area enclosed by the *black boxes* in the top photomicrographs. *B, a* and *b*, analysis of B-cell compartments in the bone marrows of $p53^{+/+}$ and $p53^{-/-}$ mice. Bone marrow cells were obtained from the femurs and tibias of either $p53^{+/+}$ or $p53^{-/-}$ mice and stained with a combination of phycoerythrin-conjugated anti-B220 and FITC-conjugated $F(ab')_2$ anti-mouse IgM. Cells were analyzed on a FACScan. Values represent the percentage of cells in each quadrant. We show one of two representative experiments. *C, a* and *b*, proliferative responses of splenic B cells. B cells were isolated from the spleens of either $p53^{+/+}$, $p53^{+/-}$, or $p53^{-/-}$ mice. B cells were cultured for 72 h with increasing concentrations of $F(ab')_2$ fragments of rabbit-anti mouse IgM (*top*), or with 50 mg/ml LPS (*bottom*). [^{3}H]Thymidine was included for the final 12 h of culture. We show one of two representative experiments.

For generation of rabbit polyclonal antibodies, New Zealand white rabbits were injected intranodally with 50 µg of purified GST-muWAF1/CIP1 on five successive occasions. Rabbit sera were initially screened by capture ELISA as described (29) and subsequently purified over Protein A Agarose (Pharmacia, Uppsala, Sweden).

For mouse monoclonals, female (BALB/c × C57B1/6) F1 mice (Charles River Breeding Laboratories) were immunized by i.p. injection with 10 µg of electroeluted GST-muWAF1/CIP1 protein in Ribi adjuvant (Ribi Immunochem Research, Inc.) at weeks 0, 4, 7, and 15. Serum was obtained from the intraorbital plexus on weeks 9 and 16. Serum titers were measured by capture ELISA using GST-muWAF1/CIP1 or GST-huMDM2 as described previously (30). Specificity toward $p21^{WAF1/CIP1}$ was determined by immunoblot using a 1:500 dilution of serum on purified GST-WAF1/CIP1 and on lysates of mouse fibroblasts expressing $p21^{WAF1/CIP1}$. $p21^{WAF1/CIP1}$ was induced in mouse fibroblasts by treatment of cells with actinomycin D at 0.5 nM final concentration for 48 h followed by lysis in Lane's lysis buffer with protease inhibitors. Antigen-antibody complexes were detected by incubation with horseradish peroxidase-conjugated goat anti-mouse IgG heavy and light chain (Pierce, Rockford, IL) followed by development with enhanced chemiluminescence (Amersham, Amersham Place, England) and exposure of blots to X-ray film. Candidate hybridomas were subcloned twice by limiting dilution. Monoclonal antibodies were purified from mouse ascites by chromatography over Protein G Plus-Agarose (Oncogene Research Products, Calbiochem, Cambridge, MA).

Mice, Sera, and Tumor Samples. Healthy 4-6-week-old female $p53^{+/+}$, $p53^{+/-}$, and $p53^{-/-}$ transgenic mice were obtained from Taconic Farms (Germantown, NY). The mice were euthanized using an approved Institutional Animal Care and Use Committee Protocol, which followed recommendations of the Panel on Euthanasia of the American Veterinary Medical Association. Spleens, intestines, and thymuses were snap frozen in liquid nitrogen and kept at −80°C until further use. Sera from normal or tumor-bearing mice were stored at −80°C until used. Tumors were harvested from tumor-bearing mice (10 $p53^{+/-}$, 9 $p53^{+/-}$, 7 $p53^{+/+}$/*wnt1*, and 7 $p53^{-/-}$/*wnt1*) and stored at −80°C until protein lysates were prepared, or until cryosectioning as described previously (30). We cryosectioned and performed H&E staining of the tumors to confirm their neoplastic origin and to assure that the samples were composed primarily (>95%) of cancer cells *versus* infiltrating cells or stromal elements (data not shown).

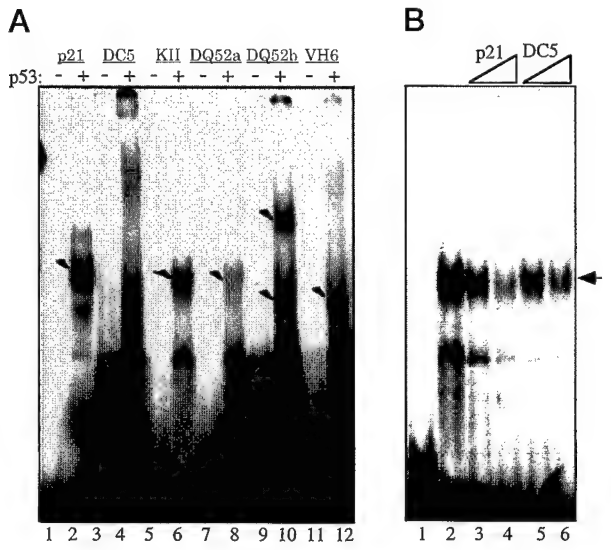

Fig. 6. Analysis of p53 binding to putative DNA consensus sites in the regulatory regions of immunoglobulin genes. *A*, EMSA results showing p53 binding to a p21 site (*Lane 2*), a nonspecific site (DC5; *Lane 4*), a KII site (*Lane 6*), DQ52 sites (*Lanes 8* and *10*), and a VH6 site (*Lane 12*). *Lanes 1, 3, 5, 7, 9,* and *11* contain no baculovirus p53 protein. *B*, EMSA results demonstrating p53 binding to a KII site (*Lane 2*) and competition by increasing concentration (10× and 20×) of a p21 site (*Lanes 3* and *4*) or a nonspecific competitor (*Lanes 5* and *6*).

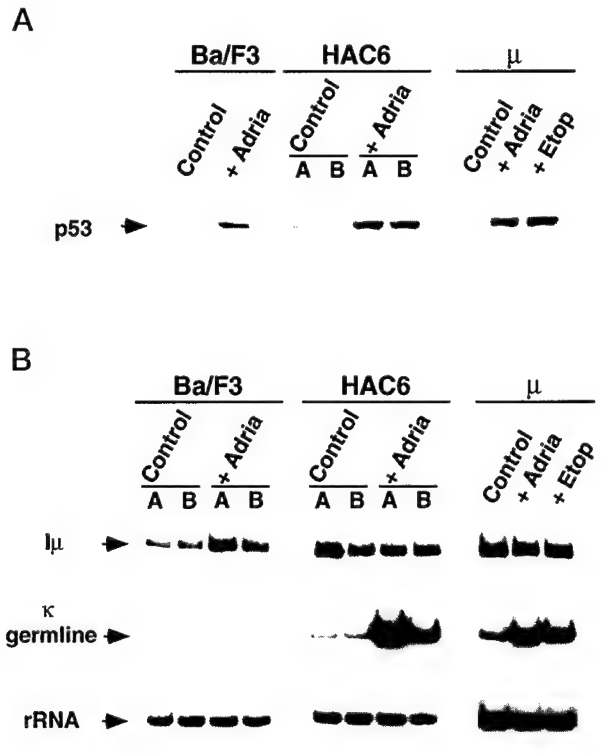

Fig. 7. Analysis of sterile transcripts after p53 induction by Adriamycin in Ba/F3, HAC6, and μ cells. p53 was detected by Western blot analysis. The following number of PCR cycles were used in the linear range: Ba/F3 cells: Iμ (30 cycles), κ germ line (30 cycles); HAC6 cells: Iμ (15 cycles), κ germ line (30 cycles); and μ cells: Iμ (15 cycles), κ germ line (25 cycles). 28S rRNA was detected using five cycles of PCR.

Western Blot Analysis. Equivalent amounts of protein from mouse tumors or cell lysates were separated by SDS-PAGE using 15% resolving gels, transferred to Immobilon P membrane (Millipore, Bedford, MA), and immunoblotted with either $p21^{WAF1/CIP1}$ antibodies (see above), anti-mouse IgG (heavy and light) antibodies (Pierce), or polyclonal mouse κ or λ chain-specific antibodies (Cappell, Durham, NC) as described previously (25).

EMSAs. The mouse anti-human p53 monoclonal antibody pAb421 (Ab1; Oncogene Research Products, Calbiochem) was used to detect specific DNA binding by p53 using EMSAs as described previously (31), except that either a p21 binding site was used as the probe (5′-CAGGAACATGTCCCAACATGTTGAGC-3′; site 1; Ref. 30), or putative p53 sites from immunoglobulin regulatory regions were used (Table 3). The DNA binding buffer contained the following in 20 μl: 10% glycerol, 20 mM HEPES (pH 7.5), 25 mM KCl, 2 mM DTT, 2 mM $MgCl_2$, 0.2% NP40, 1 μg poly(deoxyinosinic-deoxycytidylic acid), and 2 μg of baculovirus-produced wild-type p53 (32) (gift from B. Vogelstein, Johns Hopkins University). The cell lysis buffer was prepared as described previously (33), except that it also contained 1% antipain (Sigma, St. Louis, MO), 1% leupeptin (Sigma), 1% pepstatin A (Sigma), 1% chymostatin (Sigma), and 0.1% AEBSF (Oncogene Research Products, Calbiochem).

Stimulation of B-Cell Proliferation. LPS (from *Salmonella typhosa*) was purchased from Sigma. Rabbit antibody specific for mouse IgM was purified from the sera of rabbits immunized with mouse IgM by chromatography on protein A-Sepharose (Sigma). The purified immunoglobulin was digested with papain to generate F(ab′) fragments as described (34). Bone marrow cells were flushed from the femurs and tibias of individual $p53^{+/+}$ and $p53^{-/-}$ mice. Red blood cells were lysed by osmotic shock in Gey's solution (35). Mature B cells were isolated from the spleens of individual $p53^{+/+}$, $p53^{+/-}$, and $p53^{-/-}$ mice exactly as described (36). Lymph node cells were isolated from pooled axillary, brachial, inguinal, and mesenteric lymph nodes of individual $p53^{+/+}$, $p53^{+/-}$, and $p53^{-/-}$ mice. B cells (2×10^5/well) were cultured in B-cell assay medium [RPMI 1640 with 10% FCS, 0.1 mM nonessential amino acids, OPI (Life Technologies; proprietary formula), 100 mM glutamine, 100 units/ml penicillin, 100 μg/ml streptomycin, and 50 μM 2-mercaptoethanol] with either $F(ab')_2$ fragments of rabbit anti-mouse IgM, or with 50 μg/ml LPS in 96-well flat-bottom plates (Costar). To measure entry into S phase, [^{3}H]thymidine (1 μCi/well) was included for the final 12 h of a 72-h culture. Lymph node cells (2×10^5/well) were cultured with either $F(ab')_2$ fragments of rabbit anti-mouse IgM, or with concanavalin A in 96-well flat-bottom plates. To measure entry into S phase, [^{3}H]thymidine (1 μCi/well) was included for the final 12 h of culture. Thymidine incorporation was determined by liquid scintillative spectrometry.

FACS. Phycoerythrin-conjugated antibody specific for mouse CD45R (B220) and phycoerythrin-conjugated antibody specific for mouse Thy-1.2 were purchased from PharMingen (San Diego, CA). FITC-conjugated goat $F(ab')_2$ antibody specific for mouse IgM was purchased from Jackson Immunoresearch Laboratories, Inc. (West Grove, PA). Cells (5×10^5–10^6/group) were equilibrated in staining buffer (PBS with 0.1% BSA, 0.1% NaN_3) for 30 min on ice. Antibody was added (1 μg/ml in staining buffer), and cells were incubated for an additional 30 min on ice. After two washes with staining buffer, cells were fixed in 1% paraformaldehyde and kept at 4°C until analyzed on a FACScan (Becton Dickinson, San Jose, CA) using Lysis II software.

RT-PCR of Immunoglobulin Sterile Transcripts. Total RNA was isolated from μ, HAC6, and Ba/F3 cell lines using the TOTALLY RNA isolation kit (Ambion), and 5 μg was reverse transcribed using SuperScript RT II (Life Technologies) according to the manufacturer's protocol. PCR assays were carried out using one-tenth of the RT reaction in a final volume of 20 μl containing 0.1 μCi (γ-^{32}P) dCTP as described previously (37). The following primer pairs were used to amplify the Iμ transcript: 5′-GGT GGC TTT GAA GGA ACA ATT CCA C-3′ and 5′-TCT GAA CCT TCA AGG ATG CTC TTG-3′. PCR was carried out for 15 or 30 cycles of denaturing at 95°C for 30 s, annealing at 60°C for 60 s, and chain elongation at 72°C for 30 s. 28S rRNA was used as a internal control for amplification efficiency as described previously (37). Primers and conditions for κ light chain germ line transcript were done as described (4).

immunoglobulin enhancers by the helix-loop-helix protein id: implications for B-lymphoid-cell development. Mol. Cell. Biol., *11:* 6185-6191, 1991.

28. Palacios, R., and Steinmetz, M. Il-3-dependent mouse clones that express B-220 surface antigen, contain Ig genes in germ-line configuration, and generate B lymphocytes *in vivo*. Cell, *41:* 727-734, 1985.

29. Smith, K. J., Johnson, K. A., Bryan, T. M., Hill, D. E., Markowitz, S., Wilson, J. K. V., Paraskeva, C., Peterson, G. M., Hamilton, S. R., Vogelstein, B., and Kinzler, K. W. The APC gene product in normal and tumor cells. Proc. Natl. Acad. Sci. USA, *90:* 2846-2850, 1993.

30. El-Deiry, W. S., Tokino, T., Waldman, T., Oliner, J. D., Velculescu, V. E., Burrell, M., Hill, D. E., Healy, E., Rees, J. L., Hamilton, S. R., Kinzler, K. W., and Vogelstein, B. Topological control of $p21^{WAF1/CIP1}$ expression in normal and neoplastic tissues. Cancer Res., *55:* 2910-2919, 1995.

31. Hupp, T. R., Meek, D. W., Midgley, C. A., and Lane, D. P. Regulation of the specific DNA binding function of p53. Cell, *71:* 875-886, 1992.

32. El-Deiry, W. S., Kern, S. E., Pietenpol, J. A., Kinzler, K. W., and Vogelstein, B. Definition of a consensus binding site for p53. Nat. Genet., *1:* 45-49, 1992.

33. Schreiber, E., Matthias, P., Muller, M. M., and Schaffner, W. Rapid detection of octamer binding proteins with "mini-extracts," prepared from a small number of cells. Nucleic Acids Res., *17:* 6419, 1989.

34. Andrew, S. M., and Titus, J. A. Fragmentation of immunoglobulin M. *In:* J. E. Coligan, A. M. Kruisbeek, D. H. Margulies, E. M. Shevach, and W. Strober (eds.), Current Protocols in Immunology. pp. 2.10.1-2.10.2. New York: John Wiley & Sons, Inc., 1994.

35. Mishell, B. B., and Shiigi, S. M. Preparation of mouse cell suspensions. *In:* B. B. Mishell and S. M. Shiigi (eds.), Selected Methods in Cellular Immunology. New York: W. H. Freeman & Co., 1980.

36. Wechsler, R. J., and Monroe, J. G. Immature B lymphocytes are deficient in expression of the src-family kinases $p59^{fyn}$ and $p55^{fgr}$. J. Immunol., *154:* 1919-1929, 1995.

37. Choi, J. K., Shen, C. P., Radomask, H. S., Eckhardt, L. A., and Kadesch, T. E47 activates IgH and TdT loci in non-B cells. EMBO J., in press, 1996.

Deficiency of *p53* accelerates mammary tumorigenesis in *Wnt-1* transgenic mice and promotes chromosomal instability

Lawrence A. Donehower,[1] Lucy A. Godley,[2] C. Marcelo Aldaz,[3] Ruth Pyle,[1] Yu-Ping Shi,[4] Dan Pinkel,[4] Joe Gray,[4] Allan Bradley,[5] Daniel Medina,[6] and Harold E. Varmus[2,7]

[1]Division of Molecular Virology, Baylor College of Medicine, Houston, Texas 77030 USA; [2]Varmus Laboratory, National Cancer Institute, Bethesda, Maryland 20892 and Department of Biochemistry and Biophysics, University of California, San Francisco, California 94143 USA; [3]Department of Carcinogenesis, University of Texas M.D. Anderson Cancer Center—Science Park, Smithville, Texas 78957 USA; [4]Division of Molecular Cytometry, Department of Laboratory Medicine, University of California at San Francisco, San Francisco, California 94143 USA; [5] Institute for Molecular Genetics and Howard Hughes Medical Institute, Baylor College of Medicine, Houston, Texas 77030 USA; [6]Department of Cell Biology, Baylor College of Medicine, Houston, Texas 77030 USA; [7]Office of the Director, National Institutes of Health, Bethesda, Maryland 20892 and Department of Microbiology and Immunology, University of California, San Francisco, California 94143 USA

GENES & DEVELOPMENT 9:882–895 © 1995 by Cold Spring Harbor Laboratory Press ISSN 0890-9369/95 $5.00

Deficiency of *p53* accelerates mammary tumorigenesis in *Wnt-1* transgenic mice and promotes chromosomal instability

Lawrence A. Donehower,[1] Lucy A. Godley,[2] C. Marcelo Aldaz,[3] Ruth Pyle,[1] Yu-Ping Shi,[4] Dan Pinkel,[4] Joe Gray,[4] Allan Bradley,[5] Daniel Medina,[6] and Harold E. Varmus[2,7]

[1]Division of Molecular Virology, Baylor College of Medicine, Houston, Texas 77030 USA; [2]Varmus Laboratory, National Cancer Institute, Bethesda, Maryland 20892 and Department of Biochemistry and Biophysics, University of California, San Francisco, California 94143 USA; [3]Department of Carcinogenesis, University of Texas M.D. Anderson Cancer Center—Science Park, Smithville, Texas 78957 USA; [4]Division of Molecular Cytometry, Department of Laboratory Medicine, University of California at San Francisco, San Francisco, California 94143 USA; [5] Institute for Molecular Genetics and Howard Hughes Medical Institute, Baylor College of Medicine, Houston, Texas 77030 USA; [6]Department of Cell Biology, Baylor College of Medicine, Houston, Texas 77030 USA; [7]Office of the Director, National Institutes of Health, Bethesda, Maryland 20892 and Department of Microbiology and Immunology, University of California, San Francisco, California 94143 USA

By crossing mice that carry a null allele of *p53* with transgenic mice that develop mammary adenocarcinomas under the influence of a *Wnt-1* transgene, we have studied the consequences of p53 deficiency in mammary gland neoplasia. In *Wnt-1* transgenic mice homozygous for the *p53* null allele, tumors appear at an earlier age than in animals heterozygous or wild-type at the *p53* locus. About half of the tumors arising in *p53* heterozygotes exhibit loss of the normal *p53* allele, implying selection for p53-deficient cells. Mammary tumors lacking p53 display less fibrotic histopathology and increased genomic instability with aneuploidy, amplifications, and deletions, as detected by karyotype analysis and comparative genomic hybridization. In one tumor, the amplified region of chromosome 7 had an ectopically expressed *int-2/FGF3* proto-oncogene, a gene known to cooperate with *Wnt-1* in the production of mammary tumors. These findings favor a model in which p53 deficiency relaxes normal restraints on chromosomal number and organization during tumorigenesis.

[*Key Words*: *p53*; *Wnt-1*; mammary tumors; genomic instability; mouse; tumor model]

Received January 4, 1995; revised version accepted February 22, 1995.

The *p53* tumor suppressor gene is the known gene mutated most frequently in human cancers, with deletions and point mutations observed in almost half of all tumors and in about one-fourth of all sporadic breast cancers (Greenblatt et al. 1994). In addition to their frequent occurrence in spontaneously arising tumors, *p53* mutations have also been identified in the germ line of some individuals with an inherited cancer predisposition called Li–Fraumeni syndrome (Malkin et al. 1990; Srivastava et al. 1990). The presence or absence of *p53* mutations in a human tumor may have important clinical implications. A number of studies have shown that tumors missing wild-type *p53* are likely to have a relatively poor prognosis (Callahan 1992; Thor et al. 1992). Moreover, tumors with mutant *p53* appear to be significantly more resistant to the effects of radiation and other anticancer drugs (Lowe et al. 1993a, 1994).

The importance of *p53* loss in cancer is illustrated further by genetically engineered mice that contain one or two defective germ-line *p53* alleles (Donehower et al. 1992; Jacks et al. 1994; Purdie et al. 1994). Mice with two defective *p53* alleles (*p53*−/−) are developmentally normal, but all succumb to tumors by the age of 10 months (Donehower et al. 1992; Harvey et al. 1993a,b; Jacks et al. 1994; Purdie et al. 1994). Mice with a single defective *p53* allele (*p53*+/−) acquire tumors at a later age, but by 18 months half of these mice have developed cancer (Harvey et al. 1993a). Lymphomas and sarcomas are the most frequently observed tumor types in the p53-deficient animals, whereas carcinomas (including mammary adenocarcinomas) are only seen infrequently.

We have now developed an experimental model to study the role of p53 in mammary tumorigenesis by crossing mice that carry a disrupted *p53* allele with transgenic mice programmed to express a proto-oncogene in the mammary gland. We show that the biological and genetic properties of mammary tumors initiated by ectopic expression of *Wnt-1* are dramatically influenced by the presence or absence of p53. Mammary adenocarcinomas appear earlier in both male and female *p53*−/− animals. About half of the tumors arising in *p53* heterozygotes show loss of heterozygosity, although they

are not detected earlier than tumors that retain wild-type *p53*. p53-deficient tumors differ histologically from p53-containing tumors and exhibit several manifestations of genomic instability: aneuploidy in metaphase spreads and genomic regions of increased and decreased DNA sequence copy number as seen by comparative genomic hybridization. These results with transgene-induced cancers in animals extend previous studies with cultured cell lines (Bischoff et al. 1990; Livingstone et al. 1992; Yin et al. 1992) to support a model for p53 as a cell-cycle checkpoint protein whose loss leads to karyotypic instability and cancer.

Results

Mammary tumors are detected earlier in Wnt-1 *transgenic animals lacking a normal* p53 *gene*

To determine the effect of germ-line loss of *p53* alleles on *Wnt-1*-induced mammary tumorigenesis, we crossed p53-deficient mice with *Wnt-1* transgenic mice (*Wnt-1 TG*). The transgene in the *Wnt-1 TG* mice mimics a mouse mammary tumor virus (MMTV) insertion at the *Wnt-1* locus, with the MMTV long terminal repeat (MMTV LTR) in the opposite transcriptional orientation to the mouse *Wnt-1* gene. Previous studies have verified ectopic expression of the *Wnt-1* transgene in the mammary gland, accompanied by marked mammary gland hyperplasia in both female and male transgenic animals (Tsukamoto et al. 1988; Kwan et al. 1992). Because of the hyperplasia in the *Wnt-1 TG* female mammary glands, the animals are unable to nurse their pups. For this reason, we used only *Wnt-1 TG* males in crosses to the p53-deficient mice. Following the crosses, 12 categories of animals were maintained on the basis of different combinations of genotypes: males and females that carry or lack the *Wnt-1* transgene and exhibit one of the three possible *p53* genotypes (+/+, +/−, or −/−). At least 16 virgin animals in each category were maintained for up to 1 year of age while being monitored weekly for tumors (see Materials and methods).

No mammary adenocarcinomas were observed in any males and females without the *Wnt-1* transgene, regardless of *p53* genotype. As expected, nontransgenic *p53*−/− animals developed nonmammary tumors within the first several months of life and all succumbed to cancer by 9 months of age, consistent with previous experience in other genetic backgrounds (Harvey et al. 1993a,b; Jacks et al. 1994; Purdie et al. 1994). In addition, 4 of 27 *p53*+/− mice developed nonmammary tumors by 1 year of age at a rate similar to that observed previously (Harvey et al. 1993a). No tumors of any kind were observed in the nontransgenic *p53*+/+ animals.

All of the female mice containing the *Wnt-1* transgene developed mammary adenocarcinomas by 41 weeks of age (Fig. 1A). Tumors were detected in *Wnt-1 TG p53*+/+ females at a median age of 22.5 weeks, a rate similar to that observed previously for *Wnt-1 TG* females (Tsukamoto et al. 1988; Kwan et al. 1992; Shackleford et al. 1993). Likewise, tumors appeared in the *Wnt-1 TG*

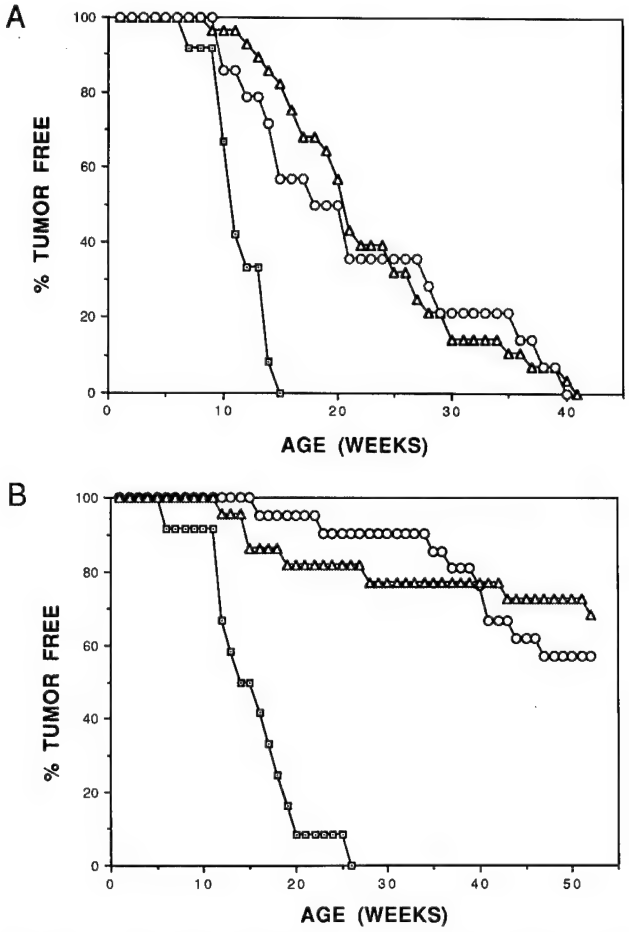

Figure 1. Tumor incidence in *Wnt-1 TG* mice with wild-type and defective germ-line *p53* alleles. The percentage of animals in each group free of palpable tumors (~0.5 cm in diam.) was plotted at weekly intervals. (*A*) *Wnt-1 TG* females. Sixteen *Wnt-1 TG p53*−/− (□), 32 *Wnt-1 TG p53*+/− (△), and 16 *Wnt-1 TG p53*+/+ (○) virgin females were monitored for mammary adenocarcinomas. (*B*) *Wnt-1 TG* males. Twelve *Wnt-1 TG p53*−/− (□), 22 *Wnt-1 TG p53*+/− (△), and 21 *Wnt-1 TG p53*+/+ (○) males were monitored for mammary tumors up to 1 year of age.

p53+/− females with a median time of 23 weeks, suggesting that inheritance of a single normal *p53* allele does not confer any increase in susceptibility to tumor formation. In contrast, tumors were detected significantly earlier in *Wnt-1 TG* females with two defective germ-line *p53* alleles (Fig. 1A). All of the females with the *Wnt-1 TG p53*−/− genotype developed at least one mammary tumor between the ages of 7 and 15 weeks, with a mean time of 11.5 weeks.

Nine of 21 (43%) *Wnt-1 TG p53*+/+ males and 7 of 22 (32%) *Wnt-1 TG p53*+/− males developed mammary tumors by the age of 1 year (Fig. 1B), proportions slightly greater than observed for *Wnt-1 TG* males in previous studies (Tsukamoto et al. 1988; Kwan et al. 1992; Shackleford et al. 1993). The Kaplan–Meier plots are not superimposable for these two cohorts, but the rates of ap-

pearance of tumors were judged to be not significantly different by the generalized Wilcoxon test. The male *Wnt-1 TG p53−/−* animals, however, displayed a dramatic increase in the rate of appearance of mammary tumors compared with their *Wnt-1 TG* p53+/− and *Wnt-1 TG* p53+/+ counterparts (Fig. 1B). Of 16 of these animals, 12 developed mammary tumors by 6 months of age, whereas the other 4 succumbed to thymic lymphomas within the first 6 months, precluding adequate evaluation for mammary tumors. (These latter animals are not included in Fig. 1B.) For those *Wnt-1 TG* p53−/− males that developed mammary adenocarcinomas, the median time required to form a detectable tumor was 15.5 weeks, nearly as short as the median time for appearance of mammary tumors in *Wnt-1 TG p53−/−* females.

Analysis of the wild-type p53 *allele(s) in mammary tumors from* Wnt-1 TG p53+/− *and* Wnt-1 TG p53+/+ *mice*

p53 allele loss accompanied by point mutation in the remaining *p53* allele is a frequent occurrence in human tumors, and we and others have observed loss of the normal *p53* allele when mesenchymal tumors and lymphomas arise in *p53+/−* mice (Harvey et al. 1993a; Jacks et al. 1994; Purdie et al. 1994). To detect loss of heterozygosity (LOH) of the wild-type allele during the development or progression of mammary tumors in *Wnt-1 TG p53+/−* mice, we analyzed the structure of the intact *p53* allele in those tumors by Southern blot hybridization. Of 18 tumors from *Wnt-1 TG p53+/−* females, 8 showed virtually complete loss of the remaining wild-type *p53* allele, whereas the other 10 tumors contained the normal allele (Fig. 2). In two of these latter tumors, comparison of the hybridization intensities of the normal and mutant *p53* alleles suggests that the normal *p53* allele is lost from some tumor cells but retained in others. Four tumors from male *Wnt-1 TG p53+/−* animals were also tested: Two lacked the wild-type allele entirely, and it was underrepresented in a third (data not shown). In tumors from *Wnt-1 TG p53+/−* animals that displayed *p53* LOH, comparison of hybridization to the mutant allele and the *p53* pseudogene suggested that the mutant allele was not duplicated in tumors from either females and males (Fig. 2; data not shown).

The appearance of LOH in a high proportion of cells from about half of the tumors in heterozygous animals indicated that cells lacking an intact *p53* gene might have a selective growth advantage. However, when we replotted the data shown in Figure 1A to separate tumors with LOH from those without LOH, p53 deficiency did not correlate with the detection of tumors at an earlier age. On average, tumors with LOH were detected slightly later than those that retained a normal *p53* allele (data not shown).

To determine whether point mutations had occurred in the wild-type *p53* allele of the *Wnt-1 TG p53+/−* tumors that had not undergone loss of heterozygosity, we sequenced nearly the entire coding region of *p53* cDNAs from four of these tumors (see Materials and methods). Because of the PCR primers used, the first 18 bp and the last 21 bp of the *p53*-protein coding sequences could not be determined, but the rest of the sequence was wild-type (data not shown).

Southern blot analyses and previous sequencing of *p53* cDNAs derived from mammary tumor RNAs from *Wnt-1 TG* mice (V. Pecenka and H.E. Varmus, unpubl.) failed to reveal any changes in the *p53* gene when both *p53* alleles are intact in the germ line.

All of the mammary tumors are adenocarcinomas, but they differ in the degree of fibrosis depending on p53 status

We performed standard histopathological examination on most of the mammary tumors in the study. A total of 40 tumors from female mice and 18 tumors from male mice were evaluated for general histoarchitecture and mammary tumor classification, without prior knowledge of *p53* genotype. The majority of the tumors in female mice (29/40) and in male mice (11/18) were type-B mammary adenocarcinomas (Sass and Dunn 1979). This pathological type was the most common regardless of the *p53* genotype or sex of the animal. The rest of the tumors were either papillary cystic adenocarcinomas or type-A adenocarcinomas, two morphological variants that are more differentiated and less aggressive than the type B adenocarcinomas.

Extensive fibrosis was observed in most of the tumors arising in the *Wnt-1 TG p53+/+* female mice (Fig. 3A). In contrast, tumors from *Wnt-1 TG p53−/−* females did

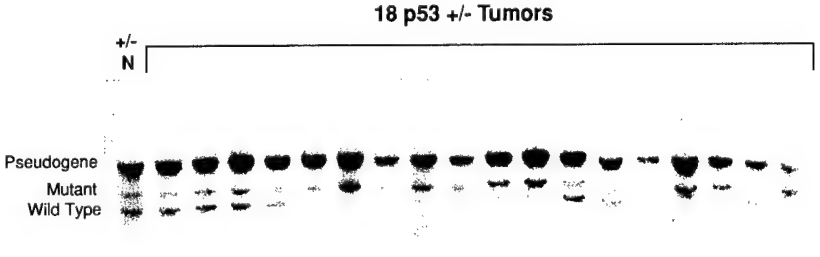

Figure 2. Loss of the wild-type allele in some *Wnt-1 TG p53+/−* tumors. Each lane contains 10 μg of tumor DNA from individual female *Wnt-1 TG p53+/−* tumors cleaved with *Bam*HI. After agarose gel electrophoresis, the DNAs were transferred to nylon and hybridized to the *p53* cDNA exon 2–6 probe. The relevant *Bam*HI fragments are ~5 kb (from the wild-type allele), 6.5 kb (from the null allele), and 10 kb (from the *p53* pseudogene). Lane N contains tail DNA from one of the tumor-bearing animals.

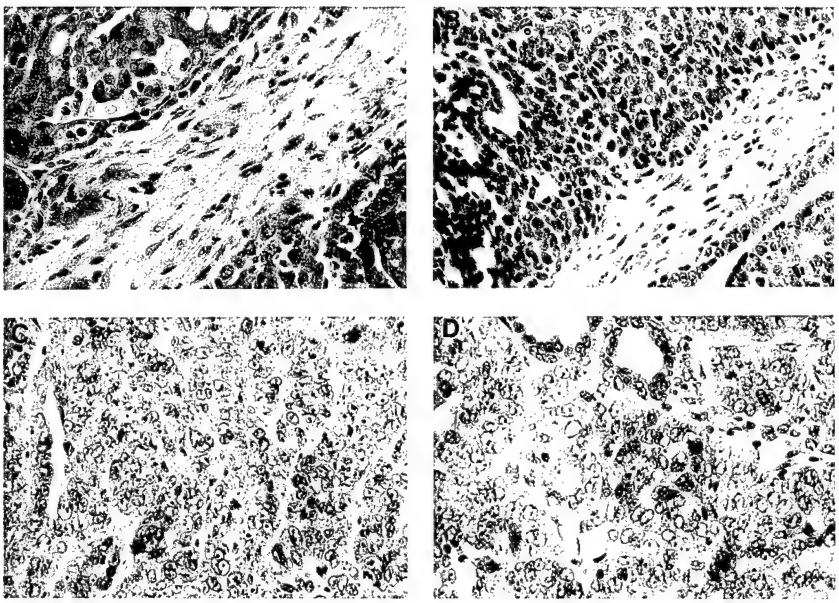

Figure 3. Fibrotic and nonfibrotic histopathology in mammary tumors from mice with different *p53* genotypes. (*A*) Histopathology section of a tumor from a *Wnt-1 TG p53+/+* female. (*B*) Histopathology section of a tumor that retained the wild-type *p53* allele from a *Wnt-1 TG p53+/−* female. (*C*) Histopathology section from a tumor that had lost the wild-type *p53* allele from a *Wnt-1 TG p53+/−* female. (*D*) Histopathology section of a tumor from a *Wnt-1 TG p53−/−* female. All slides are stained with hematoxylin and eosin. Magnification, 94×.

not exhibit significant fibrosis and frequently contained multiple mitotic cells and signs of anaplasia (Fig. 3D). Similar trends were apparent in the smaller collection of tumors from male mice (data not shown). Tumors from *Wnt-1 TG p53+/−* females varied with respect to the degree of fibrosis and number of mitotic cells. When some of these tumors were assessed for loss of the wild-type allele, as illustrated in Figure 2, retention of the wild-type allele correlated quite well with more extensive fibrosis and infrequent mitotic cells (Fig. 3B,C). Of 19 mammary adenocarcinomas with wild-type *p53* that were examined (*p53+/+* and *p53+/−* without LOH), 14 showed extensive fibrosis. In contrast, in tumors without wild-type p53 (*p53−/−* and *p53+/−* with LOH), only 1 of 12 tumors exhibited fibrosis. These findings suggest that significant biological differences may exist between those tumors that produce and those that do not produce p53 protein.

Metaphase spreads reveal a tendency to aneuploidy in p53-deficient mammary tumor cell explants

Earlier studies have revealed that p53-deficient cells in culture exhibit genomic instability as manifested by aneuploidy and susceptibility to gene amplification (Livingstone et al. 1992; Yin et al. 1992). To determine whether partial or complete loss of *p53* predisposes cells to aneuploidy during tumorigenesis in vivo, we examined the karyotypes of cultured cells from five mammary tumors from *Wnt-1 TG p53+/+* females, four mammary tumors from *Wnt-1 TG p53+/−* females, and six mammary tumors from *Wnt-1 TG p53−/−* females. Karyotyping was performed on cells grown in culture for 24–48 hr after dispersion from mammary tumors. Cultures were incubated with Colcemid, fixed, and stained according to standard procedures (Fig. 4I,J), and the chromosomes of 25–50 metaphase spreads were counted for each tumor. Any chromosome count other than 40 (the mouse diploid chromosome number) was considered aneuploid. Chromosome numbers are given in Figure 4 for all cells analyzed from eight representative tumors. Overall, the results demonstrate that the absence of *p53* predisposes tumor cells to aneuploidy.

Cells from *Wnt-1 TG p53+/+* tumors were typically exactly diploid (Fig. 4A,B). In cells from five such tumors, >70% of the metaphase spreads were diploid, and the occasional deviant cells were usually exactly tetraploid or very nearly diploid (Fig. 4A,B; data not shown).

Wnt-1 TG p53−/− tumors fell into two groups on the basis of karyotyping (Fig. 4C,D). Three tumors yielded a very high percentage of cells with grossly abnormal karyotypes, mostly subtetraploid (e.g., Fig. 4C). As is evident from the metaphase spread illustrated in Figure 4J, cells from some of these tumors demonstrated dicentric chromosomes and chromosomes with homogenously staining regions, suggesting gene amplification, in addition to increased chromosome numbers. The other three tumors from *Wnt-1 TG p53 −/−* animals displayed karyotypes similar to those from tumors with a wild-type *p53* genotype (e.g., Fig. 4D). In one case, however, >20% of the cells were tetraploid, whereas in another case nearly 30% of the cells had 39 chromosomes (data not shown). Thus, a deficiency of p53 strongly predisposes cells in mammary tumors to aneuploidy, but is not sufficient to produce it.

We also inspected metaphase spreads from four tumors arising in *Wnt-1 TG p53+/−* animals (Fig. 4E–H). The karyotypes of cells from two of these tumors were not distinguishable from tumors arising in a normal *p53* background. Over 80% of metaphases were diploid, and ~10% were tetraploid with 80 chromosomes (Fig. 4G,H). One of these two tumors retained the normal *p53* allele in most or all cells, but the other had undergone loss of heterozygosity, again demonstrating that the absence of

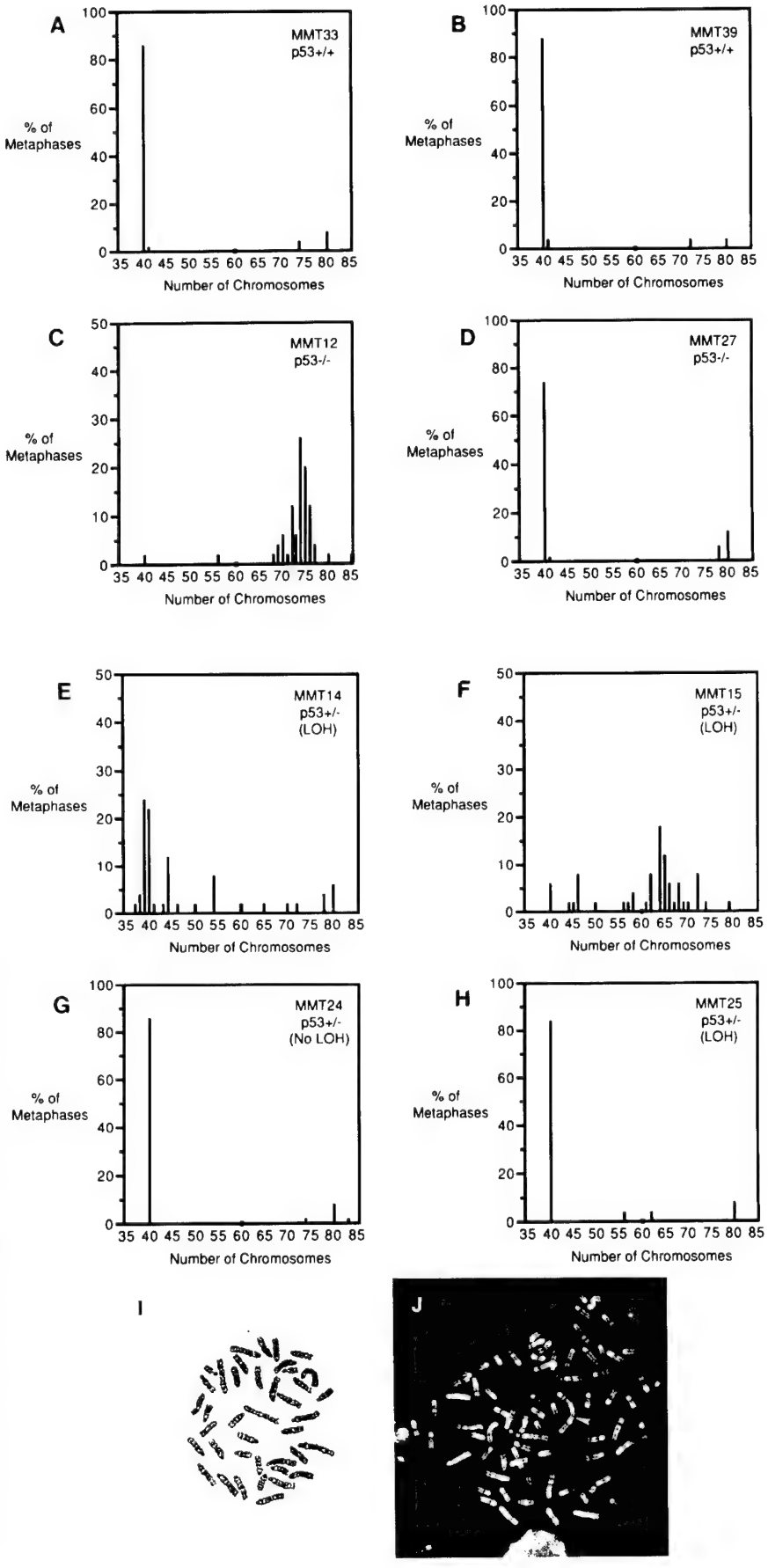

Figure 4. Karyotypes of cultured tumor cells from *Wnt-1 TG* mice with intact or defective *p53* alleles. Metaphase spreads were prepared as described previously (Aldaz et al. 1992). Chromosome numbers were determined in at least 25 different spreads from cultured cells from each tumor. Percentages of tumor cells with given chromosome numbers from representative tumors are shown. (*A,B*) Representative *Wnt-1 TG p53+/+* tumors; (*C,D*) representative *Wnt-1 TG p53−/−* tumors; (*E,F*) tumors from *Wnt-1 TG p53+/−* mice with loss of wild-type *p53* allele; (*G*) tumor from *Wnt-1 TG p53+/−* mouse with retention of the wild-type *p53* allele; (*H*) tumor from *Wnt-1 TG p53+/−* mouse with LOH; (*I*) typical metaphase spread of a tumor cell with a diploid karyotype from a *Wnt-1 TG p53+/+* female photographed after Giemsa trypsin staining; (*J*) typical metaphase spread of tumor cell with a hypotetraploid karyotype from a *Wnt-1 TG p53−/−* tumor photographed after DAPI staining. A dicentric chromosome is indicated by the arrowhead.

p53 from mammary tumor cells does not mandate aneuploidy. The other two *Wnt-1 TG p53+/−* tumors showed extensive aneuploidy, with a wide distribution of chromosome numbers, suggesting that the tumor cell population was heterogeneous and continuing to evolve at the time the animal was sacrificed (Fig. 4E,F). Both of these tumors had lost the wild-type *p53* allele from the majority of cells, as judged by Southern blotting (data not shown), suggesting that the absence of p53 contributes to karyotypic instability.

Comparative genomic hybridization and Southern blot hybridization provide further evidence of genomic instability in p53-deficient tumors

To complement the cytogenetic data and to identify recurring regions of chromosomal change in the *Wnt-1 TG* mammary tumors, we employed the comparative genomic hybridization (CGH) technique (Kallioniemi et al. 1992). This procedure detects regions of increases and decreases in DNA copy number throughout the entire genome of a tumor cell. This is achieved by differential fluorescent labeling of total genomic DNA samples from a tumor and from normal tissue. These two DNAs are hybridized to metaphase spreads of normal mouse chromosomes. Chromosomal regions showing losses and gains in the tumor can be recognized as decreases and increases, respectively, in the intensity of fluorescence from the tumor DNA relative to that from the normal DNA. Two examples of the results of such hybridizations are illustrated in Figure 5. In the first example, the tumor shows many changes by CGH (Fig. 5A,B), and in the other, a single change is observed (Fig. 5C,D). The abnormalities from all of the tumors examined are summarized in Table 1.

Four of the six *Wnt-1 TG p53+/+* mammary tumors examined by CGH had no detectable abnormalities, and the other two had only a single chromosomal alteration. Similarly, two of four tumors from *p53* heterozygous mice that retained the wild-type *p53* allele did not have detectable abnormalities, whereas two others displayed one or three subchromosomal decreases in DNA copy number. These findings are consistent with the low level of aneuploidy observed in such tumors by standard karyotyping.

In contrast, all seven of the *Wnt-1 TG p53−/−* tumors showed at least one chromosomal abnormality, and some exhibited multiple changes. Furthermore, the eight tumors that lost the wild-type *p53* allele while developing in *Wnt-1 TG p53+/−* mice showed the most chromosomal instability. Seven of the tumors displayed at least three regions of DNA gain or loss, and one tumor (W166; Fig. 5A,B) had 10 detectable genetic changes. The *Wnt-1 TG p53+/−* tumors with *p53* LOH averaged 4.2 detectable chromosomal abnormalities per tumor. In contrast, tumors that developed in *Wnt-1 TG p53+/+* mice or in *Wnt-1 TG* 53+/− without LOH averaged only 0.33 and 1.0 abnormalities per tumor. An average of 1.7 chromosomal abnormalities was observed in the tumors from animals with the *Wnt-1 TG p53−/−* genotype. Four of the p53-deficient tumors with CGH abnormalities, two from p53−/− animals and two from p53+/− animals with LOH, were also examined by standard karyotyping. One of each genotype revealed a high level of aneuploidy (see footnotes in Table 1).

Several recurring chromosomal changes were noted by CGH. As expected, many of the *Wnt-1 TG p53+/−* tumors that had lost their wild-type allele showed a loss of DNA from chromosome 11, which contains the mouse *p53* locus (Czosnek et al. 1984; Rotter et al. 1984). Other recurring alterations in the tumors included DNA losses from chromosome 4 (three tumors), chromosome 8 (four tumors), chromosome 9 (four tumors), chromosome 13 (five tumors), and the X chromosome (five tumors). Increases in DNA were also observed for chromosome 7 (two tumors) and chromosome 10 (two tumors).

As an adjunct to CGH, we used genomic Southern blot hybridization with gene-specific probes to ask whether known proto-oncogenes were amplified in *Wnt-1 TG p53*-deficient tumors. Probes for three loci known to be amplified in some human mammary tumors—c-*myc* (Escot et al. 1986), *neu* (Slamon et al. 1987), and *int-2/FGF3* (Lidereau et al. 1988)— were used to test tumor DNAs from 18 *Wnt-1 TG p53−/−* animals and from 6 *Wnt-1 TG p53+/−* animals whose tumors had lost the wild-type *p53* allele (Fig. 6A; data not shown).

In tumor B from animal W177, the *int-2/FGF3* locus was increased to about six to eight copies per cell. This change was consistent with the CGH profile for tumor 177B, which showed only one abnormality: increased representation of DNA from the distal portion of mouse chromosome 7, the chromosomal location of *int-2/FGF3* (Fig. 5C,D). A second tumor that arose independently in this animal (177A) did not show these changes by CGH or Southern blot hybridization (Table 1; Fig. 6A).

In some human breast tumors, the *int-2/FGF3* region is amplified, and the amplified domain includes the linked genes *hst/FGF4* and *PRAD-1/cyclin D1*. Because *PRAD-1/cyclin D1* is the only one of these three loci expressed in such tumors, the *cyclinD1* gene rather than either *FGF* gene is believed to be contributing to carcinogenesis (Lammie et al. 1991). However, several kinds of experiments suggest that ectopic expression of *FGF* genes can synergize with *Wnt-1* to promote mouse mammary tumors (Peters et al. 1986; Kwan et al. 1992; Shackleford et al. 1993). When we measured *int-2/FGF3, hst/FGF4*, or *PRAD-1/cyclin D1* RNAs in tumor W177B and in several other tumors, *int-2/FGF-3* RNA was abundant in W177B but undetectable in other tumors (Fig. 6B). Equally low levels of *hst/FGF4* and *PRAD-1/cyclin D1* RNA were observed in all of the samples (data not shown). These findings suggest that activated expression of *int-2/FGF-3* (by an unknown mechanism) accompanied by amplification of the gene (perhaps facilitated by p53 deficiency), participated in the oncogenic process in tumor 177B.

Discussion

Abnormalities of *p53* are common in human breast can-

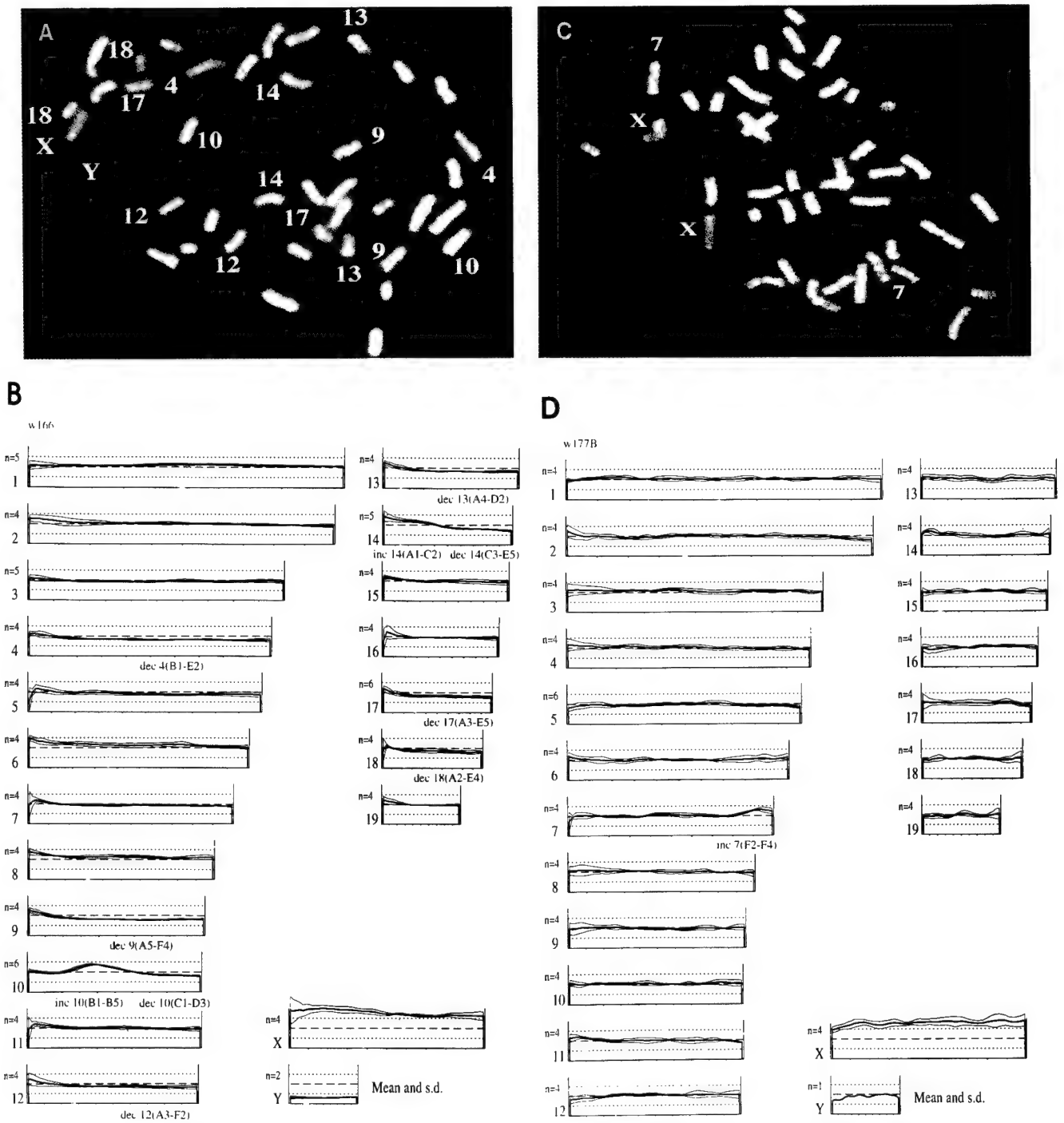

Figure 5. Representative comparative genomic hybridization images and fluorescence ratio profiles. (*A*) Composite digital image from CGH analysis of tumor W166 (*Wnt-1 TG p53+/−* tumor that had lost the wild-type *p53* allele). Tumor genomic DNA hybridization signal is displayed in green, normal genomic DNA in red, and the normal male metaphase target chromosomes in blue. Regions of relatively green fluorescence indicate increased copy number of these sequences in the tumor, and red regions indicate decreases of copy number relative to the average for the tumor. Blue regions of the target chromosomes contain repeated satellite sequences where hybridization is blocked by unlabeled C_0t-1 DNA. Those chromosomes containing regions of variant copy number are labeled in the image. The specimen is from a female mouse, and the normal DNA is male so that the X chromosome appears green and the Y chromosome appears red. (*B*) Profiles of the green to red fluorescence intensity for each of the chromosomes from tumor W166. The heavy lines show the average of profiles from several chromosomes of each type (indicated by the *n* value next to each profile); the thin lines show +/±1 S.D. from the mean. The lengths of the profiles are arbitrarily normalized and are not accurately proportional to chromosome length. The regions of variant copy number are indicated under the individual profiles and correspond to those shown in Table 1. (*C*) Composite digital image from the analysis of a *Wnt-1 TG p53−/−* tumor, W177B. (*D*) Ratio profiles of tumor W177B. The only significant variation is on the distal portion of chromosome 7 corresponding to the green region of the image in *C*.

Table 1. *Comparative genomic hybridization of tumor DNAs*

Wnt-1 tumor genotype	Tumor	Modal karyotype[a]
p53+/+	1269	normal
	1370	normal
	1477	normal
	1498	inc 8(A)
	1562	dec X(D-F)
	MMT19[b]	normal
p53+/−	W15	normal
(no *p53* LOH)	W08A	normal
	W21B	dec 3(E-H); dec 7(C-F); dec 13(A5-D)
	W55	dec 9(B-F)
p53+/−	W32	dec 8(A1-E2); dec 9(E3-F4); dec X(E-F4)
(*p53* LOH)	W108	dec 4(B-E); dec 8(B-E); dec 11
	W139	inc 1(B-H); dec 11; dec 13(A5-D); dec 14(C3-E)
	W165	dec 11(A5-E)
	W166	dec 4(B1-E2); dec 9(A5-F4); inc 10(B1-B5); dec 10(C1-D3); dec 12(A3-F2); dec 13(A4-D); dec 14(C3-E5); inc 14(A1-C2); dec 17(A3-E5); dec 18(A2-E4)
	W126	dec 4(D-E); dec 9; dec 10; dec 11; dec 13; dec 16
	MMT14[c]	dec 8; inc 10; dec 14(C-E); dec 15(D-E)
	MMT25[b]	dec 10(B-D); dec 11(C-E); dec 13(B-D)
p53−/−	W121	dec X
	W180	dec 2(G-H)
	W177A	dec X(D-F)
	W177B	inc 7F
	W154	inc 2H; inc 14B; dec X
	MMT12[c]	inc 10(A-B)
	MMT27[b]	inc 7(A-F); dec 16(C-G)

[a]Tumor DNAs were analyzed by comparative genomic hybridization (Kallioniemi et al. 1992). Chromosomal abnormalities are indicated dec for DNA copy number decreases and inc for DNA copy number increases, followed by the mouse chromosome number. Subchromosomal regions affected by these changes are indicated in parentheses by uppercase letters. Each letter represents a band visible by DAPI staining; A is the band closest to the centromere.
[b]Tumor diploid by karyotyping.
[c]Tumor aneuploid by karyotyping.

cer (Greenblatt et al. 1994), yet mammary tumors have rarely been encountered in mice with null alleles at the *p53* locus (Donehower et al. 1992; Jacks et al. 1994; Purdie et al. 1994) or with mutant *p53* transgenes (Lavigueur et al. 1989). To examine the role of *p53* in mammary tumorigenesis in an animal model, we have introduced a *Wnt-1* transgene, known to induce mammary hyperplasia and a strong predisposition to mammary cancer, into mice bearing one or two copies of a targeted null mutation of *p53*. Two major findings with the progeny of this cross strongly support our conclusion that a deficiency of *p53* influences the formation of mammary tumors in the presence of the *Wnt-1* transgene: (1) Tumors arise much earlier in animals that do not inherit an intact *p53* gene (Fig. 1), and (2) tumors that develop in animals constitutively heterozygous at the *p53* locus often show loss of heterozygosity (Fig. 2), implying a selective growth advantage for mammary tumor cells in which no functional *p53* gene remains.

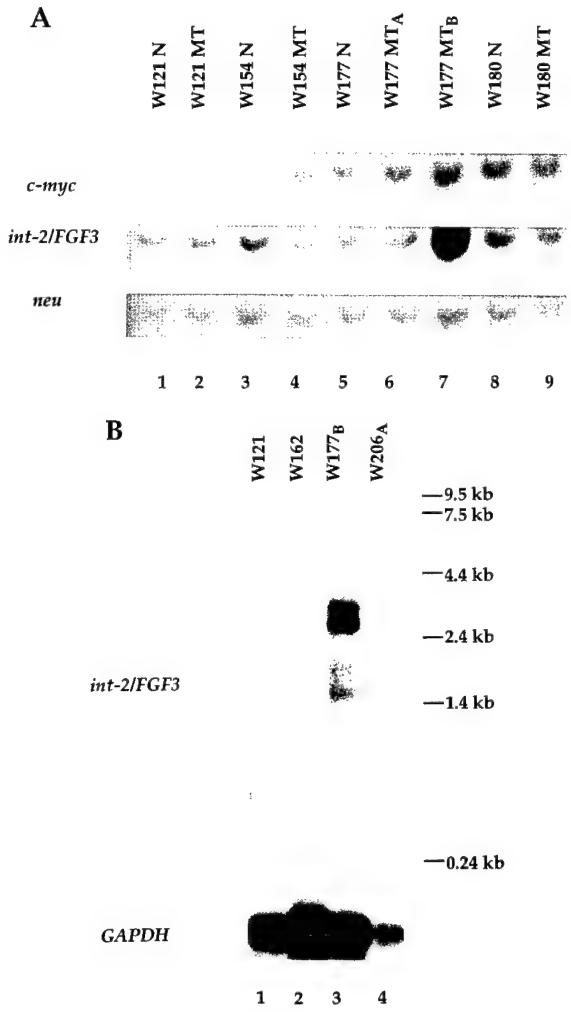

Figure 6. Southern and Northern blotting analyses of *Wnt-1 TG p53*−/− mammary tumors. (*A*) Gene amplification of the *int-2/FGF3* locus in *Wnt-1 TG p53*−/− tumor W177B. Southern blotting was performed with multiple probes on paired samples from *Wnt-1 TG p53*−/− tumors. At the *top* of each lane, the mouse identification number is given: (N) normal tail DNA; (MT), mammary tumor DNA. Subscript letters distinguish independently arising tumors in a single animal. The gene from which each probe is derived is given at *left*. (*B*) Overexpression of *int-2/FGF3* in *Wnt-1 TG p53*−/− mammary tumor W177B. Northern blotting of RNA from *Wnt-1 TG p53*−/− tumors was performed with multiple probes. The gene from which each probe is derived is given at *left*, and RNA sizing is at *right*.

Three striking correlations have emerged from our efforts to understand the contribution that a deficiency of *p53* might make to the oncogenic process in these animals: (1) We noted histopathological differences between tumors that retained and those that lacked a *p53* gene. p53-Deficient tumors were, in general, less fibrotic, and contained more mitotic and anaplastic cells; (2) aneuploidy was frequent in cells derived from tumors lacking *p53* and much less common in tumor cells that retained *p53*; and (3) relative gains and losses of chromosomal DNA, as measured by CGH, were more common in tumors that lacked p53, especially in those p53-deficient tumors resulting from loss of a wild-type *p53* gene in a heterozygous background. These findings imply that there are at least two pathogenic routes by which mammary tumors can arise in *Wnt-1* transgenic mice. In one, p53 continues to function, tumor cells show little aneuploidy or chromosomal rearrangement, and the tumors contain extensive fibrosis. In the other, p53 function is lost, the tumor cell genome is destabilized, and the tumors are minimally fibrotic.

p53 deficiency and the kinetics of tumorigenesis

We initiated the experiments described here in hopes of understanding the multistep process of carcinogenesis in greater detail. Our results have provoked at least two perplexing questions about the number, timing, and functional consequence of the events in mammary tumorigenesis: (1) Why do tumors appear relatively early in p53-deficient mice? and (2) why do tumors fail to appear early in heterozygous mice when the normal *p53* gene has been eliminated? We have considered possible answers to these questions in the context of two models that posit cell-autonomous and non-cell-autonomous functions for p53 protein (Fig. 7A,B).

Loss of one or more of the cell-autonomous functions previously proposed for the *p53* gene product might foster the development of a tumor and thereby help to explain the early onset of tumors in *Wnt-1 TG p53−/−* animals (Fig. 7A): (1) Loss of cell-cycle control and accompanying genomic instability (Livingstone et al. 1992; Yin et al. 1992; Harvey et al. 1993c) might favor the more rapid accumulation of additional mutations necessary for tumor development; (2) changes in control of p53-dependent transcription (Farmer et al. 1992; Kern et al 1992) might affect cell growth rates or other cell processes; (3) resistance to apoptosis (Yonish-Rouach et al. 1991; Clarke et al. 1993; Lowe et al. 1993a,b) might increase cell numbers during tumor growth, because p53-

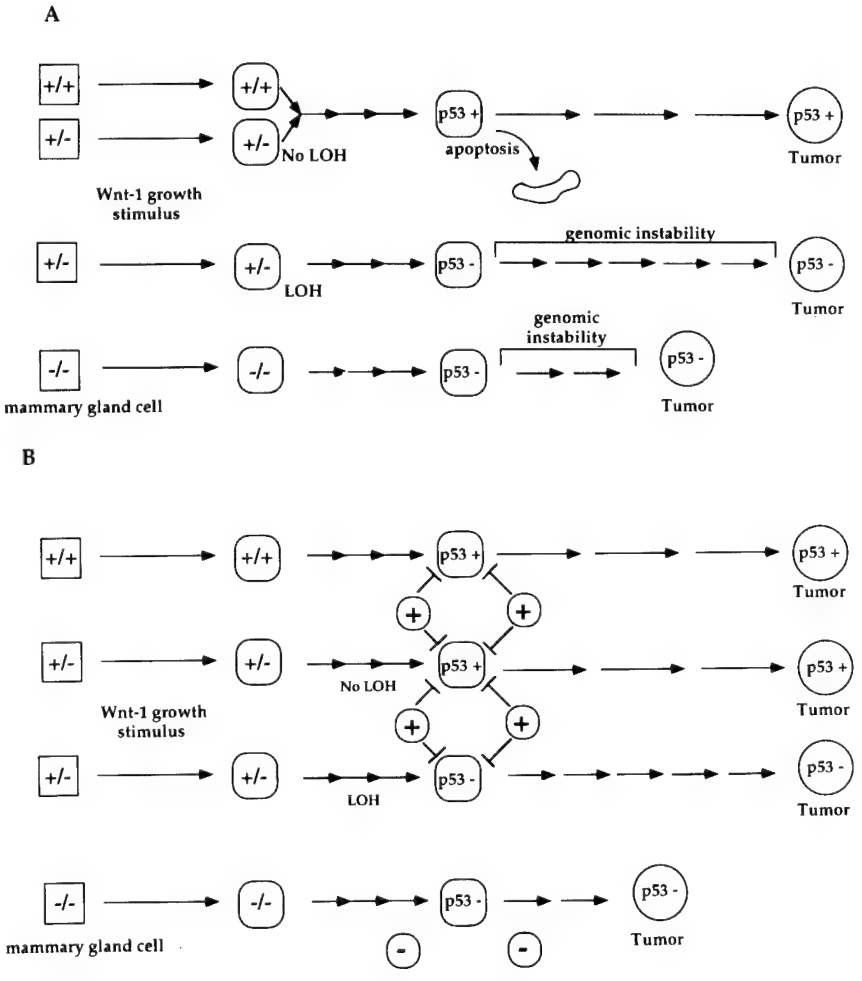

Figure 7. Multistep models of mammary tumorigenesis in *Wnt-1 TG p53* mice. (Squares) Normal mammary gland epithelial cells; (squares with rounded edges) preneoplastic cells; and (circles) the dominant cell population in a tumor. Arrows between cells indicate genetic or epigenetic changes that occur during tumor cell initiation and progression. (*A*) The cell-autonomous model. Initially in all *Wnt-1 TG* mice, ectopic expression of Wnt-1 protein in normal mammary gland cells induces polyclonal hyperplastic growth. Further growth stimulation by Wnt-1 accompanies additional genetic or epigenetic changes that produce clonal tumor growth. In this model the rate of progression depends on the *p53* status of the initiated cell. Cells that retain wild-type *p53* produce tumors at a delayed rate, possibly because of a lower frequency of genetic change and *p53*-mediated apoptosis. (*B*) The non-cell-autonomous model. In this model tumor cell progression is regulated in part by events extrinsic to that cell that will give rise ultimately to a tumor. The *p53* genotype of the host animal, not the genotype of the nascent tumor cell, determines the speed of tumor formation. It is hypothesized that surrounding cells that have wild-type *p53* (*p53+/+* and *p53+/−* animals) inhibit expansion of the tumor cell clone, whereas in *p53−/−* animals this inhibitory effect does not occur. Fewer genetic changes may be necessary for the nascent tumor cell in *p53−/−* animals to form a tumor because of the reduction of inhibition by surrounding cells.

mediated programmed cell death no longer counterbalances Wnt-1-stimulated proliferation. Although we have provided considerable support for the first of these three explanations, we have not yet tested directly for contributions by the latter two. Moreover, we have identified only a single specific mutation, amplification of *int-2/FGF-3* in tumor 177B, that is likely to participate in carcinogenesis, despite abundance evidence for genomic instability.

These proposed effects of p53 on cell growth are not, however, sufficient to account for the observation that *p53* LOH failed to accelerate the development of tumors in *Wnt-1 TG p53+/−* animals. Perhaps the simplest explanation for this observation is that *p53* LOH is a late event in this tumorigenesis model. This hypothesis can be tested further by comparison of the frequency of *p53* LOH as a function of tumor size. A non-cell-autonomous model is presented in Figure 7B to account for the paradoxical finding that *Wnt-1 TG p53+/−* tumors with LOH display more evidence of genomic instability than *Wnt-1 TG p53−/−* tumors. *Wnt-1 TG p53−/−* mice might develop mammary tumors earlier than their *Wnt-1 TG p53+/−* and *Wnt-1 TG p53+/+* counterparts because of a permissive environment afforded by *p53−/−* cells surrounding nascent tumor cells. Conversely, p53-containing cells that surround neoplastic cells, including p53-deficient tumor cells, might provide an inhibitory influence and retard growth of the tumor clone, demanding that the clone undergo further mutations to overcome the inhibition.

The idea that normal cells surrounding a transformed cell can influence its growth potential has been demonstrated previously both in vitro and in vivo, as assayed by focus formation in primary rodent fibroblasts (Land et al. 1983) and by tumorigenic potential of mixtures of normal and preneoplastic mammary cells (Medina et al. 1978). Such a model implies that wild-type p53 may have an extracellular inhibitory role in growth control, in addition to its well-characterized intracellular effects. For example, wild-type p53 was shown to stimulate expression of thrombospondin-1, a potent inhibitor of angiogenesis (Dameron et al. 1994).

p53 and genomic stability

Our findings of aneuploidy and CGH abnormalities in mammary tumors in conjunction with p53 deficiency are consistent with previous reports that the lack of p53 predisposes cultured cells to aneuploidy and amplification of selectable genes (Livingstone et al. 1992; Yin et al. 1992). By extending these observations to a tumor model in an intact animal, we provide support for the hypothesis that p53 deficiency contributes to carcinogenesis by promoting chromosomal rearrangements that favor tumor cell growth. But the findings also emphasize the importance of two largely unresolved questions.

1. What is the mechanism by which p53 protects a cell from genomic instability? p53 is believed to defend cells from premature entry into the S phase of the cell cycle, an idea that has been especially well-documented after exposure of cells to genotoxic agents (Kastan et al. 1991, 1992; Lu and Lane 1993). Failure to block passage through the cell cycle could result in permanent genetic change if the genome has been assaulted by radiation or chemical mutagens, without sufficient opportunity for repair. Deficiency of p53 per se does not produce chromosomal abnormalities because mice carrying targeted germ-line mutations of *p53* can develop normally despite a total absence of p53 protein (Donehower et al. 1992; Jacks et al. 1994; Purdie et al. 1994). Also, some mammary tumors from p53-deficient animals are composed largely of diploid cells with relatively few abnormalities seen by CGH (Fig. 5). However, the absence or loss of p53 causes a predisposition to genomic instability in established cell lines and in cultured fibroblasts from p53-deficient animals (Bischoff et al. 1990; Livingstone et al. 1992; Yin et al. 1992; Harvey et al. 1993c), and we have observed a higher frequency of aneuploidy and abnormalities detectable with CGH in p53-deficient tumors (Figs. 4 and 5; Table 1). The factors that provoke genomic instability in p53-deficient cells remain unknown. Their identity might be useful in considering both the origins and treatment of cancers.

2. What are the specific genetic consequences of p53 deficiency that promote the growth of tumor cells? In at least one instance, tumor 177B, we were able to provide some answer to this question, because the amplified DNA included a gene, *int-2/FGF-3*, that is known from several other kinds of experiments, to collaborate with *Wnt-1* when expressed ectopically in mammary tissue (Peters et al. 1986; Kwan et al. 1992; Shackleford et al. 1993). The increases and decreases of several other chromosomal domains may also be functionally important, because the changes were encountered in multiple tumors or because the domains are syntenic with those implicated in human or experimental tumors. Recurring decreases in DNA occurred on chromosomes 4, 8, 9, 11, 13, and X, arguing that the genomic instability in this model is at least partially nonrandom and may represent genetic events that provide a selective growth advantage during tumor progression. The role such genomic losses play in the progression of mammary cancer remains to be elucidated. However, the largely normal karyological and CGH patterns observed in tumors that retain p53 show that the abnormalities detectable with these methods are not absolutely required for Wnt-1-promoted tumorigenesis. In addition, it should be noted that increased genomic instability did not necessarily correlate with accelerated tumorigenesis, as the *Wnt-1 TG p53+/−* tumors with LOH displayed the greatest numbers of karyotypic abnormalities but did not show an increase in rate of formation in comparison to *Wnt-1 TG p53+/+* tumors and *Wnt-1 TG p53+/−* tumors without LOH. This lack of correlation suggests that genomic instability may provide a selective advantage during tumor progression, but does not necessarily affect the rate at which the tumors appear.

Further definition of multistep mammary tumorigenesis

Our work demonstrates that the proto-oncogene *Wnt-1* and the tumor suppressor gene *p53* can collaborate to produce mammary cancers in mice, but it is evident from the kinetics of appearance of new tumors that other events are required. We presume these to be mutations, at least some of which are represented by the genomic abnormalities observed by CGH. Moreover, we do not know how many mutations are required, how many oncogenic combinations of mutations are possible (even in the limited context of a Wnt-1-stimulated, hyperplastic mammary gland), or what constraints are placed on the order in which the mutations occur.

Multistep carcinogenesis has been documented in some human cancers (Fearon and Vogelstein 1990) and often involves the *p53* gene (Greenblatt et al. 1994). p53 mutations have been associated with genomic instability during tumor development in at least one clinical setting, esophageal cancer (Neshat et al. 1994), although in general human tissues are difficult to obtain at different stages of tumorigenesis in a single patient or in a genetically homogeneous population. For this reason, many laboratories are using mouse models to explore multistep models for carcinogenesis (Cardiff and Muller 1993; Kemp et al. 1993; Christofori and Hanahan 1994). Some of these models incorporate, as ours has done, a gene that is frequently mutated in the same type of cancer in human patients (Dietrich et al. 1993; Oltvai and Korsmeyer 1994). It is evident from recent work with such models that important physiological events—such as augmented angiogenic activity (Kandel et al. 1991; Shing et al. 1993; Fidler and Ellis 1994) or a diminished rate of apoptosis (Symonds et al. 1994)—can have major consequences during tumor progression. The *Wnt-1* transgenic model has special advantages in this regard, because it is possible to examine mammary tissue at several stages of tumor development, ranging from early hyperplasia to metastatic growth (Tsukamoto et al. 1988). It will now be important to ask whether changes in angiogenic and apoptotic activity accompany the changes we have described here in histology, genomic composition, and integrity of specific genes.

Materials and methods

Mice

The *Wnt-1 TG* mice used in the crosses described here were the offspring of two *Wnt-1 TG* males from line 303 described previously (Tsukamoto et al. 1988). These mice were of mixed SJL×C57/BL/6 genetic background. The p53-deficient mice were from a pure 129/Sv line of mice containing one or two germ-line *p53* null alleles (Harvey et al. 1993b). The two *Wnt-1* males were crossed to heterozygous (*p53*+/−) 129/Sv females to derive F_1 mice of four possible genotypes (*p53*+/+; *Wnt-1 TG p53*+/+; *p53*+/−; *Wnt-1 TG p53*+/−). F_1 *p53*+/− females were crossed to F_1 *Wnt-1 TG p53*+/− males to obtain F_2 mice that carried any of the *Wnt-1 TG p53* genotypes found in the F_1 population as well as *Wnt-1 TG p53*−/− or *p53*−/−. To obtain larger numbers of mice with *p53*−/− genotypes with or without the *Wnt-1* transgene, F_2 *p53*−/− females were mated to *Wnt-1 TG p53* −/− males. All of the mice were monitored visually twice weekly for the appearance of tumors for up to 1 year. When a tumor of ~0.5 cm in diameter was detected, the age of the mouse was recorded and used to generate the Kaplan–Meier plots in Figure 1. Once a tumor reached 1.5–2 cm in diameter, the tumor-bearing mouse was sacrificed, and tissue sections removed for histopathology. The remainder of the tumor was frozen at −70°C for nucleic acid analyses.

Nucleic acid isolation and analysis

We determined the *p53* and *Wnt-1* genotypes of the offspring from the crosses by use of methods described previously (Tsukamoto et al. 1988; Donehower et al. 1992; Harvey et al. 1993a). To determine the coding sequence of the remaining *p53* allele in *Wnt-1 TG p53*+/− mammary tumors that did not show LOH, total cellular RNA from a small tissue segment from each of four tumors was prepared using the RNAzol B kit (Tel-Test, Inc.) according to the manufacturer's instructions. We then used reverse transcriptase–PCR (with the RT–PCR kit from Perkin-Elmer Cetus) to amplify the *p53* cDNA from the four tumor RNAs.

Initially, the amplification primers used were derived from exons 4 and 10 of the mouse cDNA, and these amplified exons 5–9 of the murine *p53* gene. The nucleotide sequences of these primers were 5′-CAGTCTGGGACAGCCAAGTC-3′ (exon 4) and 5′-CTCCCGGAACATCTGGAAGC-3′ (exon 10). The amplified exon 4–10 fragments were purified from a low-temperature agarose gel following electrophoresis, treated with Klenow polymerase and T4 polynucleotide kinase, and then ligated into the plasmid cloning vector Bluescript II (Stratagene) at the *SmaI* site. Sequencing was performed on the Applied Biosystems automated sequencer with the SP6 and T7 universal sequencing primers adjacent to the insertion site. Standard dideoxy sequencing with the Sequenase sequencing kit (U.S. Biochemical) was also performed on parts of the cloned cDNA with two internal primers from exons 5 and 9: 5′-CGTGAGACGCTGCCCCCACCATG-3′ (exon 5) and 5′-TTGCGGGGGAGAGGCGCTTGTGC-3′ (exon 9).

Subsequently, fragments containing the remainder of the *p53* coding exons were also obtained by amplifying exons 2–4 and exons 10–11. The sequences of these primers used were 5′-GGAATTCGCCATGGAGGAGTCACAGTCG-3′ (exon 2); 5′-GCAGAATAGCTTATTGAGGGGAGG-3′ (exon 5); 5′-GCGCAAAGAGAGCGCTGCCC-3′ (exon 8–9); 5′-CCCAAGCTTCAGTCTGAGTCAGGCCCCAC-3′ (exon 11).

Karyotype analysis

Cytogenetic preparations were obtained essentially as described in Aldaz et al. (1992).

Comparative genomic hybridization

Comparative genomic hybridization was performed essentially as described in Kallioniemi et al. (1992). Briefly, tumor genomic DNA and normal genomic DNA were labeled with biotin 14 dATP (GIBCO-BRL) and digoxigenin-11-dUTP (Boehringer Mannheim) by nick translation or random priming. Double stranded labeled DNA with a fragment size distribution of 600–1000 bp gave optimal signals if labeled by nick translation. The size distribution was between 150 and 500 bp when random primer labeling was used. Random priming was used in most of this work because it required less input DNA and more reliably produced good hybridization signals. Labeled tumor and normal

genomic DNAs (60–100ng) and unlabeled mouse Cot-1 DNA (GIBCO-BRL) (10–20 μg) were coprecipitated and dissolved in 10 μl of hybridization solution to obtain a final composition of 50% formamide, 10% dextran sulfate, and 2× SSC (pH 7). This mixture was heated to 70°C for 5 min to denature the DNAs and incubated at 37°C for 5–30 min. Normal mouse metaphase chromosomes prepared from fibroblast cultures were denatured at 80–85°C in 70% formamide, 2× SSC, for 5 min and dehydrated through an ethanol series. The hybridization mixture was applied to the slides, the coverslip sealed with rubber cement, and the slide incubated at 37°C for 4–5 days. After hybridization, the slides were washed and stained with a single layer of avidin–FITC (Vector Laboratories) and anti-digoxigenin–rhodamine (Boehringer Mannheim). Slides were counterstained with 0.1–0.2 μM DAPI in an antifade solution. The low DAPI concentration produced sufficient banding to permit identification of the mouse chromosomes.

Digital images of each of the fluorochromes in the specimens were obtained under computer control with a fluorescence microscope equipped with a CCD camera. Profiles of the fluorescence intensities of the normal and tumor DNA hybridization signals, and the intensity ratio profiles were calculated as described in Piper et al. (1995). The profiles were normalized so that the average value was 1.0 for the entire genome. Chromosomal regions where the ratio profile deviated significantly from the average were classified as either increases or decreases in DNA copy number.

Histopathology of tumor tissue

Histopathology of tumor tissues was as described previously (Medina 1973).

Southern blotting analysis of mammary tumors for gene amplification

DNA was isolated from tail and tumor tissue and 5 μg was digested with *Bam*HI as described previously (Donehower et al. 1992; Harvey et al. 1993a). The Southern blot was hybridized sequentially with several probes at the indicated temperatures: the 420-bp *Bam*HI fragment of rat *neu* (Bargmann et al. 1986) at 55°C, the 2.15-kb *Hin*dIII fragment of mouse *int-2/FGF3* (Mansour and Martin 1988) at 65°C, and the 600-bp *Cla*I–*Hin*dIII fragment of human c-*myc* (Stone et al. 1987) at 55°C. Following each hybridization, the blot was stripped of probe as recommended by the manufacturer. Quantitation was performed with a PhosphorImager (Molecular Dynamics).

Northern blotting analysis of mammary tumors

Portions of each tumor were used for RNA isolation by RNazol B reagent (Tel-Test, Inc.) according to manufacturer's protocol. One microgram of poly(-A)$^+$ RNA was electrophoresed through a 1% agarose formaldehyde gel and transfered to Hybond N (Amersham) in 20× SSC. Hybridizations were performed as described above. Additional probes and the corresponding hybridization temperatures used were the 1.7-kb *Bam*HI–*Eco*RI fragment of human *PRAD-1/cyclin D1* (Arnold et al. 1989) at 55°C and the 1.6-kb *Hin*dIII fragment of mouse *hst /FGF4* (Peters et al. 1989) at 65°C. The blot was stripped following each hybridization, as recommended by the manufacturer and as confirmed by autoradiography.

Acknowledgments

We thank E. Aguilar-Cordova and J. Jones for helpful discussions. We are grateful to W. Fang, M. McArthur, F. Kittrell, T. Doigg, A. Paladugu, and L. Yuschenkoff for excellent technical assistance, and R.F. Ramig for allowing us to use his mouse facility. We thank P. Hevezi, S. Sukumar, V. Pecenka, A. Arnold, G. Shackleford, and G. Lozano for gifts of plasmids. We also thank P. Wyde for help with the statistical assays. This work was supported by National Cancer Institute grants CA59967 (C.M.A.), CA54897 (L.A.D.), CA25215 (D.M.), CA45919 (D.P.), CA39832 (H.E.V.), a grant from the U.S. Army Breast Cancer Program (L.A.D.), and a grant from the Melanie Mann Bronfman Trust (H.E.V). L.A.D. is the recipient of a Research Career Development Award from the National Cancer Institute, and H.E.V. was an American Cancer Society research professor.

The publication costs of this article were defrayed in part by payment of page charges. This article must therefore be hereby marked "advertisement" in accordance with 18 USC section 1734 solely to indicate this fact.

References

Aldaz, C.M., A. Chen, L.S. Gollahon, J. Russo, and K. Zappler. 1992. Nonrandom abnormalities involving chromosome 1 and Harvey-ras-1 alleles in rat mammary tumor progression. *Cancer Res.* **52:** 4791–4798.

Arnold, A., H.G. Kim, R.D. Gaz, R.L. Eddy, Y. Fukushima, M.G. Byers, T.B. Shows, and H.M. Kronenberg. 1989. Molecular cloning and chromosomal mapping of DNA rearranged with parathyroid hormone gene in a parathyroid adenoma. *J. Clin. Invest.* **83:** 2034–2040.

Bargmann, C., M.-C. Hung, and R.A. Weinberg. 1986. Multiple independent activations of the neu oncogene by a point mutation altering the transmembrane domain of p185. *Cell* **45:** 649–657.

Bischoff, F.Z., S.O. Yim, S. Pathak, G. Grant, M.J. Siciliano, B.C. Giovanella, L.C. Strong, and M.A. Tainsky. 1990. Spontaneous immortalization of normal fibroblasts from patients with Li-Fraumeni cancer syndrome: Aneuploidy and immortalization. *Cancer Res.* **50:** 7979–7984.

Callahan, R. 1992. p53 mutations, another breast cancer prognostic factor. *J. Natl. Cancer Inst.* **84:** 826–827.

Cardiff, R.D. and W.J. Muller. 1993. Transgenic models of mammary tumorigenesis. *Cancer Surv.* **16:** 97–113.

Christofori, G. and D. Hanahan. 1994. Molecular dissection of multi-stage tumorigenesis in transgenic mice. *Sem. Cancer Biol.* **5:** 3–12.

Clarke, A.R., C.A. Purdie, D.J. Harrison, R.G. Morris, C.C. Bird, M.L. Hooper, and A.H. Wyllie. 1993. Thymocyte apoptosis induced by p53-dependent and independent pathways. *Nature* **352:** 849–852.

Czosnek, H.H., B. Bienz, D. Givol, R. Zakut-Houri, D.D. Pravtcheva, F.H. Ruddle, and M. Oren. 1984. The gene and the pseudogene for mouse p53 cellular tumor antigen are located on different chromosomes. *Mol. Cell. Biol.* **4:** 1638–1640.

Dameron, K.M., O.V. Volpert, M.A. Tainsky, and N. Bouck. 1994. Control of angiogenesis in fibroblasts by p53 regulation of thrombospondin-1. *Science* **265:** 1582–1584.

Dietrich, W.F., E.S. Lander, J.S. Smith, A.R. Moser, K.A. Gould, C. Luongo, N. Borenstein, and W. Dove. 1993. Genetic identification of Mom-1, a major modifier locus affecting Min-induced intestinal neoplasia in the mouse. *Cell* **75:** 631–639.

Donehower, L.A., M. Harvey, B.L. Slagle, M.J. McArthur, C.A. Montgomery, Jr., J.S. Butel, and A. Bradley. 1992. Mice deficient for p53 are developmentally normal but susceptible to spontaneous tumours. *Nature* **356:** 215–221.

Escot, C., C. Theillet, R. Lidereau, F. Spyratos, M.-H. Champeme, J. Gest, and R. Callahan. 1986. Genetic alteration of the c-myc protooncogene (MYC) in human primary breast carcinomas. *Proc. Natl. Acad. Sci.* **83:** 4834–4838.

Farmer, G., J. Bargonetti, H. Zhu, P. Friedman, R. Prywes, and C. Prives. 1992. Wild type p53 activates transcription in vitro. *Nature* **358:** 83–86.

Fearon, E.R. and B. Vogelstein. 1990. A genetic model for colorectal tumorigenesis. *Cell* **61:** 759–767.

Fidler, I.J. and L.M. Ellis. 1994. The implications of angiogenesis for the biology and therapy of cancer metastasis. *Cell* **79:** 185–188.

Greenblatt, M.S., W.P. Bennett, M. Hollstein, and C.C. Harris. 1994. Mutations in the p53 tumor suppressor gene: Clues to cancer etiology and molecular pathogenesis. *Cancer Res.* **54:** 4855–4878.

Harvey, M., M.J. McArthur, C.A. Montgomery, Jr., J.S. Butel, A. Bradley, and L.A. Donehower. 1993a. Spontaneous and carcinogen-induced tumorigenesis in p53-deficient mice. *Nature Genet.* **5:** 225–229.

Harvey, M., M.J. McArthur, C.A. Montgomery, Jr., A. Bradley, and L.A. Donehower. 1993b. Genetic background alters the spectrum of tumors that develop in p53-deficient mice. *FASEB J.* **7:** 938–943.

Harvey, M., A.T. Sands, R.S. Weiss, M.E. Hegi, R.W. Wiseman, P. Panayotis, B.C. Giovanella, M.A. Tainsky, A. Bradley, and L.A. Donehower. 1993c. In vitro growth characteristics of embryo fibroblasts isolated from p53-deficient mice. *Oncogene* **8:** 2457–2467.

Jacks, T., L. Remington, B.O. Williams, E.M. Schmitt, S. Halachmi, R.T. Bronson, and R.A. Weinberg. 1994. Tumor spectrum analysis in p53-mutant mice. *Curr. Biol.* **4:** 1–7.

Kallioniemi, A., O.-P. Kallioniemi, D. Sudar, D. Rutovitz, J.W. Gray, F. Waldman, and D. Pinkel. 1992. Comparative genomic hybridization for molecular cytogenetic analysis of solid tumors. *Science* **258:** 818–821.

Kandel, J., E. Bossy-Wetzel, F. Radvanyi, M. Klagsbrun, J. Folkman, and D. Hanahan. 1991. Neovascularization is associated with a switch to the export of bFGF in the multistep development of fibrosarcoma. *Cell* **66:** 1095–1104.

Kastan, M.B., O. Onyekwere, D. Sidransky, B. Vogelstein, and R.W. Craig. 1991. Participation of p53 protein in the cellular response to DNA damage. *Cancer Res.* **51:** 6304–6311.

Kastan, M.B., Q. Zhan, W.S. El-Deiry, F. Carrier, T. Jacks, W.V. Walsh, B.S. Plunkett, B. Vogelstein, and A.J. Fornace, Jr. 1992. A mammalian cell cycle checkpoint pathway utilizing p53 and GADD45 is defective in ataxia-telangiectiasia. *Cell* **71:** 587–597.

Kemp, C., L.A. Donehower, A. Bradley, and A. Balmain. 1993. Reduction of p53 gene dosage does not increase initiation or promotion but enhances malignant progression of chemically induced skin tumors. *Cell* **74:** 813–822.

Kern, S.E., J.A. Pietenpol, S. Thiagalingam, A. Seymour, K.W. Kinzler, and B. Vogelstein. 1992. Oncogenic forms of p53 inhibit p53-regulated gene expression. *Science* **256:** 827–830.

Kwan, H., V. Pecenka, A. Tsukamoto, T.G. Parslow, R. Guzman, T.-P. Lin, W.J. Muller, F.S. Lee, P. Leder, and H.E. Varmus. 1992. Transgenes expressing the *Wnt-1* and *int-2* protooncogenes cooperate during mammary carcinogenesis in doubly transgenic mice. *Mol. Cell. Biol.* **12:** 147–154.

Lammie, G.A., V. Fantl, R. Smith, E. Schuuring, S. Brookes, R. Michalides, C. Dickson, A. Arnold, and G. Peters. 1991. D11S287, a putative oncogene on chromosome 11q13, is amplified and expressed in squamous cell and mammary carcinomas and linked to BCL-1. *Oncogene* **6:** 439–444.

Land, H., L. Parada, and R.A. Weinberg. 1983. Tumorigenic conversion of primary embryo fibroblasts requires at least two cooperating oncogenes. *Nature* **304:** 596–602.

Lavigueur, A.L., V. Maltby, D. Mock, J. Rossant, T. Pawson, and A. Bernstein. 1989. High incidence of lung, bone, and lymphoid tumors in transgenic mice overexpressing mutant alleles of the p53 oncogene. *Mol. Cell. Biol.* **9:** 3982–3991.

Lidereau, R., R. Callahan, C. Dickson, G. Peters, C. Escot, and I.U. Ali 1988. Amplification of the *int-2* gene in primary human breast tumors. *Oncogene Res.* **2:** 285–291.

Livingstone, L.R., A. White, J. Sprouse, E. Livanos, T. Jacks, and T. Tlsty. 1992. Altered cell cycle arrest and gene amplification potential accompany loss of wild-type p53. *Cell* **70:** 923–935.

Lowe, S.W., H.E. Ruley, T. Jacks, and D.E. Housman. 1993a. p53-dependent apoptosis modulates the cytotoxicity of anticancer agents. *Cell* **74:** 957–967.

Lowe, S.W., E.M. Schmitt, S.W. Smith, B.A. Osborne, and T. Jacks. 1993b. p53 is required for radiation-induced apoptosis in mouse thymocytes. *Nature* **362:** 847–849.

Lowe, S.W., S. Bodis, A. McClatchey, L. Remington, H.E. Ruley, D.E. Fisher, D.E. Housman, and T. Jacks. 1994. p53 status and the efficacy of cancer therapy *in vivo*. *Science* **266:** 807–810.

Lu, X. and D.P. Lane. 1993. Differential induction of transcriptionally active p53 following UV or ionizing radiation: Defects in chromosome instability syndromes? *Cell* **75:** 765–778.

Malkin, D., F.P. Li, L.C. Strong, J.F. Fraumeni, Jr., C.E. Nelson, D.H. Kim, J. Kassel, M.A. Gryka, F.Z. Bischoff, M.A. Tainsky, and S.H. Friend. 1990. Germ line p53 mutations in a familial syndrome of breast cancer, sarcomas, and other neoplasms. *Science* **250:** 1233–1238.

Mansour, S.L. and G.R. Martin. 1988. Four classes of mRNA are expressed from the mouse *int-2* gene, a member of the FGF gene family. *EMBO J.* **7:** 2035–2041.

Medina, D. 1973. Preneoplastic lesions in mouse mammary tumorigenesis. *Methods Cancer Res.* **7:** 3–53.

Medina, D., F. Shepherd, and T. Gropp. 1978. Enhancement of the tumorigenicity of preneoplastic mammary lines by enzymatic dissociation. *J. Natl. Cancer Inst.* **60:** 1121–1126.

Neshat, K., C.A. Sanchez, P.C. Galipeau, P.L. Blount, D.S. Levine, G. Joslyn, and B. Reid. 1994. *p53* mutations in Barrett's adenocarcinoma and high-grade dysplasia. *Gastroenterology* **106:** 1589–1595.

Oltvai, Z.N. and S.J. Korsmeyer. 1994. Checkpoints of dueling dimers foil death wishes. *Cell* **79:** 189–192.

Peters, G., A.E. Lee, and C. Dickson. 1986. Concerted activation of two potential proto-oncogenes in carcinomas induced by mouse mammary tumour virus. *Nature* **320:** 628–631.

Peters, G., S. Brookes, R. Smith, M. Placzek, and C. Dickson. 1989. The mouse homolog of the *hst/k-FGF* gene is adjacent to *int-2* and is activated by proviral insertion in some virally induced mammary tumors. *Proc. Natl. Acad. Sci.* **86:** 5678–5682.

Piper, J., D. Rutovitz, D. Sudar, A. Kallioniemi, O.-P. Kallioniemi, F.W. Waldman, J.W. Gray, and D. Pinkel. 1995. Computer image analysis of comparative genomic hybridization. *Cytometry* **19:** 10–26.

Purdie, C.A., D.J. Harrison, A. Peter, L. Dobbie, S. White, S.E.M. Howie, D.M. Salter, C.C. Bird, A.H. Wyllie, M.L. Hooper, and A.R. Clarke. 1994. Tumour incidence, spectrum and ploidy in mice with a large deletion in the p53 gene. *Oncogene* **9:** 603–609.

Rotter, V., D. Wolf, D. Pravtcheva, and F.H. Ruddle. 1984. Chromosomal assignment of the murine gene encoding the trans-

formation-related protein p53. *Mol. Cell. Biol.* **4:** 383–385.
Sass, B. and T.B. Dunn. 1979. Classification of mouse mammary tumors in Dunn's miscellaneous group, including recently reported types. *J. Natl. Cancer Inst.* **62:** 1287–1293.
Shackleford, G.M., C.A. McArthur, H.C. Kwan, and H.E. Varmus. 1993. Mouse mammary tumor virus infection accelerates mammary carcinogenesis in *Wnt-1* transgenic mice by insertional activation of *int-2/Fgf-3* and *hst/Fgf-4*. *Proc. Natl. Acad. Sci.* **90:** 740–744.
Shing, Y., G. Christofori, D. Hanahan, Y. Ono, R. Sasada, K. Igarashi, and J. Folkman. 1993. Betacellulin: A mitogen from pancreatic beta cell tumors. *Science* **259:** 1604–1607.
Slamon, D.J., G.M. Clark, S.G. Wong, W.J. Levin, A. Ullrich, and W.L. McGuire. 1987. Human breast cancer: Correlation of relapse and survival with amplification of the HER-2/neu oncogene. *Science* **235:** 177–182.
Srivastava, S., Z. Zou, K. Pirollo, W. Blattner, and E.H. Chang. 1990. Germ-line transmission of a mutated p53 gene in a cancer prone family with Li-Fraumeni syndrome. *Nature* **348:** 747–749.
Stone, J., T. de Lange, G. Ramsay, E. Jakobovits, J.M. Bishop, H. Varmus, and W. Lee. 1987. Definition of regions in human c-*myc* that are involved in transformation and nuclear localization. *Mol. Cell. Biol.* **7:** 1697–1709.
Symonds, H., L. Krall, L. Remington, M. Saenz-Robles, S. Lowe, T. Jacks, and T. Van Dyke. 1994. p53-dependent apoptosis suppresses tumor growth and progression *in vivo*. *Cell* **78:** 703–711.
Thor, A.D., D.H. Moore, S.M. Edgerton, E.S. Kawasaki, E. Reihsaus, H.T. Lynch, J.N. Marcus, L. Schwartz, L.-C. Chen, B.H. Mayall, and H.S. Smith. 1992. Accumulation of p53 tumor suppressor gene protein: An independent marker of prognosis in breast cancers. *J. Natl. Cancer Inst.* **84:** 845–855.
Tsukamoto, A.S., R. Grosschedl, R.C. Guman, T. Parslow, and H.E. Varmus. 1988. Expression of the *int-1* gene in transgenic mice is associated with mammary gland hyperplasia and adenocarcinomas in male and female mice. *Cell* **55:** 619–625.
Yin, H., M.A. Tainsky, F.Z. Bischoff, L.C. Strong, and G.M. Wahl. 1992. Wild-type p53 restores cell cycle control and inhibits gene amplification in cells with mutant p53 alleles. *Cell* **70:** 937–948.
Yonish-Rouach, E., D. Resnitzky, J. Lotem, L. Sachs, A. Kimchi, and M. Oren. 1991. Wild-type p53 induces apoptosis of myeloid leukemic cells that is inhibited by interleukin-6. *Nature* **352:** 345–347.